**SKB**

# Task description of Task 9A – modelling of REPRO experiments WPDE-1 and WPDE-2

## Task 9 of SKB Task Force GWFTS – Increasing the realism in solute transport modelling based on the field experiments REPRO and LTDE-SD

**Martin Löfgren**

**Kersti Nilsson**

SVENSK KÄRNBRÄNSLEHANTERING

# Task description of Task 9A – modelling of REPRO experiments WPDE-1 and WPDE-2

## Task 9 of SKB Task Force GWFTS – Increasing the realism in solute transport modelling based on the field experiments REPRO and LTDE-SD

Martin Löfgren, Niressa AB

Kersti Nilsson, Geosigma AB

This report concerns a study which was conducted for Svensk Kärnbränslehantering AB (SKB). The conclusions and viewpoints presented in the report are those of the authors. SKB may draw modified conclusions, based on additional literature sources and/or expert opinions.

Data in SKB's database can be changed for different reasons. Minor changes in SKB's database will not necessarily result in a revised report. Data revisions may also be presented as supplements, available at www.skb.se.

A pdf version of this document can be downloaded from www.skb.se.

# Abstract

This report concerns Task 9 of the SKB Task Force GWFTS – Increasing the realism in solute transport modelling – Modelling the field experiments of REPRO and LTDE-SD. The purpose of this report is to publish the Task 9A description, as well as accompanying data deliveries, in the open literature. These documents have previously been distributed to the modelling groups of Task 9.

Task 9A concerns the semi-predictive modelling of tracer breakthrough curves of the Water Phase Diffusion Experiments (WPDE) 1 and 2. These in situ tracer tests have been carried out within the REPRO programme at about 400 m depth at the ONKALO underground rock characterisation facility in Olkiluoto, Finland, by Posiva. The Task 9A description gives the prerequisites of the experiments, accompanying laboratory data on rock matrix retention properties and guidance on the semi-predictive modelling of the breakthrough curves. The actual modelling within Task 9A is not presented here but in a separate report.

This report also gives a discussion on scientific challenges regarding solute diffusion, sorption and speciation in the heterogeneous rock matrix, as well as some other background documentation, which have been used when justifying the start-up of Task 9.

# Sammanfattning

Den här rapporten berör Task 9 inom ramen för SKB Task Force GWFTS – Förbättring av realismen vid transportmodellering av lösta ämnen – Modellering av fältexperimenten REPRO och LTDE-SD. Syftet med denna rapport är att publicera modelleringsbeskrivningen för Task 9A, samt de medföljande dataleveranserna, i den öppna litteraturen. Dessa dokument har tidigare distribuerats till modelleringsgrupperna i Task 9.

Task 9A berör semiprediktiv modellering av genombrottskurvor för spårämnen i experimentserien Water Phase Diffusion Experiments (WPDE – diffusionsexperiment i vattenfas) 1 och 2. Dessa spårämnesförsök har utförts in situ på ca 400 m djup i underjordslaboratoriet ONKALO i Olkiluoto, Finland. Detta har utförts av Posiva inom ramen för undersökningsprogrammet REPRO. Modelleringsbeskrivningen för Task 9A ger förutsättningarna för experimenten, kompletterande laborativa data gällande matrisbergets retentionsegenskaper, samt vägledning angående den semiprediktiva modelleringen av genombrottskurvorna. Den faktiska modelleringen inom Task 9A presenteras inte här utan i en annan rapport.

Denna rapport innehåller även en diskussion om vetenskapliga utmaningar gällande diffusion, sorption och speciering av lösta ämnen i den heterogena bergmatrisen, samt övrigt bakgrundsmaterial som tillämpats för att motivera uppstarten av Task 9.

# Contents

# 1 Introduction

## 1.1 SKB Taskforce GWFTS – Task 9

Task 9 is part of the SKB Task Force on Modelling of Groundwater Flow and Transport of Solutes (Task Force GWFTS), which focuses on the fractured crystalline host rock surrounding present and future repositories for spent fuel and other radioactive waste. Special interest is taken in work on fracture flow and solute transport made by the Äspö Hard Rock Laboratory (HRL), Sweden.

The title of Task 9 is "Increasing the realism in solute transport modelling – Modelling the field experiments of REPRO and LTDE-SD". The task focuses on the realistic modelling of coupled matrix diffusion and sorption in the heterogeneous crystalline rock matrix at depth. This is done in the context of inverse and predictive modelling of tracer concentrations of the in situ experiments performed within LTDE-SD at the Äspö HRL in Sweden, as well as within the REPRO project at ONKALO in Finland, focusing on sorption and diffusion. The ultimate aim is to develop models that in a more realistic way represent retardation in the natural rock matrix at depth. The following waste management organisations are part of Task 9:

- Svensk Kärnbränslehantering AB, SKB, Sweden.
- Bundesministerium für Wirtschaft und Technologie, BMWi, Germany.
- Japan Atomic Energy Agency, JAEA, Japan.
- Korea Atomic Energy Research Institute. KAERI, South Korea.
- Posiva Oy, Finland.
- Department of Energy, DOE, USA.
- Radioactive Waste Repository Authority (RAWRA), SURAO, Czech Republic.

These waste management organisations assign modelling groups that perform the actual modelling within Task 9.

## 1.2 Organisation of Task 9A

Task 9 is divided into subtasks that model different in situ tracer tests. The framework of Task 9A was first established by the Technical Committee of Task 9:

- Jan-Olof Selroos, Svensk Kärnbränslehantering AB.
- Björn Gylling, Svensk Kärnbränslehantering AB.
- Lasse Koskinen, Posiva Oy.
- Martin Löfgren, Niressa AB.
- Kersti Nilsson, Geosigma AB.
- Antti Poteri, VTT Technical Research Centre of Finland.

The Scientific Chairman of Task 9:

- Bill Lanyon, Fracture Systems Ltd.

The Scientific Chairman was also included in the discussion when setting up the framework of Task 9A. The subtask was thereafter detailed in the Task 9A description, primarily authored by the Principal Investigators Martin Löfgren and Kersti Nilsson but with valuable input from the technical committee and also Bill Lanyon. Task 9A was initiated in April 2015 at a workshop in Helsinki where modelling groups also were present. The setup of Task 9A, and the modelling groups' work on the subtask, is evaluated by the Task 9 Evaluator:

- Josep Maria Soler Matamala, IDAEA-CSIC.

The outcome of Task 9A is reported in two SKB reports, including this present report. The other report (Soler et al. in prep) compiles the modelling groups' accounts of, and results from, Task 9A, as well as the Task 9 Evaluator's evaluation of the task description and the performed modelling work.

> **Clarification or comment***
> Soler et al. in prep should be Soler et al. 2019.

* Modification to the original text is avoided and instead clarifications and comments are inserted in grey text boxes below the paragraphs concerned.

## 1.3    REPRO experiments WPDE-1 and WPDE-2

This section gives an overview of the in situ tracer tests in focus of Task 9A, i.e. the Water Phase Diffusion Experiments (WPDE) 1 and 2 that have been carried out at the ONKALO underground rock characterisation facility in Olkiluoto, Finland. Details of the experiments are given in the task definition in Chapter 2.

The experiments are part of Posiva's extensive research programme REPRO (Rock matrix REtention PROperties) that includes both studies in situ and in the laboratory (Poteri et al. in prep a, b, Ikonen et al. 2015, Voutilainen et al. in prep a, b). The programme focuses on investigating the rock that surrounds the investigation niche ONK-TKU-4219 at ONKALO, which is also called the REPRO niche. The niche is found at about 400 m depth and from the niche, several drillholes extend into the rock. The location of the REPRO niche is provided in Figure 1-1 and a close-up of the niche and also the drillholes extending from it is illustrated in Figure 1-2.

> **Clarification or comment**
> Poteri et al. in prep a, b should be Poteri et al. 2018 a, b.
> Voutilainen et al. in prep a, b should be Voutilainen et al. 2018 a, b.
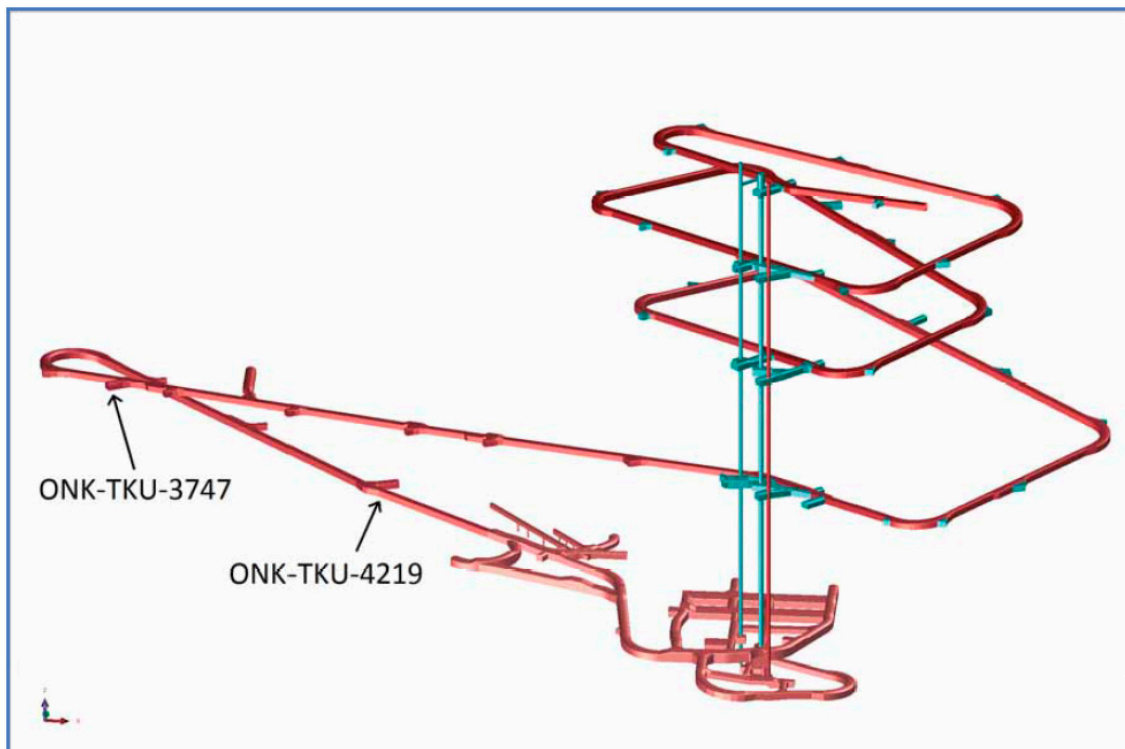


**Figure 1-1.** *Location of the REPRO niche (ONK-TKU-4219) at ONKALO. Reproduced from (Toropainen 2012, Figure 1).*

Two types of in situ tracer tests in the water phase are carried out within the REPRO campaign, using drillholes extending from the REPRO niche. The experiments that Task 9A focuses upon, i.e. WPDE 1 and 2, have been carried out in drillhole ONK-PP323, which is labelled 323 in Figure 1-2. The other in situ tracer test is the Through Diffusion Experiment (TDE) which is carried out between a section in injection drillhole ONK-PP326 and sections in monitoring drillholes ONK-PP324 and ONK-PP327.

The WPDE campaign features advection-diffusion-sorption experiments which are carried out in a defined section of drillhole ONK-PP323, about 18 to 20 m away from the niche wall. Here a 1.905 m long section has been packed off, and in this section a dummy has been placed that is coaxially oriented with the drillhole (cf. Figure 1-3).
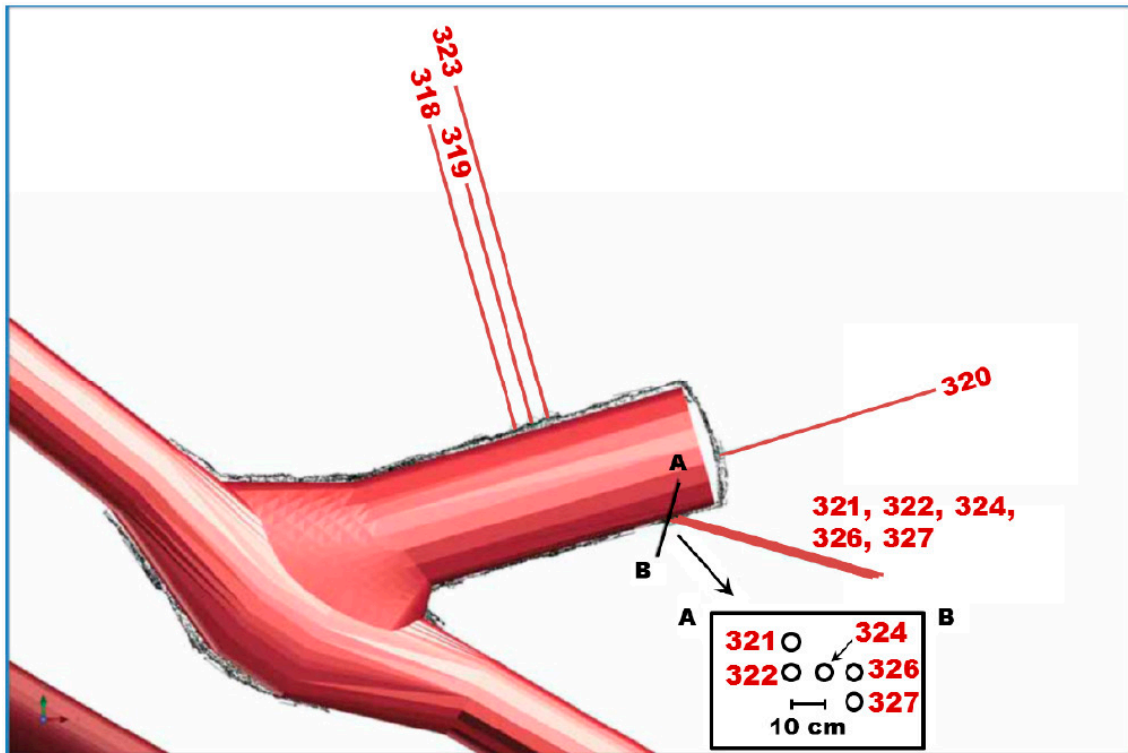


*Figure 1-2.* *The REPRO niche at the 401 m level at ONKALO, and some of the drillholes drilled from the niche. Drillhole ONK-PP323 (labelled 323 in the illustration) is utilised for WPDE 1 and 2, and drillholes ONK-PP324, ONK-PP326, and ONK-PP327 for TDE. Reproduced from (Ikonen et al. 2015, Figure 2).*
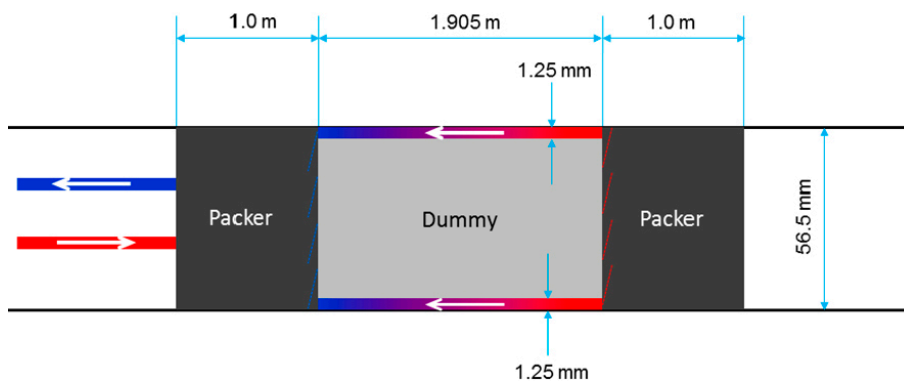


*Figure 1-3.* *The packed-off section in drillhole ONK-PP323 where the tracer tests are carried out in flowing water at different flow rates in a slot between the drillhole wall and a dummy. The red colour in the illustration signifies the injected tracer pulse and the blue colour the displaced non-traced water.*

The dummy diameter is 54 mm whereas the drillhole diameter is 56.5 mm, leaving a 1.25 mm slot between the drillhole wall and the dummy. This slot is regarded as an artificial fracture of relatively well-defined geometry. In this slot a very low steady-state water flow has been applied, directed towards the niche. This was achieved by injecting the water at the far end of the packed-off section, as shown in Figure 1-3. To date, two experiments have been performed at different flow rates; WPDE-1 (20.1 µL/min) and WPDE-2 (10.0 µL/min). In this water flow, the active tracers HTO, Na-22, Cl-36, and I-125 were injected in WPDE-1, and HTO, Na-22, Cl-36, Sr-85 and Ba-133 in WPDE-2. For each experiment, the tracer injection took the form of an extended pulse of a few hours duration at the far end of the experimental section. The tracer cocktails in WPDE-1 and WPDE-2 consisted only of the tracer stock solutions (Cl-36 stock solution containing Cl⁻ carrier) and no added salts. The idea behind the experimental setup is that as the tracer pulse is carried with the water flow, the tracers diffuse into the rock matrix surrounding the drillhole, where they may also sorb. As the pulse passes, the concentration gradients are reversed and the tracers then diffuse out of the rock matrix and into the flowing water. By detecting their activities in the water phase at the end of the drillhole, breakthrough curves are obtained which can be analysed by modelling.

As part of the REPRO programme, numerous drill core samples have been analysed in the laboratory with respect to their retention properties (cf. Section 2.4). The bulk of the samples have been collected from the drillholes extending from the REPRO niche, with the exception of several reference samples taken from other drillholes.

## 1.4 Task description and data deliveries of Task 9A

The main purpose of this report is to publish the Task 9A description, as well as accompanying data deliveries, in the open literature. These documents were provided to the modelling groups during the course of Task 9A. The final task description for Task 9A was sent out to the modellers in the later part of 2015, and is dated the 22$^{nd}$ of November, 2015. In addition to the task description, there are several accompanying data deliveries. These are tabulated in Table 1-1, where also the data delivery number relating to the SKB Task Force website is provided. These data deliveries are appended to this report and the rightmost column of Table 1-1 provides the link to the corresponding appendix. The first few rows concern the task description, and links to where the different chapters and appendices are found in this present report.

The Task 9A definition (section 2) is primarily written in present tense, as presented to the modellers prior to Task 9A, although the planned modelling at the time for publishing of this report has already been performed.

**Table 1-1. Mapping of task description and data deliveries to this report.**

| Delivery Number | Description of data delivery | Link to location in this report |
|---|---|---|
| 1 | Task 9A Description (2015-11-22) | |
| | Chapter 1: Introduction | Appendix 1 |
| | Chapter 2: Task definition of Task 9A | Chapter 2 |
| | Chapter 3: References | Reference list |
| | Appendix A: List of scientific challenges | Appendix 2 |
| | Appendix B: List of revisions | Revisions incorporated in final task description. Not included in this report. |
| | Appendix C: Letter to modellers | Appendix 3 |
| 2 | Data for Task Description 9A | Appendix 4 |
| 3 | Description of the tracer inlet for task 9A | Appendix 5 |
| | WPDE Photographs with higher resolution than earlier distributed | Appendix 6 |
| 4 | Template for reporting of Task 9A and Template for delivering results of Task 9A | Not included in this report |
| 10 | Experimental data of REPRO WPDE 1 and 2 | Not included in this report |
| 17 | Update concerning tracer cocktail density | Not included in this report |
| #20 | Update 2 concerning tracer cocktail density | Appendix 7 |

Chapter 1 of the Task 9A description in Delivery #1 serves as an introduction to Task 9, and includes general information that is not directly relevant for Task 9A. This can be exemplified by information on the LTDE-SD experiment at the Äspö HRL in Sweden. Accordingly, the chapter is not presented in the main part of this present report but instead reproduced without modifications in Appendix 1.

Chapter 2 of the Task 9A description contains the core definition of the subtask, and is reproduced in Chapter 2 of this present report. Modification to the original text is avoided and instead clarifications and comments are inserted in grey text boxes below the paragraphs concerned. An example of such a text box is provided below.

> **Clarification or comment**
> Text providing a brief clarification of comment.

Only with regard to one issue has the original text been corrected on multiple occasions. This concerns an erroneous reference that is now replaced by Ikonen et al. (2015), as detailed in a text box in Section 2.4.1.

Appendices A and C of the Task 9A description in Delivery #1 are reproduced without modification in Appendix 2 and 3, respectively. Appendix B of the task description describes revisions that were already incorporated in the final version dated November 22th, 2015, and is not provided in this present report.

Delivery #2 concerns tabulated numerical data that accompany Task 9A. These data have been copied from the Excel spreadsheets to Appendix 4, with no modifications except for their placement on the pages. The intention is that one should be able to easily copy the data back to a spreadsheet for further calculations. In instances where the number of rows or columns exceeds what is reasonable in a report, the data have been plotted and the link to the data within the data delivery is provided.

Part of Delivery #3 is reproduced without changes in Appendix 5. The high resolution photos of data delivery #3 are copies of the same photos provided in Chapter 2, with the exception that in Chapter 2 the resolution is lower. To obtain the high resolution photos, the reader must download the data delivery #3 from the SKB Task Force website.

Delivery #4 only contains templates for the modellers to use when reporting Task 9A. These templates are not reproduced in this report. Delivery #10 concerns tracer breakthrough data from the WPDE-1 and WPDE-2 experiments that were not delivered to the modellers as part of the semi-predictive phase of the modelling. These data are not appended to this present report.

Delivery #17 concerns clarifications on the water densities of the injected tracer solution and synthetic groundwater used as carrier in WPDE-1. This clarification has been updated in Delivery #20, where also data has been added for WPDE-2. None of these data deliveries are part of the actual task description but should rather be seen as complementary and clarifying information provided at the conclusion of Task 9A. The choice has been made to only include Delivery #20 in this report, as presented in Appendix 7.

Appendix 8 contains the General Task Description for GWTFS Task 9.

The main reference list of this report is extended to also cover references given in the appendices.

# 2 Task definition of Task 9A

## 2.1 Introduction

Task 9A is intended as a relatively simple "warm-up" case for Task 9. It includes the semi-predictive modelling of the REPRO in situ experiments WPDE-1 and WPDE-2, where the tracer breakthrough curves should be predicted by using "standard" solute transport codes, parameters, and data. Typical processes that may be represented in the modelling of this warm-up case are advection and dispersion, Fickian matrix diffusion, and linear equilibrium sorption. The rock matrix should be assumed to be homogenous or heterogeneous with a simple microstructure.

Preliminary results from WPDE-1 and WPDE-2 were shown in PowerPoint presentations at a few Task Force meetings and workshops during 2013 and 2014. In addition, the official WPDE-1 report is intended to be published by Posiva in 2015. The modellers are requested to disregard these presentations and this publication during the subtask. Even so, the modelling cannot properly qualify as being fully predictive (blinded) and is consequently considered to be only semi-predictive.

The starting point of the subtask is the Task Force GWFTS workshop in Helsinki between the 22nd and 23rd of April 2015 and the first chance to present modelling results is at the Task Force meeting #33 that will be held in Kalmar, Sweden, between the 20th and 22nd of October, 2015.

> **Clarification or comment**
> The official WPDE-1 report was not published in 2015 by Posiva, but the plan for publication is instead in 2018 (Poteri et al. 2018 a).

## 2.2 Scope and objectives

As discussed in Appendix 1, the ultimate aim of Task 9 is to develop models that in a more realistic way represent solute transport and retardation in the natural rock matrix. This may be done by more realistically representing the rock heterogeneity and microstructural features, by incorporating a broader range of processes involved, or by other means.

However, Task 9A is intended as a relatively simple "warm-up" case where no significant effort should be made to improve the modelling codes. Instead, there are a number of soft objectives associated with the subtask, as specified below:

- To gather a group of modellers, researchers, and delegates of nuclear waste management organisations around a simple modelling case, allowing them to familiarise themselves with:
  - the framework of the GWFTS Task Force, and
  - the general geoscientific settings of the REPRO experimental site.

- To allow the modellers to familiarise themselves with the experimental setup of the WPDE campaign, in terms of geometries, flows, boundary conditions, supporting laboratory data, etc. The proper incorporation of such basic information in the models will also be of use when modelling the experiments in a later subtask.

- To use the WPDE-1 and WPDE-2 experiments as a framework for discussing the heterogeneous nature of the rock, as well as processes that may or may not be relevant for solute transport and retardation in the rock matrix.

- To obtain comparable results that could form the basis of a scientific discussion at coming workshops and meetings. In this instance the results will consist of predicted tracer breakthrough curves of the WPDE campaign.

- An optional objective would be to perform predictive modelling of a third WPDE experiment, which may or may not be launched within REPRO, using higher or lower flow rates that in WPDE 1 and 2. Whether, or not to pursue this option will be decided at a later stage, and such predictive modelling will not be initiated until after the Task Force meeting #33 in October 2015.

Concerning the models, the modellers should intentionally avoid further development within Task 9A, other than adjusting them to represent the experimental set-up of the WPDE-1 and WPDE-2 experiments. As such, the modellers should use what they perceive to be traditional solute transport codes. The following simplifications may be made:

- Conventional advection and dispersion may be assumed in the experimental drillhole section; in the water filled annular slot between the drillhole wall and the dummy. The modellers may also choose to model advection and dispersion in the tubing connecting the experimental section with injection and water sampling equipment in the REPRO niche. No detailed information on the flow distribution or potential channelling pattern in the experimental section is provided. Instead a single value of the total water flow rate through the experimental section is provided, with the intention that a simple flow distribution should be assumed when modelling the central prediction of breakthrough curves (cf. Section 2.5). However, as it is reasonable that channelized flow occurs to some degree, potential impacts can be explored in alternative predictions.

- Fickian matrix diffusion may be assumed as the only transport mechanism in the rock matrix. Possible effects from multicomponent transport should be disregarded. If the modeller is in possession of computational codes that treat matrix diffusion as non-Fickian, such codes may be used if this is judged to simplify matters.

- Equilibrium linear sorption may be assumed in the rock matrix, effectively meaning that the customary, conditionally constant $K_d$ concept can be used. Furthermore, geochemical conditions should be assumed to be constant in space and time. The synthetic groundwater of the tracer cocktail should be assumed to represent the matrix pore water.

- It is left to the discretion of the modellers whether surface sorption on the drillhole is to be considered. However, no specific data supporting such an approach is provided (that is only $K_d$ values are provided from the laboratory investigations of the rock matrix, but no $K_a$ values).

- The rock matrix may be assumed to be either homogenous or heterogeneous. However, if choosing a heterogeneous representation, a simple microstructural configuration should be assumed. Two examples of simple heterogeneous configurations are:
  – a layered rock matrix representation featuring cylindrical layers that are coaxial with the drillhole;
  – dividing the rock along the experimental sections into a few different rock volumes based on, for example, the rock type characterisation of the drill core.

The modellers are not limited by the above examples, but the level of complexity should be constrained when setting up a heterogeneous rock model. The assumed heterogeneity may reflect on the porosity, effective diffusivity, and/or sorption partitioning coefficients.

- The breakthrough of I-125 in WPDE-1 is not modelled in Task 9A, as its speciation may change in a manner that is outside the scope of the subtask.

The outcome of the modelling should be the prediction of the breakthrough curves of WPDE-1 and WPDE-2; for all the tracers used, except I-125. To facilitate comparison between results from different modelling groups, common performance measures are preferably used. Modellers are also encouraged to discuss uncertainties associated with the model and to explore the model's sensitivity to input data uncertainty and other unknowns. This is further described in Section 2.5.

## 2.3    Specifics of the in situ experiment

The in situ part of the WPDE campaign has been summarised in Appendix 1. In the sections below a more detailed account is given, with focus on data that may be needed as input to the modelling of Task 9A. Additional information and data are also given with the aim of providing deeper familiarity with the circumstances under which the experiments have been carried out. Such additional data may also prove to be of use when revising the experiments in a later subtask.

### 2.3.1 Experimental setup and geometries

The WPDE campaign is carried out in drillhole ONK-PP323, which is a 21.65 m long hole that is drilled from the left-hand wall of the REPRO niche. The drillhole has a dip of −10°, meaning that it is drilled almost horizontally but with a slight dip downwards. The experimental setup consists of installations in the borehole, equipment in a container in the REPRO niche and connecting tubing.

The upper image of Figure 2-1 shows a side view illustration of the experimental section utilised in the campaign. A 1.905 m long drillhole section has been packed off using inflatable packers. The section is located between the drillhole lengths 17.95–19.85 m. The ends of the packers, facing the experimental section, have been Teflon-coated to avoid interactions with the tracers. An inert and non-porous dummy of PEEK (PolyEtherEtherKetone) has been placed within the packed-off drillhole section, coaxially oriented with the drillhole.

The diameter of the dummy is 54 mm, while the diameter of the drillhole is about 56.5 mm (and not 56 mm as stated in previous presentations). This leaves a $1.25 \pm 0.1$ mm annular slot between the dummy and the drillhole wall. Locally, the borehole diameter may change[1] due to surface roughness and minor irregularities of the drillhole wall.
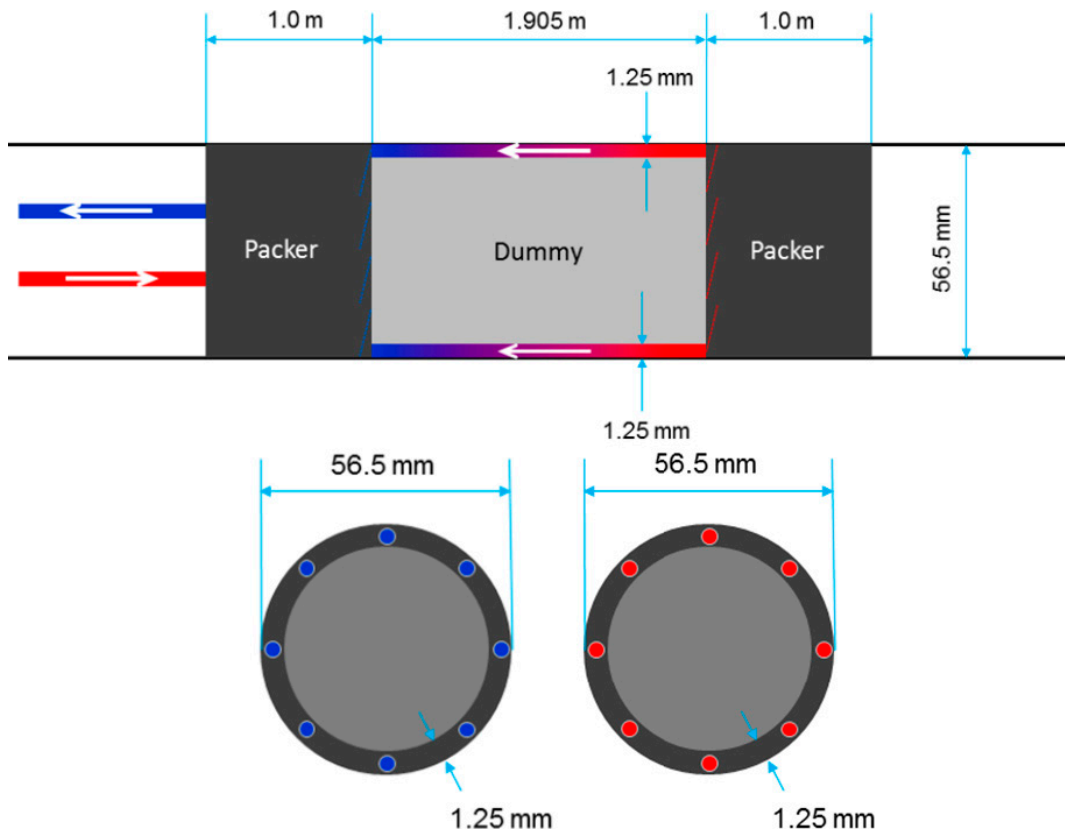


**Figure 2-1.** *The experimental setup of the WPDE in situ campaign. Upper: Side view of the experimental section. Lower left: Schematic cross-section view of the outlet to the experimental section, showing the eight outlet points. Lower right: Cross-section view of the inlet to the experimental section, showing the eight inlet points. The actual geometry of the inlet and outlet points is not circular, as indicated in Figure 2-2.*

---

[1]  Recent diameter measurements with calliper indicate an average drillhole diameter of 56.72 mm in the WPDE section. Max and min values are 56.90 and 56.58 mm, respectively. The standard deviation is 68 μm. The data are unpublished and presently we cannot account for data uncertainty.

***Figure 2-2.*** *Grooves are applied on the equipment to facilitate the mixing of the injected tracer solution with the synthetic groundwater; rubber sealing is covering the grooves.*

The lower images of Figure 2-1 show cross-sectional views of the inlet to, and outlet from, the annular slot. At the inlet, the water flows from eight distinct points which are equally spaced. The part that connects the annular slot with the inlet tube is shown in Figure 2-2. The PEEK dummy is inserted in the pipe featuring spiral grooves, and a tight fit is secured by a rubber seal. The grooves aim to further facilitate mixing of the injected tracer solution with the synthetic groundwater carrying the tracer pulse. They also facilitate a more dispersed flow during the experiment. In this setup, the water injection takes place at the far side end of the annular slot, at the drillhole length 19.85 m. The same design is applied at the outlet of the experimental section, which is located at the drillhole length 17.95 m.

---

**Clarification or comment**

Several modelling groups asked for additional information on the tracer inlet, which was provided in data delivery #3 and is reproduced in Appendix 5.

Unpublished calliper data on the borehole diameter are archived in Posiva's research database POTTI.

---

The experimental section is connected to various pieces of equipment fitted in a container that is placed next to the drillhole in the Repro niche. The inside of this container is displayed in Figure 2-3. The connections are made by PEEK tubing of the inner diameter 1/25 inch (1.0 mm). The length of the inlet tube, from the end of the injection loop to the start of experimental section, is estimated to be 24.2 m. The length of the spiral grooves shown in Figure 2-2 is included in this estimate.

The length of the outlet tube from the end of the experimental section to the online gamma detection equipment (cf. Section 2.3.5) is 25.7 m. An additional tube length is added when water samples are collected from a 6-way valve for analyses in the laboratory. The total length between the end of the experimental section and the valve is 30.3 m. The length of the spiral grooves of the outlet is included in these estimates. The main geometries of the WPDE experiments are summarised in Table 2-1.

**Table 2-1. Geometries of the WPDE in situ campaign.**

| Description | Measure | Unit |
|---|---|---|
| Aperture of annular slot | 1.25 ± 0.1 | mm |
| Outer diameter of dummy | 54.0 | mm |
| Length of annular slot (also distance between inlet and outlet) | 1.905 | m |
| PEEK tubing – inner diameter | 1.0 | mm |
| Length of PEEK inlet tube | 24.2 | m |
| Length of PEEK outlet tube to online detector | 25.7 | m |
| Length of PEEK outlet tube to sample collection point | 30.3 | m |

### 2.3.2 Flows, experimental pressures and temperature

In the WPDE campaign the aim has been to maintain a steady-state flow of synthetic groundwater through the experimental section prior, during, and after tracer injection. The target flow rates of WPDE-1 and WPDE-2 were 20 and 10 μL/min, respectively. The injection flow was regulated by using a calibrated piston pump and the actual flow rate was measured by logging the position of the piston. For WPDE-1, the measured flow rate was 20.1 ± 0.6 μL/min and for WPDE-2 the measured flow rate was 10.0 ± 0.4 μL/min. These data are given as the arithmetic mean of the daily average flow rate ± two standard deviations, and are based on logged piston movements during the entire experimental time. The logged flow rates can be seen in Figure 2-4 (upper row). The larger fluctuations seen at regular intervals are due to pump stops in order to fill the piston pump with synthetic groundwater under atmospheric pressure.



*Figure 2-3. Container in the REPRO niche, containing equipment such as sampling- and injection loops (a), data taker (b), online detector (c), pressure regulation unit (membrane chamber; d), and piston pump (e).*
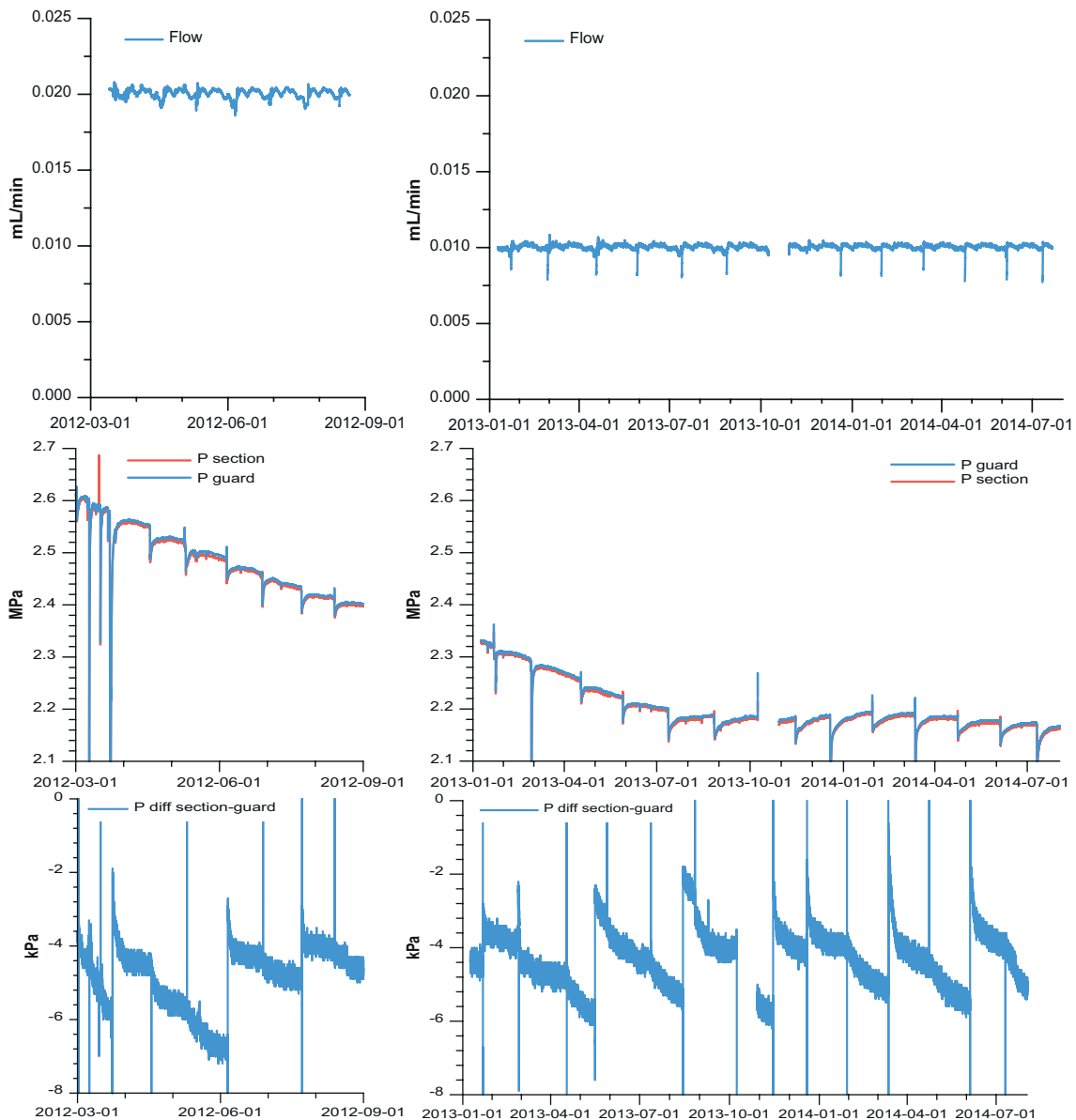
***Figure 2-4.*** *The logged flow rates of injected synthetic groundwater in WPDE-1 (upper left) and WPDE-2 (upper right); the pressures in the experimental and guard sections of WPDE-1 (middle left) and WPDE-2 (middle right); and the pressure difference between the experimental and guard sections in WPDE-1 (lower left) and WPDE-2 (lower right). The injection date for WPDE-1 was 2012-03-08 and for WPDE-2 2013-01-23.*

**Clarification or comment**

Diagrams in Figure 2-4 from (Poteri et al. ***2018 a, b).***

The flow rate, or total volume, of the synthetic groundwater flowing out of the experimental system, that is from the outlet tube, was not measured. Hence, no direct data exist for estimating the recovery of the synthetic groundwater. Such data could have been used for estimating if there had been a leakage into, or out of, the experimental system.

The experimental section, as well as an adjacent guard section, were pressurised throughout the experiments and the pressures were monitored. The packer installations of the drillhole, as well as the installed tubing, are displayed in Figure 2-5. Note that there is a short-circuiting tube connecting the two sections surrounding the experimental section. The blue curves in the middle row of

Figure 2-4 correspond to the pressure of the experimental section and the red curves correspond to that of the guard section. It should be noted that the regular drops in pressure corresponds to the event of refilling the piston pump with synthetic groundwater.

In the early part of the WPDE-1 experiment there are four major pressure fluctuations. The first two short-term pressure drops coincide with minor leakages. These were quickly discovered and their impact on the flow through the experimental section can be neglected. The third pressure drop coincides with a larger leakage from ~19:30 on the 22nd of March to 16:11 on the 23rd of March. During this time the inflow can be assumed to have halted. The short-term pressure increase in the experimental section corresponds to a mistakenly closed valve but should have no significant impact on the results.

The pressure in the experimental section was regulated by a pressure regulation membrane to almost match the ambient pressure, as measured in the adjacent packed-off guard section, featuring a hydraulically conductive fracture. The fracture is found at the drillhole length 7.64 m. A perfect match was not strived for but rather the experimental section should be at a slightly lower pressure compared to the ambient pressure. The intention was to hinder an advective flow of tracers from the experimental section and into the rock matrix; or over the packer system. The difference between the experimental and ambient pressures was regulated to be within the limits −4 to −7 kPa for WPDE-1 and −2 to −6 kPa for WPDE-2. The variations in the pressure differences over time are shown in Figure 2-4 (lower row).

During the experimental time of WPDE-1, the pressure in the experimental section decreased from 2.6 MPa at tracer injection to 2.4 MPa at the end of the experiment. For WPDE-2 the experimental pressure decreased from 2.3 MPa to 2.2 MPa. As can be seen in Figure 2-4 (middle row), this decrease matches the decrease in ambient pressure. Such pressure decrease is expected around a newly constructed tunnel due to drainage, and a similar trend can be observed in the nearby located drillhole ONK-KR14.

The temperature of both the WPDE experiments should coincide with the ambient in situ temperature. The in situ temperature at the Olkiluoto site is in general between 10 and 11 °C at the –400 m level (Sedighi et al. 2014, Section 3.1). The temperature in the REPRO niche (i.e. at the experimental container) was within the range 14 to 17 °C during the experiments, but the elevated temperature in the tunnel should have limited impact on the experimental section that is shielded by almost 20 m of rock. For the purpose of Task 9A, the experimental temperature 11 °C can be used.
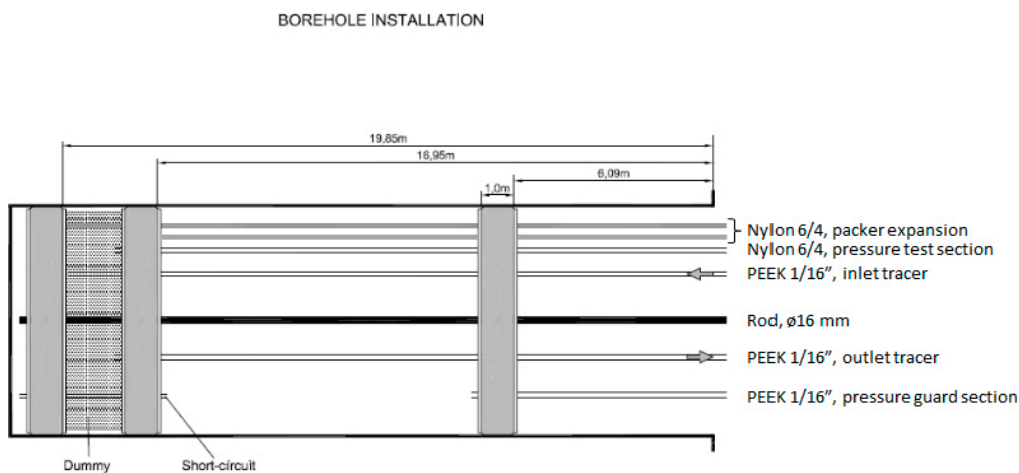
BOREHOLE INSTALLATION



*Figure 2-5. Installations in drillhole ONK-PP323. The packed-off section in the middle is the guard section, which features a hydraulically conductive fracture at the borehole length 7.64 m.*

### 2.3.3 The tracer injection solution and injection data

*WPDE-1*

For the WPDE-1 experiment, a small amount of concentrated injection solution that contained the tracers HTO, Na-22, Cl-36, and I-125 was injected into the experimental section as a short pulse. This was done by filling a 124 cm long PEEK tube, called the injection loop, with the injection solution, where the total weight of the solution was 999 mg (total volume of ~1 mL).

Prior to and during injection, a low steady state flow of synthetic groundwater (~20 μL/min) was upheld through the experimental section. During the injection, a 6-way valve was switched forcing the synthetic groundwater to flow through the injection loop, bringing the tracers into the inlet tube connected to the experimental section. After about three hours the valve was again switched, disconnecting the injection loop. The tracer injection was initiated at 14:12 on the 8th of March 2012. It should be noted that the injection loop was placed in the container in the REPRO niche (see Figure 2-3). This means that the tracer pulse needed to travel through a PEEK tube of significant length between the injection loop and the experimental section (cf. Section 2.3.1), which affected the arrival time of the tracer injection pulse in the experimental section.

The activities of the tracers in WPDE-1 that initially filled the injection loop are provided in Table 2-2, save for data for the tracer I-125 that is not intended to be modelled in Task 9A. The amounts of residual tracers in the loop after injection were not measured but likely they are insignificant, as three hours of injection roughly corresponds to three exchanges of the volume in the injection loop.

---

**Clarification or comment**

At near completion of the semi-predictive modelling phase of Task 9A, additional information was asked for regarding the contrast in density between the tracer cocktail within the injection loop and the synthetic groundwater carrying the plug of tracer cocktail to the experimental section. Such additional information is given in Appendix 7.

---

*WPDE-2*

The injection procedure in WPDE-2 was similar to that of WPDE-1. The tracers HTO, Na-22, Cl-36, Sr-85, and Ba-133 were injected. This time, a 370-cm long injection loop was used, containing 2.963 mg, or about 3 mL, of injection solution. Once more the injection solution was flushed into the inlet tube connected to the experimental section by a steady-state flow of synthetic groundwater (10 μL/min). The flushing time of the injection loop was about 25 hours. As for WPDE-1, the tracer pulse needed to travel through a PEEK tube of significant length before reaching the experimental section. The tracer injection was initiated at 14:27 on the 23rd of January, 2013.

The activities of the tracers in that initially filled the injection loop are provided in Table 2-2. As in WPDE-1, the amounts of residual WPDE-2 tracers in the loop after injection were not measured.

*Specifics of the tracers*

Table 2-2 provides data on the injected activities[2], together with some specifics of the tracers. It should be noted that all measured activities in the WPDE campaign are presented as decay corrected activities, using the injection date as time zero. This means that measured activities are recalculated in a way that effectively negates the concentration decreasing effect of decay.

---

[2] To convert the injected activity to number of injected moles; take the activity (Bq) times the half-life (s) divided by the product of ln(2) and Avogadro's number.

**Table 2-2. Specifics of the tracers used in the WPDE campaign.**

| Tracer | Injected activity WPDE-1 (Bq) | Injected activity WPDE-2 (Bq) | Decay mode | Half-life |
|---|---|---|---|---|
| HTO | $17.1(\pm0.3) \times 10^6$ | $31.1(\pm0.7) \times 10^6$ | $\beta^-$ | 12.3 y |
| Na-22 | $1.38(\pm0.03) \times 10^6$ | $2.04(\pm0.09) \times 10^6$ | EC, $\beta^+$ | 2.6 y |
| Cl-36 | $1.25(\pm0.03) \times 10^6$ | $5.09(\pm0.07) \times 10^6$ | EC, $\beta^-$ | $3.01 \times 10^5$ y |
| Sr-85 | | $4.12(\pm0.11) \times 10^6$ | EC, g | 64.8 d |
| Ba-133 | | $2.46(\pm0.12) \times 10^6$ | g, $\beta^-$ | 10.5 y |

### 2.3.4 Water chemistry

Synthetic groundwater has been injected throughout the WPDE experiments. The recipe of this synthetic groundwater has been designed to match the groundwater composition in the rock surrounding the ONKALO tunnel, at the corresponding location of the WPDE experiments. The recipe was initially made to match groundwater composition data from a flowing fracture in drillhole ONK-KR14 (drillhole section 28.1–29.6 m), which is also drilled from the REPRO niche parallel to drillhole ONK-PP320. The ONKALO tunnel and drillholes ONK-KR14, as well as ONK-KR13, are shown in Figure 2-6.

The recipe of the synthetic groundwater is provided in Table 2-3, together with measured groundwater compositions in drillholes ONK-KR13, ONK-KR14, and ONK-PP319. The latter drillhole is drilled in close proximity to, and parallel with, drillhole ONK-PP323 in which the WPDE campaign is carried out (cf. Figure 1-2). The composition of the actually produced synthetic groundwater was measured just prior to the initiation of WPDE-1, and measurement data are provided in Table 2-4. The provided groundwater composition data are primarily intended as general background information, and do not necessarily need to be included in the modelling for Task 9A.
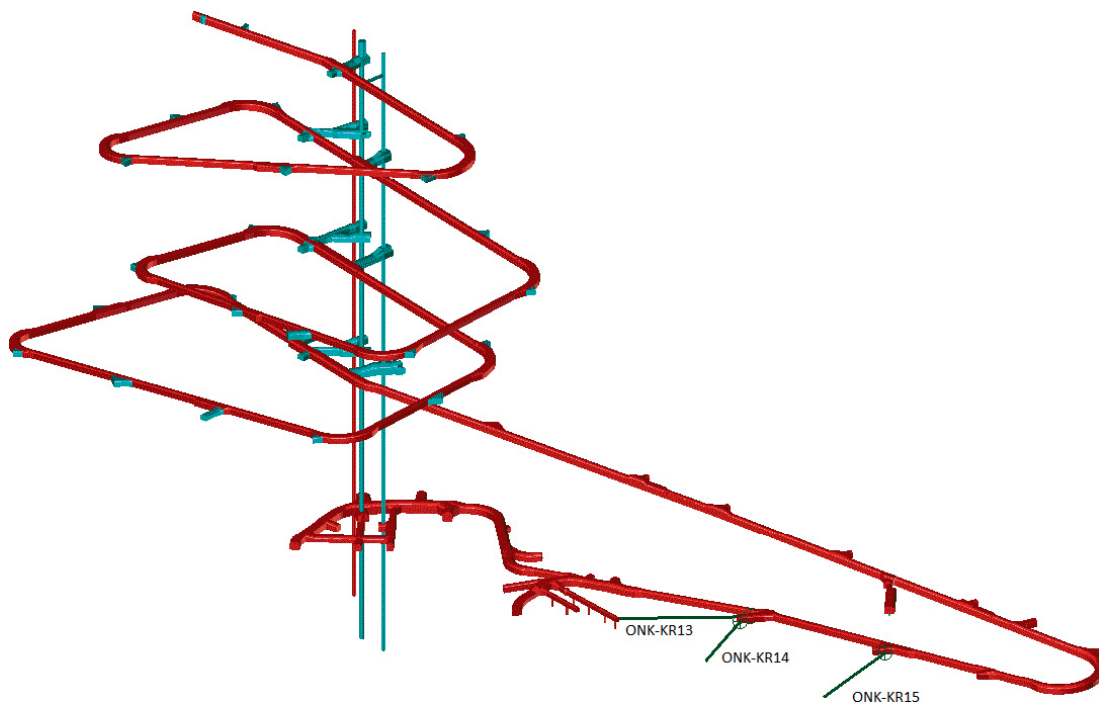


***Figure 2-6.*** *The ONKALO tunnel, also showing drillholes ONK-KR13 and ONK-KR14 that are drilled from the Investigation niche 5 (the REPRO niche). Image reproduced from Toropainen (2012).*

**Table 2-3. Recipe of synthetic groundwater and groundwater compositions in nearby drillholes.**

| ACTIVITY_ID | 55727 | 55731 | 57518 | 72108 | Synthetic groundwater, recipe | Unit |
|---|---|---|---|---|---|---|
| HOLE_ID | ONK-KR13 | ONK-KR13 | ONK-KR14 | ONK-PP319 | | |
| DATE_START | 25.1.2011 | 28.2.2011 | 20.6.2011 | 21.2.2013 | | |
| LENGTH_FROM | 81.1 | 89 | 28.1 | | – | |
| LENGTH_TO | 82.1 | 120 | 29.6 | | – | |
| SAMPLE_ID | 1834 | 1835 | 1964 | 72108 | – | |
| WATER_TYPE | Na-Cl | Na-Cl | Na-Cl | Na-Cl | – | |
| Sodium fluorescein | < 1 | < 1 | 1.2 | < 1 | – | µg/l |
| pH | 7.9 | 8.1 | 7.0 | 7.9 | 7.0 | |
| Conductivity | 14.99 | 22.1 | 15.33 | 17.27 | – | mS/cm |
| Iron, $Fe^{2+}$ | < 0.02 | < 0.02 | – | < 0.02 | – | mg/l |
| Total acidity, NaOH uptake | 0.2 | 0.06 | 0.06 | – | – | mmol/l |
| Total dissolved solids | 8 475 | 12 620 | 8 601 | 9 559 | – | mg/l |
| Bromide, Br | 37 | 59.3 | 33 | 34 | 33 | mg/l |
| Calcium, Ca | 780 | 1 600 | 520 | 690 | 520 | mg/l |
| Carbonate alkalinity, HCl uptake | < 0.05 | < 0.05 | < 0.05 | < 0.05 | – | mmol/l |
| Dissolved inorg. Carbon | 2 | 2.2 | 2 | 8.9 | – | mg/l |
| Iron, Fe | 12 | 35 | 11 | – | – | µg/l- |
| Nitrogen, N total | 1.1 | 0.54 | 6 | – | – | mg/l |
| Non Purgeable Organic Carbon | 11 | 7.2 | 50 | 2.1 | – | mg/l |
| Potassium, K | 7.5 | 9.2 | 7.9 | 14 | 7.9 | mg/l |
| Strontium, Sr | 15.2 | 6.7 | 4.5 | 5.7 | 4.5 | mg/l |
| Sulphide, $S^{2-}$ | < 0.02 | < 0.02 | – | < 0.02 | – | mg/l |
| Magnesium, Mg | 19 | 33 | 35 | 34 | 35 | mg/l |
| Sulphur, S total | 1.6 | 1 | 1.4 | – | – | mg/l |
| Total alkalinity, HCl uptake | 0.15 | 0.14 | 0.2 | 0.73 | – | mmol/l |
| Bicarbonate, $HCO_3$ | 9.2 | 8.5 | 12.2 | 45 | 12.2 | mg/l |
| Fluoride, F | 1.9 | 1.6 | 1.5 | – | 1.5 | mg/l |
| Nitrite, $NO_2$ | < 0.01 | < 0.01 | 0.035 | – | – | mg/l |
| Silicate, $SiO_2$ | 5.6 | 5.9 | 6.2 | 5.4 | 13 | mg/l |
| Sodium, Na | 2 480 | 2 980 | 2 770 | 2 840 | 2 670 | mg/l |
| Sulphate, $SO_4$ | < 0.1 | 0.2 | 0.3 | 1.1 | 0.3 | mg/l |
| Charge balance, calculated from $HCO_3$ | 1.28 | −2.64 | 0.66 | −1.85 | – | % |
| Ammonium, $NH_4$ | 0.02 | 0.02 | 0.10 | – | – | mg/l |
| Chloride, Cl | 5 120 | 7 910 | 5 210 | 5 890 | 5 130 | mg/l |
| Nitrate, $NO_3$ | < 0.02 | < 0.02 | 0.086 | – | – | mg/l |
| Uranium, U | < 0.1 | < 0.1 | 0.14 | – | – | µg/l |
| Colour | < 5 | < 5 | < 5 | – | – | mg/l Pt |
| Turbidity | < 5 | < 5 | < 5 | – | – | FTU |
| Deuterium, $^2H$ | – | – | – | −56.5 | – | ‰ VSMOW |
| Oxygen-18, $^{18}O$ | – | – | – | −10.19 | – | ‰ VSMOW |

**Table 2-4. Measurement data on the actually produced synthetic groundwater, prior to injection in WPDE-1.**

| Bromide, Br | Calcium, Ca | Potassium, K | Strontium, Sr | Magnesium, Mg | Fluoride, F |
|---|---|---|---|---|---|
| 31.9 mg/l | 474 mg/l | 9.87 mg/l | 4.19 mg/l | 27.7 mg/l | 0.86 mg/l |

| Silicate, $SiO_2$ | Sodium, Na | Sulphate, $SO_4$ | Chloride, Cl | Manganese, Mn | Nickel, Ni |
|---|---|---|---|---|---|
| 10* mg/l | 2 580 mg/l | 2.87 mg/l | 5 410 mg/l | 3.39 µg/l | 4.6 µg/l |

* Reported as Si, recalculated to $SiO_2$

It should be noted that the redox conditions in the experimental section likely deviated from the natural redox conditions at the site. This is because the redox conditions of the synthetic groundwater were not controlled, or measured, prior to injection. Given the handling of the synthetic groundwater it is judged, by the personnel performing the experiments, to be oxic in nature. Moreover, the neutral pH that was prescribed for the synthetic groundwater can be assumed to quickly have increased to be comparable to what was measured in drillhole ONK-PP319 (see Table 2-3), due to fast buffering reactions with the rock.

### 2.3.5 Detection of tracers

The WPDE tracer cocktails contain radionuclides that emit gamma and/or beta radiation. Na-22, Sr-85 and Ba-133 are gamma active, and could therefore be detected by online gamma measurements using Na(Tl)I-scintillation detection in addition to laboratory analyses of collected samples. At the laboratory, the gamma emitting radiotracers Na-22, Sr-85 and Ba-133 were detected by gamma spectroscopy while HTO and Cl-36 were detected by Liquid Scintillation Counting (LSC). Chemical separation was necessary before measuring Cl-36 by LSC, due to interference from Na-22 beta emission.

For WPDE-1, online detection was carried on between the dates March 8th and August 16th, 2012. Water samples were taken for subsequent analysis in the laboratory between the dates March 8th and August 21st, 2012.

For WPDE-2, online detection was carried on between the dates January 23rd, 2013 and August 13th, 2014. Water samples were collected for subsequent analysis in the laboratory between the dates January 21st, 2013 and July 7th, 2014.

During the course of the performed WDPE experiments, two of the tracers reached activities below the detection limits. For samples analysed in the laboratory this was the case for Cl-36 in WPDE-1. Concerning the online detection, Sr-85 reached the detection limit in the WPDE-2 campaign.

## 2.4 The REPRO laboratory campaign and other supporting data

### 2.4.1 Rock type, lithology, and mineralogy

The drill cores of the concerned drillholes at the REPRO niche have been subjected to geological core logging. This is detailed in Toropainen (2012) where a large amount of quantitative core logging data is tabulated. Concerning the intact rock matrix, the rock type, lithology, foliation and degree of weathering have been documented. In addition, a number of fracture related indicators, as well as other indicators, have been logged. Toropainen (2012) also provides photos of the drill cores concerned. The report is thus recommended reading for understanding the general geological settings of the REPRO experiments.

The entire drill core of the WPDE drillhole is described as consisting of sparsely fractured unweathered/unaltered rock. In the two meters of drill core closest to the tunnel, the dominant rock type is DGN (migmatitic metamorphic gneiss; subdivision diatexitic gneiss). Thereafter, the dominant rock type is VGN (migmatitic metamorphic gneiss; subdivision veined gneiss) for four meters after which PGR (coarse-grained pegmatitic granite) dominates for the next 12 meters. At the end of the drillhole, where the WPDE experimental section is located, the dominant rock type is VGN. While the PGR is generally massive (non-foliated), the VGN typically exhibits a banded foliation of weak foliation intensity. The entire drill core of ONK-PP323 is displayed in Figure 2-7.
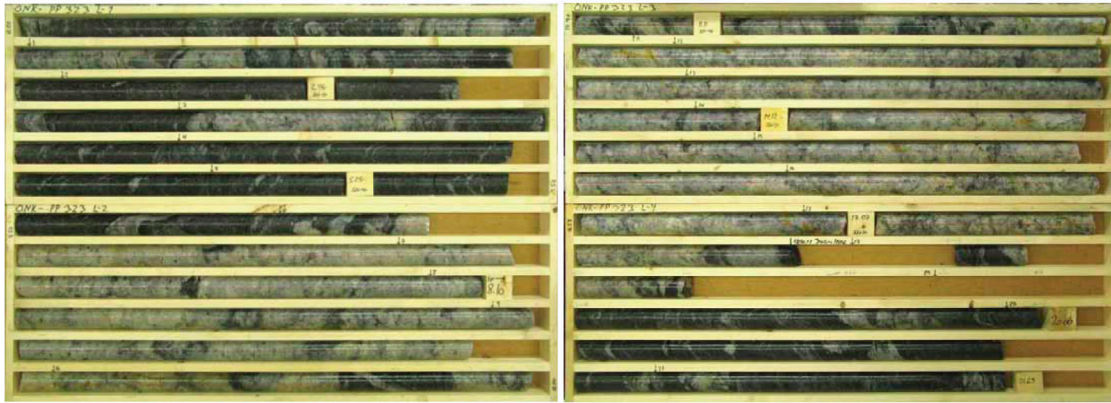
**Figure 2-7.** *Photos of the entire drill core of drillhole ONK-PP323. Some drill core pieces were taken to the laboratory prior to taking the photos. The drill core is wetted. Reproduced from Toropainen (2012).*

**Clarification or comment**
Photos of rock samples in Figure 2-7 and Figure 2-8 are given in higher resolution in Appendix 6.

The lithology of drillhole ONK-PP323, as descried by Toropainen (2012), is summarised in Table 2-5.

**Table 2-5. Lithology of drillhole ONK-PP323 from geological core logging. From Toropainen (2012).**

| Drillhole section (m) | Rock type | Fraction of leucosome (%) | Desciption |
|---|---|---|---|
| 0.00–1.85 | DGN | 70 | Irregular to weakly banded DGN with cordierite. Unweathered/ unaltered. |
| 1.85–6.20 | VGN | 40 | Weakly to moderately banded VGN with sillimanite, cordierite in leucosome. Unweathered/unaltered. |
| 6.20–17.88 | PGR | | Pale coloured massive coarse-grained PGR with garnet. Few cordierite patches. Low amount of mica. Few mica rich stripes. Unweathered/unaltered. |
| 17.88–21.65 | VGN | 40 | Weakly to moderately banded VGN with sillimanite, cordierite in leucosome. Shear bands of sillimanite and biotite. Unweathered/ unaltered. |

The description given in Toropainen (2012) is coarsely resolved, compared to the scale of interest for the WPDE campaign. Therefore, a more detailed description focusing on the experimental section (17.95–19.85 m) is provided below. The section is predominantly surrounded by the rock type VGN, which is from this point referred to as veined gneiss. However, a fraction of the drill core, such as the section from about 18.30–18.45 m, is predominantly of the rock type PGR; from this point referred to as pegmatitic granite. It has been roughly estimated[3] that little over 90 % of the experimental section is surrounded by veined gneiss, while a little less than 10 % is surrounded by pegmatitic granite. This is indicated from the photos of the local drill core, provided in Figure 2-8, as well as from the drillhole images provided in Figure 2-9 and Figure 2-10. For the purpose of Task 9A, it can be assumed that 90 % of the experimental section is surrounded by veined gneiss and 10 % by pegmatitic granite.

---

[3] Estimation made by Mikko Voutilainen at Helsinki University.

***Figure 2-8.*** *Drill core from the WPDE experimental section 17.95–19.85 m. Missing piece from 17.90–18.20 m was taken to the laboratory experiments before logging of the drill core, and is shown separately in the lower photo. All displayed fractures in the experimental section are judged to be mechanically induced (broken) in the core drilling, and there is no natural fracture. Photos from Helsinki University.*

By studying the drill core from drillhole section 19.42 m to 20.22 m, corresponding to about 40 % of the WPDE experimental section, it was estimated that the maximum foliation angle ranges from 60° to 90° relative to the axis of the drill core. The foliation of this drill core section fluctuates considerably since it consists of migmatitic rock; however, the main direction of the foliation is almost perpendicular to the drill core axis. The foliation estimate was made at Helsinki University. The pegmatitic granite of the section can be considered non-foliated.
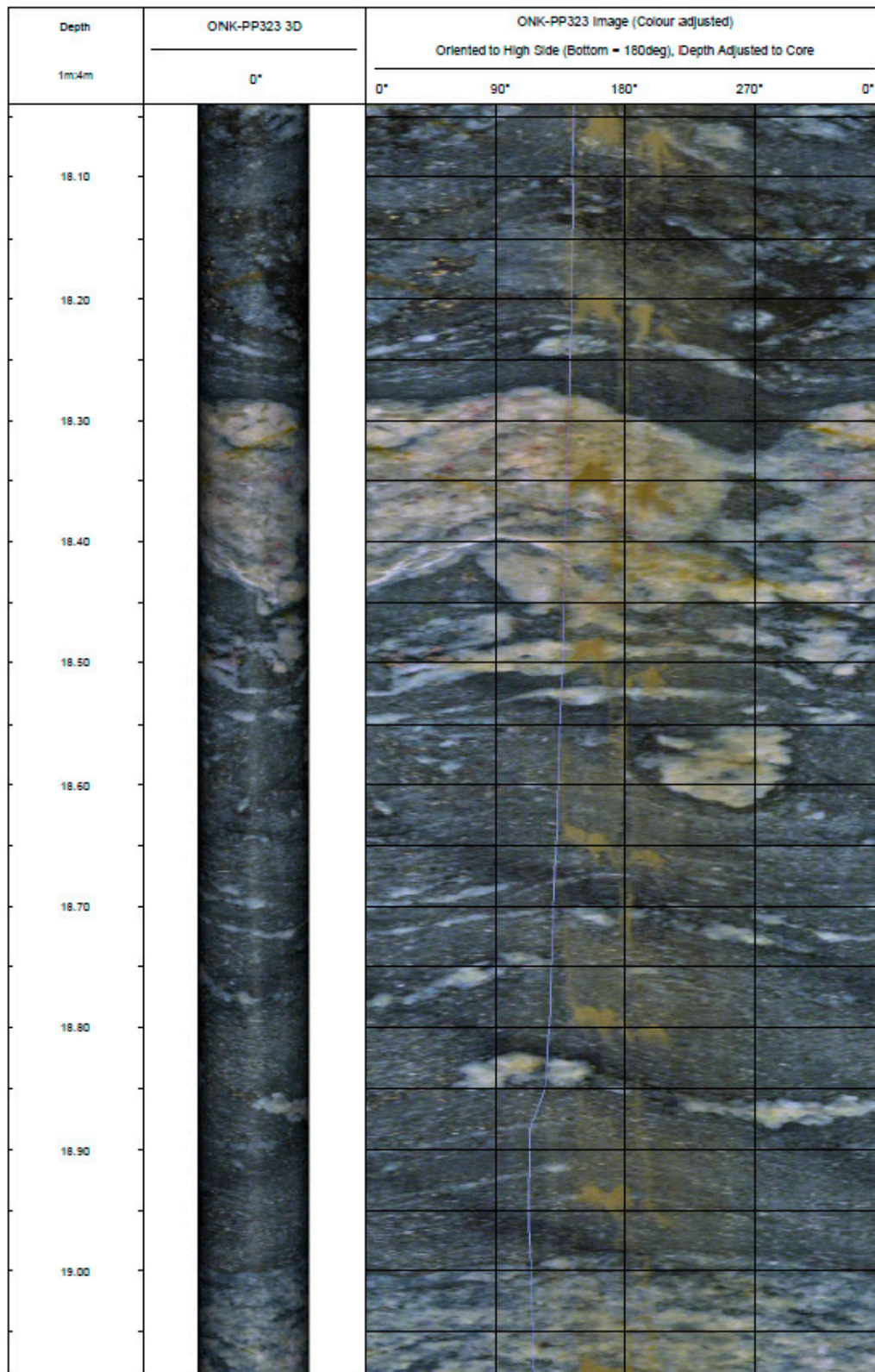
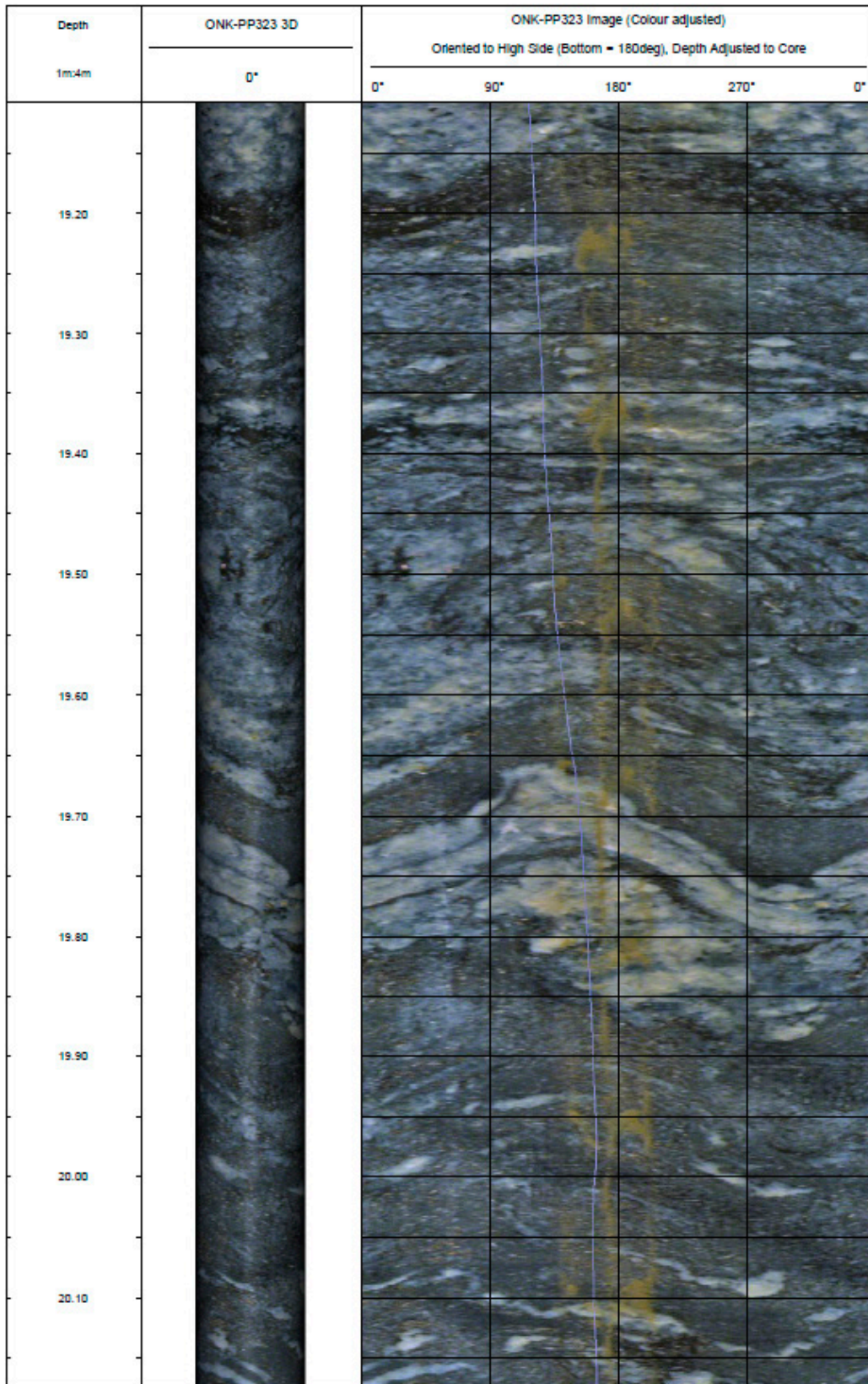***Figure 2-9.*** *Image from drillhole camera covering one part of the WPDE experimental section.*

**Figure 2-10.** *Image from drillhole camera covering the other part of the WPDE experimental section.*

Rock samples have been collected from the drill core of ONK-PP323, as well as from other drill-holes of the REPRO niche, for mineralogical analysis in the laboratory. Five samples from drillhole ONK-PP323 (cf. Table 2-6) were analysed by using polarized microscopy and point counting, with 500 points per sample (Ikonen et al. 2015). All five rock samples were classified as veined gneiss. By averaging the results from these thin sections, an average mineralogy of the veined gneiss rock matrix of the drillhole section has been produced and is shown in Figure 2-11.

---

**Clarification or comment**

At the time of issuing the first version of the Task 9A description, the Posiva working report 2014-68 had not yet been published. At the time the preliminary reference was:

**Sammaljärvi J, Ikonen J, Voutilainen M, Kuva J, Lindberg A, Siitari-Kauppi M, Timonen J, 2015.** Investigation of Rock Matrix Retention Properties. Supporting laboratory studies I: Mineralogy, porosity, and pore structure. POSIVA Working Report 2014-68, Posiva Oy, Finland.

This reference was used in the task description, also in the final version, and in the text (Sammaljärvi et al. 2015) was referred to. When the report was finally pubished, the reference was modified to:

**Ikonen J, Sammaljärvi J, Siitari-Kauppi M, Voutilainen M, Lindberg A, Kuva J, Timonen J, 2015.** Investigation of Rock Matrix Retention Properties Supporting Laboratory Studies I: Mineralogy, Porosity, and Pore Structure. POSIVA Working Report 2014-68, Posiva Oy, Finland.

In this present report, we have chaged the text of the task description to avoid the erronerous reference. Hence, all instances previously refering to (Sammaljärvi et al. 2015) now refer to (Ikonen et al. 2015).

---

Although the experimental section is also surrounded by pegmatitic granite, no such samples were collected for mineralogical analysis from drillhole ONK-PP323. However, pegmatitic granite samples were collected from the closely located drillhole ONK-PP318, which is drilled parallel to drillhole ONK-PP323. By analysing several thin sections, and averaging the results, the averaged mineralogical composition of the pegmatitic granite samples from ONK-PP318 was obtained (cf. Figure 2-12). In Task 9, this mineralogical composition is suggested to be used as a proxy of the mineralogical composition of the pegmatitic granite surrounding the WPDE experimental section.
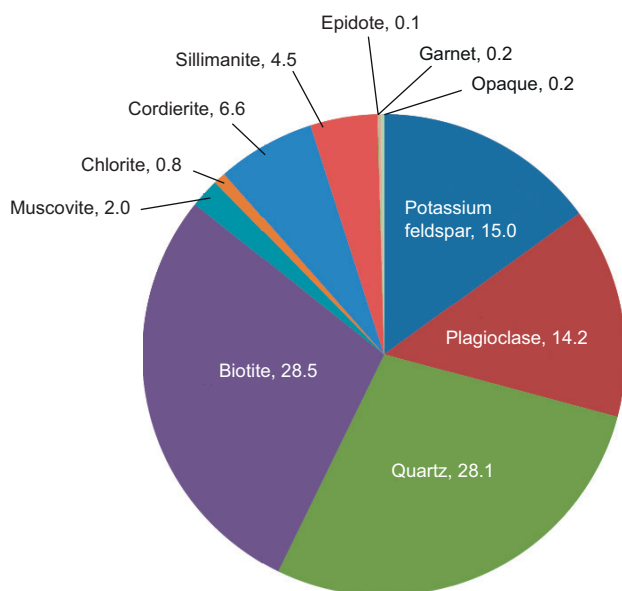


*Figure 2-11.* *Average mineralogical composition of veined gneiss samples from the WPDE experimental section of ONK-PP323. Diagram reproduced from Ikonen et al. (2015).*
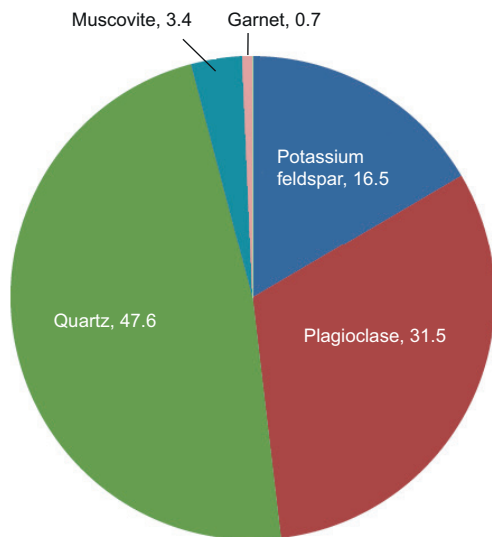
*Figure 2-12.* *Average mineralogical composition of pegmatitic granite from several samples from drillhole ONK-PP318. Diagram reproduced from Ikonen et al. (2015).*

## 2.4.2 Rock samples of the REPRO laboratory campaign

Rock samples have been collected from the drill core corresponding to the WPDE experimental section, as well as from other sections and drillholes of the REPRO niche. As described above, the experimental section is surrounded by two main rock types, where the dominant rock type is veined gneiss and the subordinate rock type is pegmatitic granite. The rock samples from ONK-PP323, which have been analysed in the laboratory in respect to conventional rock matrix transport and retention parameters, have all been of the rock type veined gneiss. To also provide data on pegmatitic granite, data from the drillhole section 13.92 to 15.84 m of ONK-PP318 are provided.

One outcome of writing this task description is the revelation that the labelling of laboratory samples was partly incorrect in the earlier documents[4] (Kuva et al. 2015, Ikonen et al. 2015). The labelling should reflect the position in the drillhole from where the sample is taken. The labelling has now been double-checked and updated.

> **Clarification or comment**
> The report (Ikonen et al. 2015) still contains incorrect sample coordinates in Table 3 relating to results from Ar-pycnometry. All porosities have been compared to the now published version and they are in agreement, except for one occasion where one significant digit less is used in the report (1.2 vs 1.24 % for sample ONK-PP323: 18.83–18.89 m in Table 2-8).

### ONK-PP323

14 cylindrical rock samples, between 1 and 5 cm in length, have been sawed from the drill core section 18.02 to 19.17 m for subsequent analysis in the laboratory. This can be compared with the drillhole section of the WPDE experiments, which is from 17.95 to 19.85 m. This means that about half of the drill core from the experimental section has been used for sawing rock samples for subsequent analysis.

---

[4]  Ikonen et al. (2015) is presently being prepared for printing. Therefore, it is unclear if the errors found in the sample labelling can still be corrected for. Presently there is no plan to correct the errors in Kuva et al. (2015).

Five of the 14 samples have been divided into two equal parts A and B by sawing a straight cut along the drillhole axis. Such samples have been used for ^{14}C-PMMA autoradiography for porosity characterisation and thin sections for mineralogical analysis. The cylindrical samples have been used for:

- Water phase through-diffusion experiments.
- Gas phase measurements of porosity, effective diffusivity, and permeability.
- Porosity measurements by water gravimetry.
- Effective diffusivity measurements by electrical methods.
- Batch sorption experiments, after grinding and sieving.

The links between different samples and applied laboratory methods are provided in Table 2-6. Photos of the sampled drill core section are provided in Figure 2-8.

**Table 2-6. Partition of drill core of ONK-PP323 into rock samples, based on partition diagrams in Ikonen et al. (2015) as well as on recently updated information (i.e. the sample labelling is updated). Water gravimetry analyses were performed on cylindrical samples and after partition-ing of the sample, autoradiography and thin section analyses were performed on the respective A and B samples.**

| Drillhole lengths (m) | Cylindrical sample | Parted A sample | Parted B sample |
| --- | --- | --- | --- |
| 18.02–18.07 | Gas phase methods | | |
| 18.12–18.15 | Gas phase methods | | |
| 18.71–18.74 | | Autoradiography | Thin section |
| 18.75–18.78 | Water gravimetry | Autoradiography | Thin section |
| 18.78–18.83 | Electrical methods Water gravimetry | | |
| 18.83–18.89 | Gas phase methods | | |
| 18.89–18.94 | Water phase through-diffusion | | |
| 18.94–18.96 | Water phase through-diffusion | | |
| 18.96–18.98 | Water phase through-diffusion | | |
| 19.02–19.07 | Gas phase methods | | |
| 19.07–19.10 | Water gravimetry | Autoradiography | Thin section |
| 19.10–19.12 | | Autoradiography | Thin section |
| 19.12–19.17 | | Autoradiography | Thin section |
| 19.17–19.19 | Batch sorption | | |

In addition, an 80 cm long intact section of the drill core has been used in the laboratory for an advection-diffusion tracer test that can be regarded as a mirror replicate experiment to the WPDE campaign. In this experiment, the intact drill core is surrounded by an inert and non-porous tube of a slightly larger radius. This creates an annular slot around the drill core in which a steady state water flow and a tracer pulse is injected, much as in the WPDE campaign.

### ONK-PP318

Eight cylindrical rock samples, between 1 and 5 cm in length, have been sawed from the drill core section 13.92 to 15.84 m for subsequent analysis in the laboratory. Three of the eight samples have been divided into two equal parts A and B, one by sawing normal to the drillhole axis, creating two cylindrical subsamples, and two samples were divided by sawing a straight cut along the drillhole axis, resulting in totally six A and B subsamples. The subsamples have been used for ^{14}C-PMMA autoradiography and thin sections. The links between different samples and applied laboratory methods are provided in Table 2-7. A photo of part of the sampled drill core section is provided in Figure 2-13.

**Table 2-7. Partition of drill core of ONK-PP318 into rock samples, based on partition diagrams in Ikonen et al. (2015), as well as on recently updated information (i.e. the sample labelling is updated). Water gravimetry analyses were performed on the cylindrical sample and after partitioning of the sample, autoradiography and thin section analyses were performed on the respective A and B samples.**

| Drillhole lengths (m) | Cylindrical sample | Parted A sample | Parted B sample |
|---|---|---|---|
| 13.92–13.95 | Gas phase methods | | |
| 13.97–14.02 | Gas phase methods | | |
| 15.62–15.65 (parallel cut) | | Autoradiography | Thin section |
| 15.65–15.66 (tangentially cut) | | Autoradiography | Thin section |
| 15.66–15.69 (parallel cut) | Water gravimetry | Autoradiography | Thin section |
| 15.69–15.74 | Electrical methods Water gravimetry | | |
| 15.74–15.79 | Gas phase methods | | |
| 15.79–15.84 | Water phase through-diffusion | | |

### 2.4.3 Porosity

This section provides quantitative data on porosities obtained on the drill core samples described in Section 2.4.2 by water gravimetry, argon pycnometry (which is a gas phase method) and $^{14}$C-PMMA autoradiography. The data are reproduced from Kuva et al. (2015) and Ikonen et al. (2015), in which descriptions of the experimental procedures and other details can be found. (Ikonen et al. 2015) is recommended reading for better understanding of the rock matrix around the WPDE experimental section, as well as the general surroundings of the REPRO niche. The porosity data are tabulated in Table 2-8.
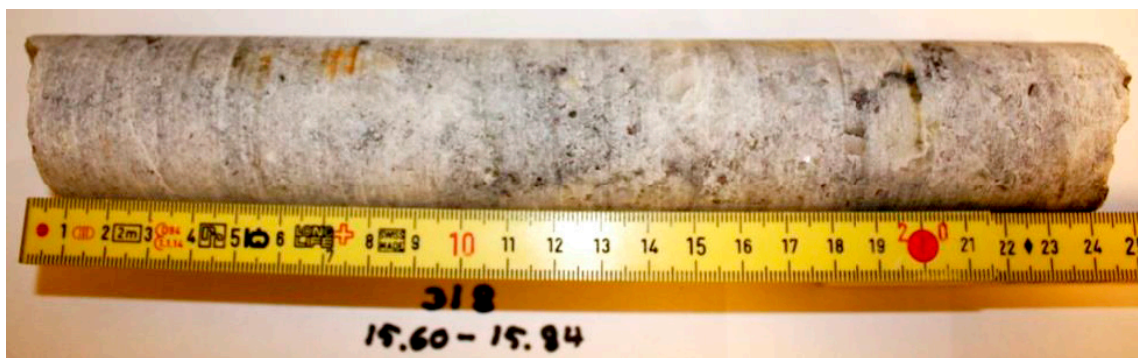


***Figure 2-13.*** *Photo of the drill core section ~15.60–15.86 m in ONK-PP318. Excerpt of image in Ikonen et al. (2015).*

**Table 2-8. Rock matrix porosities obtained in the REPRO laboratory campaign. Data are reproduced from Ikonen et al. (2015) and, where noted, from Kuva et al. (2015). The sample labelling is updated.**

| Drillhole | Drillhole lengths (m) | Porosity (%) | Method |
|---|---|---|---|
| ONK-PP323 | 18.02–18.07 | 0.82 ± 0.13 | Ar-pycnometry (Kuva et al. 2015) |
| ONK-PP323 | 18.12–18.15 | 2.7 ± 0.3 | Ar-pycnometry (Kuva et al. 2015) |
| ONK-PP323 | 18.71–18.74 | 1.20 ± 0.12 | Autoradiography |
| ONK-PP323 | 18.75–18.78 | 0.64 ± 0.16<br>0.40 ± 0.04 | Water gravimetry<br>Autoradiography |
| ONK-PP323 | 18.78–18.83 | 0.85 ± 0.23 | Water gravimetry |
| ONK-PP323 | 18.83–18.89 | 1.24 ± 0.14 | Ar-pycnometry |
| ONK-PP323 | 19.02–19.07 | 0.65 ± 0.05 | Ar-pycnometry |
| ONK-PP323 | 19.07–19.10 | 0.45 ± 0.12<br>0.50 ± 0.05 | Water gravimetry<br>Autoradiography |
| ONK-PP323 | 19.10–19.12 | 0.70 ± 0.07 | Autoradiography |
| ONK-PP323 | 19.12–19.17 | 0.30 ± 0.03 | Autoradiography |
| ONK-PP323 | 20.89–20.91 | 0.19 ± 0.08 | Ar-pycnometry (Kuva et al. 2015) |
| ONK-PP318 | 13.92–13.95 | 0.6 ± 0.3 | Ar-pycnometry (Kuva et al. 2015) |
| ONK-PP318 | 13.97–14.02 | 0.63 ± 0.05 | Ar-pycnometry (Kuva et al. 2015) |
| ONK-PP318 | 15.62–15.65 | 0.30 ± 0.04 | Autoradiography |
| ONK-PP318 | 15.65–15.66 | 0.70 ± 0.07 | Autoradiography |
| ONK-PP318 | 15.66–15.69 | 0.42 ± 0.12<br>0.50 ± 0.05 | Water gravimetry<br>Autoradiography |
| ONK-PP318 | 15.69–15.74 | 0.49 ± 0.14 | Water gravimetry |
| ONK-PP318 | 15.74–15.79 | 0.44 ± 0.05 | Ar-pycnometry |

## 2.4.4 Rock matrix effective diffusivity and permeability

This section provides numerical data of the effective diffusivity obtained by water-phase through-diffusion measurements. These data have not been published and, hence, details in the experimental setup and performance are not provided for Task 9A. What can be said is that the active tracers HTO and Cl-36 have been used simultaneously in trace amounts in a synthetic groundwater background. The experiments were carried out under ambient conditions normal for the laboratory (at room temperature and atmospheric pressure) in standard through-diffusion cells. Data are provided for three veined gneiss samples from ONK-PP323 and one pegmatitic granite sample from ONK-PP318 in Table 2-9.

Concerning the uncertainty estimates in Table 2-9 are given as 1-sigma standard deviations.

**Table 2-9. Rock matrix effective diffusivity obtained by water phase through-diffusion experiments at Helsinki University (unpublished data).**

| Drillhole | Drillhole lengths (m) | Tracer | Effective diffusivity, $D_e$ (m²/s) | Rock capacity factor, a (–) |
|---|---|---|---|---|
| ONK-PP323 | 18.89–18.94 | HTO | $(2.5 ± 0.3) \cdot 10^{-13}$ | 0.0070 ± 0.0005 |
| ONK-PP323 | 18.94–18.96 | HTO<br>Cl-36 | $(1.6 ± 0.3) \cdot 10^{-13}$<br>$(0.05 ± 0.03) \cdot 10^{-13}$ | 0.011 ± 0.001<br>0.0002 ± 0.0005 |
| ONK-PP323 | 18.96–18.98 | HTO<br>Cl-36 | $(1.4 ± 0.2) \cdot 10^{-13}$<br>$(0.05 ± 0.03) \cdot 10^{-13}$ | 0.011 ± 0.001<br>0.00015 ± 0.0005 |
| ONK-PP318 | 15.79–15.84 | HTO<br>Cl-36 | $(5.7 ± 0.6) \cdot 10^{-13}$<br>$(5 ± 1) \cdot 10^{-13}$ | 0.013 ± 0.001<br>0.013 ± 0.002 |

**Clarification or comment**
The data in Table 2-9 will be published in Voutilainen et al. (2018 b).

Here, the effective diffusivity, $D_e$ (m$^2$/s) and rock capacity factor, $\alpha$ (–) are parameters of Fick's second law of diffusion in porous media, together with the tracer concentration, $C$ (mol/m$^3$), diffusion distance, $x$ (m), and time, $t$ (s):

$$\alpha \frac{\partial C}{\partial t} = D_e \frac{\partial^2 C}{\partial x^2}$$

(2-1)

In addition, the effective diffusivity and permeability of several rock samples from the REPRO rock volume have been determined by He gas-phase methods. Here, a rock sample is dried for a substantial period of time and is subsequently placed in a nitrogen gas environment. By introducing helium and measuring the helium flow through the rock sample, the gas phase effective diffusivity and permeability can be measured. This is done in separate runs using different pressure boundary conditions. Details of the experimental campaign as well as methodological issues are described in Kuva et al. (2015). Gas-phase results have been converted to effective diffusivities in the water phase by using a conversion factor of 11 600 (Kuva et al. 2015). In general, the conversion is adequate, although if the main transport routes include non-negligible amounts of nanometer scale apertures, gas-phase measurements may underestimate the effective diffusion coefficient in water phase.

The data in Table 2-10 are reproduced from Kuva et al. (2015), although the sample labelling is updated. As can be seen from the Table, the data correspond to a larger group of rock samples than is described in Section 2.4.2, including results for samples having a foliation that is parallel to the axis of the drill core (ONK-PP324, ONK-PP326, and ONK-PP327). These samples are, however, from the right-hand side of the REPRO niche, whereas ONK-PP323 is located on the left-hand side. The porosities given in the table are obtained by the Ar-pycnometry method.

**Table 2-10. Measured porosities, effective diffusion coefficients, and permeabilities, as well as rock types of the REPRO samples. Error estimates are given as ±1 σ. Data are reproduced from Kuva et al. (2015, Table 2) but sample labelling has been updated and sample foliation is added for borehole ONK PP323-PP327.**

| Sample | Porosity ε [%] | Gas diffusion $D_e \times 10^{-9}$ (m$^2$/s) | Permeability $k \times 10^{-19}$ (m$^2$) | Rock type | Foliation |
|---|---|---|---|---|---|
| ONK-PP318 13.92–13.95 | 0.6 ± 0.3 | 8.2 ± 0.8 | 860 ± 70 | PGR | – |
| ONK-PP318 13.97–14.02 | 0.63 ± 0.05 | 3.2 ± 0.6 | 64 ± 1 | PGR | – |
| ONK-PP318 15.74–15.79 | 0.44 ± 0.14 | 5.7 ± 0.5 | 5.9 ± 0.2 | PGR | – |
| ONK-PP318 16.87–16.92 | 0.70 ± 0.05 | 6.7 ± 0.7 | 9 ± 1 | VGN | – |
| ONK-PP319 9.16–9.21 | 0.34 ± 0.14 | 2.0 ± 0.2 | 1.3 ± 0.2 | VGN | – |
| ONK-PP319 9.47–9.52 | 2.4 ± 0.2 | 1.4 ± 0.3 | 6 ± 1 | VGN | – |
| ONK-PP319 12.46–12.51 | 0.77 ± 0.15 | 2.8 ± 0.2 | 1.1 ± 0.1 | VGN | – |
| ONK-PP319 12.70–12.75 | 0.6 ± 0.14 | 3.8 ± 0.5 | 49 ± 5 | VGN | – |
| ONK-PP321 10.26–10.31 | 0.55 ± 0.14 | 1.9 ± 0.7 | 39 ± 1 | VGN | – |
| ONK-PP323 18.02–18.07 | 0.82 ± 0.13 | 3 ± 1 | 11.3 ± 0.1 | VGN | ⊥ |
| ONK-PP323 18.12-18.15 | 2.7 ± 0.3 | 5.4 ± 0.5 | 53 ± 5 | VGN | ⊥ |
| ONK-PP323 18.83–18.89 | 1.24 ± 0.14 | 0.58 ± 0.05 | 0.2 ± 0.1 | VGN | ⊥ |
| ONK-PP323 19.02–19.07 | 0.7 ± 0.2 | 0.50 ± 0.05 | 0.14 ± 0.02 | VGN | ⊥ |
| ONK-PP323 20.89–20.91 | 0.19 ± 0.08 | 0.75 ± 0.1 | 0.9 ± 0.1 | VGN | ⊥ |
| ONK-PP324 11.49–11.51 | 1.02 ± 0.05 | 0.8 ± 0.1 | 3.6 ± 0.4 | VGN | ∥ |
| ONK-PP326 11.42–11.44 | 2.9 ± 0.1 | 1.4 ± 0.1 | 2.0 ± 0.2 | VGN | ∥ |
| ONK-PP326 11.72–11.74 | 0.68 ± 0.08 | 1.1 ± 0.1 | 9.5 ± 0.2 | VGN | ∥ |
| ONK-PP327 12.05–12.07 | 0.7 ± 0.1 | 1.2 ± 0.1 | 0.2 ± 0.1 | VGN | ∥ |

### 2.4.5    Sorption partitioning coefficients

This section provides quantitative data on sorption partitioning coefficients for the tracers Na-22, Sr-85, and Ba-133, based on batch experiments. These data have not been published and, hence, details in the experimental setup and performance are not provided for Task 9A. What can be said is that multiple samples that were either classified as "pure" veined gneiss or "pure" pegmatitic granite were taken from different drill core locations. The samples were crushed/ground and sieved and the size fraction < 0.3 mm was used for batch experiments using synthetic groundwater as background. The sorption partitioning coefficients are provided in Table 2-11.

**Table 2-11. Sorption partitioning coefficients obtained in batch experiments on crushed rock of different size fractions by Helsinki University (unpublished data). Uncertainty estimates represent one standard deviation.**

| Radionuclide | Rock type | Grain size (mm) | Sorption partitioning coefficients ($m^3$/kg) |
|---|---|---|---|
| Na-22 | Veined gneiss | Average over < 0.3, 0.3 < D > 0.85 and 0.85 < D > 2 | 0.0013 ± 0.0003 |
| | Pegmatitic granite | < 0.3 | 0.0008 ± 0.0003 |
| Sr-85 | Veined gneiss | < 0.3 | 0.0011 ± 0.0003 |
| | Pegmatitic granite | < 0.3 | 0.0011 ± 0.0003 |
| Ba-133 | Veined gneiss | < 0.3 | 0.06 ± 0.02 |
| | Pegmatitic granite | < 0.3 | 0.08 ± 0.02 |

Concerning the two other tracers of interest for Task 9A, HTO and Cl-36, they are normally treated as being non-sorbing. This is also the recommendation of the personnel[5] at Helsinki University involved in the experimental campaign, based on their experience from the water phase through diffusion experiments where HTO and Cl-36 are used as tracers. The non-sorbing behaviour of HTO and Cl-36 is indicated by the low rock capacity factor in Table 2-9.

## 2.5    Expected outcome and reporting

### 2.5.1    Comparable breakthrough curves

The main result of the predictive modelling of Task 9A is breakthrough curves for all active tracers involved in the WPDE-1 and WPDE-2 experiments except for I-125. This means that the modellers should predict the decay-corrected activities of the tracers, over time, as they reach the end of the outlet tube in the REPRO niche.

A number of different modelling groups will perform the predictive modelling. To facilitate a graphical cross-comparison of the central prediction of the breakthrough curves at meetings and workshops, they should preferably be presented in a specific, mutually-agreed upon format. Two graphs should be presented for each experiment where one has the time scale (on the x-axis) in arithmetic units and the other in $\log_{10}$-units. Hours should be used as the time unit and the starting point (time = 0 hours) should be when the valve to the tracer injection loop is switched on (see Section 2.3.3). The y-axis for all graphs should represent the normalised decay-corrected activity flow ((Bq/h)/Bq), in $\log_{10}$-space. This means the activity flux at the outlet, per time unit, divided by the total injected activity of that particular tracer. Hence, the normalisation should be based on the total activity of each tracer in the injection loop (cf. Table 2-2). When performing the decay correction, the initiation of the injection should be set as time zero. Alternatively, one could neglect to account for decay in the first place in the modelling, as no decay chain is involved, as long as linear reversible sorption is assumed. The modelled time-period of WPDE-1 should extend for one year, while the modelled time-period of WPDE-2 should extend for two years. Corresponding data should also be delivered in an Excel file, based on a provided template. This will facilitate the evaluator of Task 9, as well as the editor of the Task 9A report (see Section 2.5.4), to present data in a uniform graphical format.

---

[5] Personal communication with Marja Siitari-Kauppi and Mikko Voutilainen.

To facilitate a quick comparison between central predictions of the breakthrough curves, we encourage the use of performance measures. For the Kalmar meeting, we recommend that you note discrete points in time when each tracer reaches specified concentrations at the outlet tube, relative to the tracer´s peak concentration. These times should correspond to the attainment of:

- 10 % and 50 % of tracer peak concentration in the leading edge of the tracer pulse.
- Tracer peak concentration.
- 10 %, 1 %, 1 ‰, and 0.1 ‰ of tracer peak concentration in the tail of the tracer pulse (if this occurs within the modelled time-period).

At the Kalmar meeting, it was decided to add one more performance measure, namely:

- Recovery fraction.

This means that the decay corrected recovery fraction should be predicted at the end of the modelling period (1 year for WPDE-1 and two years for WPDE-2) for each tracer, relative to the total amount of injected tracer.

Each modelling group should also deliver alternative predictions (see Section 2.5.3), although no particular format is requested when presenting them.

The modellers may also choose to present other modelling results, which are not intended to be graphically cross-compared with those of other groups. For such results there is no particular requirement on the format in which they are presented. However, we encourage that the modelling groups also deliver such results in a readily comprehensible Excel file.

## 2.5.2 Description of the model and the handling of processes, features, etc

The conceptual model used and how it is incorporated in the computational code should be described in a transparent manner. It is also encouraged that the authors give detailed references to documents providing a comprehensive background on such issues.

A very important part of reporting the modelling is also presenting how the model has handled different processes and features, as well as experimental conditions and supporting data. In most modelling, a simplified representation of reality is incorporated. Typical simplifications include neglecting processes and features, or streamlining them so that they fit in a reasonably simple mathematical representation. Other efforts may involve simplifying geometrical constraints, boundary conditions, the initial state, supporting data, etc.

In this respect it is important to both describe processes, conditions, data, and other features that are incorporated in the models, as well as those which are intentionally neglected or simplified. Unless the handling is self-evident, steps taken when simplifying the real system should be justified and the impact of the simplification should be discussed (cf. Section 2.5.3).

It is important to acknowledge that the final reporting of the above-issues is only part of the expected outcome of Task 9A. The journey to arriving at the final models and results, preferably involving scientific discussions with fellow scientists within and outside the Task Force framework, can also be considered an important outcome.

## 2.5.3 Uncertainty treatment and sensitivity studies

The development of multiple models describing similar systems (REPRO and LTDE-SD) together with "blind" prediction of experiment results provides an opportunity to examine both parameter and model uncertainty. Task 9A involves semi-predictive modelling of the WPDE experiments, prior to more detailed inverse modelling of the experiments intended in a later subtask.

As part of the semi-predictive work, modellers are encouraged to consider the uncertainties associated with their predictions. Ideally this should include an initial consideration of both parameter uncertainty (sensitivity) and some assessment of the conceptual model uncertainty.

Conceptual model uncertainty has been widely shown to have significant impact and documenting the decisions made during conceptual model development, together with the associated uncertainties, is essential when trying to gain improved system understanding.

As is always the case, there is some data uncertainty in the main parameters delivered from the WPDE in situ campaign and supporting laboratory programme of REPRO. Moreover, the relatively limited laboratory programme may not have captured the spatial variability of the heterogeneous rock matrix at the site. It should also be remembered that there is concern regarding how well laboratory data in general can represent in situ conditions. There are also other unknowns, which can be exemplified by the lack of knowledge if there was a minor water leakage out of, or into, the in situ experimental section. Such input data uncertainty prompts the need to perform sensitivity studies. Which sources of uncertainty have a minor and, respectively, a major impact on the breakthrough results, and within what uncertainty ranges does this apply?

Hence, we encourage the modellers to perform sensitivity studies within Task 9A. As a minimum each modelling group should deliver two alternative breakthrough curves for each tracer of the WPDE-1 and WPDE-2 experiments, except I-125, which complement the central predictions discussed in Section 2.5.1. These curves should represent upper and lower predictions. It is left to the modelling groups to determine, and justify, the grounds for the alternative predictions. We encourage that the modelling groups also deliver these alternative results in a readily comprehensible Excel file.

At the Kalmar meeting, it became apparent that the assumptions made by the modelling groups concerning the dispersivity had an effect on the predicted breakthrough curves that overshadowed the effect of the groups' individual treatment of matrix diffusion. More on this is provided in Appendix C. We encourage all modelling groups to perform an alternative simulation of their central prediction where dispersivity is arbitrarily set to 0.19 m (unless this is the dispersivity that you already used). Using a predefined dispersivity places this particular simulation outside the realm of predictive modelling, but facilitates a straight-forward comparison of how different groups' treatments of matrix diffusion and retention affect their breakthrough curves.

**Clarification or comment**
Appendix C, which is a letter to the modellers on the issues of dispersivity, is called Appendix 3 in this present report.

## 2.5.4   Reporting

Task 9A is intended as an introduction to the modelling of the REPRO experiments, which will be revisited in greater detail in later subtasks. For this reason, it is intended to limit reporting of the modelling groups' work to a short document of less than 30 pages. These documents will be assembled together with a description of Task 9A, and a statement from the evaluator, into a single Task 9A report.

**Clarification or comment**
It was later decided to break out this task description to a stand-alone report.

A Microsoft Word template that should be used when reporting Task 9A will be provided in May/June 2015. The template will not only include headings and formats, but also short instructions. In general, the reporting document should describe:

• The conceptual model implemented, including the significant assumptions underlying the model.

• The results of key simulations.

• Sensitivity studies and discussion of uncertainty.

• The assessment of each modelling group of their own model.

The aim is not only to document the work performed but also to provide a base-line assessment of the different modelling approaches at the start of the task.

Modelling groups are of course free to produce additional, more detailed reports, or to publish in the open literature. Please provide a copy of any paper submitted to the Task Force Secretary so that publications of the different modelling groups and experimenters can be coordinated.

### 2.5.5 Timeline for deliveries within Task 9A

A reasonable timeline for deliveries within Task 9A was discussed at the Helsinki workshop and at the Kalmar meeting. Based on these discussions, and on the overall progress of the subtask, the following can be said:

As the Kalmar meeting was also the starting point of Task 9B-1, one can expect that the focus shifts from Task 9A to 9B-1 after the meeting. For modelling groups that have joined Task 9 at a later time, perhaps as late as at the Kalmar meeting, they have the opportunity to cover as much as possible of Task 9A until the spring meeting. This spring meeting, i.e. the Task Force meeting #34, will tentatively be held in May 2016, in Prague, Czech Republic. The spring meeting will be last chance for all modelling groups to orally present their results on Task 9A and no such oral presentations are foreseen at later meetings or workshops. In the interest of not falling too far behind, newcomers are permitted to skip modelling Task 9A altogether and instead commence modelling Task 9B-1.

Two weeks prior to the spring meeting the modelling groups should send their breakthrough curve and performance measure data to the task evaluator, as inserted in the provided Microsoft Excel template (see Sections 2.5.1 and 2.6). This follows the same procedure as prior to the Kalmar meeting. However, please add your recovery data and possible data for the variant of your central prediction, using a dispersivity of 0.19 m.

Shortly after the spring meeting, no later than the 30<sup>th</sup> of June 2016, the modelling groups should submit a complete draft report of their Task 9A work. The groups' reports should be compiled into a single Task 9A report that aims to be completed in autumn 2016.

In previous versions of this document it was stated that a decision may be made at the Kalmar meeting to include a predictive modelling of a future WPDE-3 experiment (cf. Section 2.2) in Task 9A. However, it was later decided not to do this.

**Clarification or comment**
The timeline for completing the Task 9A report has been revised and work with the modellers' contribution and the evaluation is ongoing.

## 2.6 Additional data, documentation, and information

During the course of Task 9, additional data and documentation, as well as presentations held at meetings and workshops, will be uploaded to the member area of the SKB Task Force website (www.skb.se/taskforce). During May and June 2015, the following Task 9A documents will be uploaded:

- This version of the task description.
- A Microsoft Excel file in which the data found in this task description are compiled, including data behind some of the shown graphs.
- High resolution photographs of, for example, the drill core and drillhole wall.
- A Microsoft Word template, with further instructions, that should be used by the modelling groups when reporting Task 9A.
- A Microsoft Excel template, with short instructions, that should be used by the modelling groups for delivering numerical data within Task 9A concerning the breakthrough curves.

**Clarification or comment**
For a complete overview of additional data and supporting documents (data deliveries), turn to Chapter 1.

For additional information on the experimental setup or geoscientific settings, as well as for additional data, please send an e-mail to both

- Martin Löfgren (martin.lofgren@niressa.se), and
- Kersti Nilsson (kersti.nilsson@geosigma.se).

Please do not hesitate to ask questions, as we have been assigned to deal with such requests. You may also request a telephone meeting in order to receive additional explanations or help.

# References

SKB's (Svensk Kärnbränslehantering AB) publications can be found at www.skb.com/publications.

**Ikonen J, Sammaljärvi J, Siitari-Kauppi M, Voutilainen M, Lindberg A, Kuva J, Timonen J, 2015.** Investigation of rock matrix retention properties supporting laboratory studies I: Mineralogy, porosity, and pore structure. Posiva Working Report 2014-68, Posiva Oy, Finland.

**Kuva J, Voutilainen M, Kekäläinen P, Siitari-Kauppi M, Timonen J, Koskinen L, 2015.** Gas phase measurements of porosity, diffusion coefficient, and permeability in rock samples from Olkiluoto bedrock, Finland. Transport in Porous Media 107, 187–204.

**Nilsson K, Byegård J, Selnert E, Widestrand H, Höglund S, Gustafsson E, 2010.** Äspö Hard Rock Laboratory. Long Term Sorption Diffusion Experiment (LTDE-SD). Results from rock sample analyses and modelling. SKB R-10-68, Svensk Kärnbränslehantering AB.

**Parkhurst D L, Appelo C A J, 1999.** User's guide to PHREEQC (version 2): a computer program for speciation, batch-reaction, one-dimensional transport, and inverse geochemical calculations. Water-Resources Investigations Report 99-4259, U.S. Geological Survey, Denver, Colorado.

**Posiva, 2012.** Safety case for the disposal of spent nuclear fuel at Olkiluoto – Performance assessment 2012. Posiva 2012-04, Posiva Oy, Finland.

**Poteri A, Andersson P, Nilsson K, Byegård J, Skålberg M, Siitari-Kauppi M, Helariutta K, Voutilainen M, Kekäläinen P, Ikonen J, Sammaljärvi J, Lindberg A, Kuva J, Timonen J, Koskinen L, 2018a.** The first matrix diffusion experiment in the water phase of the REPRO project: WPDE-1. Posiva Working Report 2017-23, Posiva Oy, Finland.

**Poteri A, Andersson P, Nilsson K, Byegård J, Skålberg M, Siitari-Kauppi,M, Helariutta K, Voutilainen M, Kekäläinen P, 2018b.** The second matrix diffusion experiment in the water phase of the REPRO project: WPDE-2. Posiva Working Report 2017-24, Posiva Oy, Finland.

**Sedighi M, Bennett D, Masum S A, Thomas H R, Johansson J, 2014.** Analysis of temperature data at the Olkiluoto. Posiva Working Report 2013-58, Posiva Oy, Finland.

**SKB, 2011.** Long-term safety for the final repository for spent nuclear fuel at Forsmark. Main report of the SR-Site project. SKB TR-11-01, Svensk Kärnbränslehantering AB.

**Soler J, Neretnieks I, Moreno L, Liu L, Meng S, Svensson U, Trinchero P, Iraola A, Ebrahimi H, Molinero J, Vidstrand P, Deissmann G, Říha J, Hokr M, Vetešník A, Vopálka D, Gvoždík L, Polák M, Trpkošová D, Havlová V, Park D-K, Ji S-H, Tachi Y, Ito T, 2019.** Evaluation and modelling report of Task 9A based on comparisons and analyses of modelling results on REPRO experiments. Task 9 of SKB Task Force GWFTS – Increasing the realism in solute transport modelling based on the field experiments REPRO and LTDE-SD, SKB R-17-10, Svensk Kärnbränslehantering AB.

**Toropainen V, 2012.** Core drilling of REPRO drillholes in ONKALO at Olkiluoto 2010–2011. Posiva Working Report 2012-26, Posiva Oy, Finland.

**Voutilainen M, Ikonen J, Kekäläinen P, Sammaljärvi J, Siitari-Kauppi M, Lindberg A, Kuva J, Timonen J, 2018a.** Matrix pore water study on REPRO samples. Posiva Working Report 2017-22, Posiva Oy, Finland.

**Voutilainen M, Ikonen J, Sammaljärvi J, Siitari-Kauppi M, Lindberg A, Kuva J, Timonen J, Löfgren M, 2018b.** Investigation of rock matrix retention properties – Supporting laboratory studies II: Diffusion coefficient and permeability. Posiva Working Report 2017-39, Posiva Oy, Finland.

**Widestrand H, Byegård J, Selnert E, Skålberg M, Höglund S, Gustafsson E, 2010a.** Long Term Sorption Diffusion Experiment (LTDE-SD). Supporting laboratory program – Sorption diffusion experiments and rock material characterisation. With supplement of adsorption studies on intact rock samples from the Forsmark and Laxemar site investigations. SKB R-10-66, Svensk Kärnbränslehantering AB.

**Widestrand H, Byegård J, Nilsson K, Höglund S, Gustafsson E, Kronberg M, 2010b.** Long Term Sorption Diffusion Experiment (LTDE-SD). Performance of main in situ experiment and results from water phase measurements. SKB R-10-67, Svensk Kärnbränslehantering AB.

# Chapter 1 of Task description 9A

In this appendix, Chapter 1 of the final task description of Task 9A (dated the 22nd of November 2015) is reproduced without changes. The purpose is to provide a historical record of the task, and it is asked of the reader not to reference this appendix regarding technical descriptions of the experiments, or the actual progress of Task 9. Some of the below information is outdated and technical information of the described experiments may have become inaccurate due to replanning of the campaigns or that new information has been brought to light.

## A1.1    Introduction

Task 9 focuses on the realistic modelling of coupled matrix diffusion and sorption in heterogeneous crystalline rock matrix at depth. This is done in the context of inverse and predictive modelling of tracer concentrations of the in-situ experiments performed within LTDE-SD at the Äspö Hard Rock Laboratory in Sweden, and the REPRO project at the ONKALO underground rock characterisation facility in Finland, focusing on sorption and diffusion. The ultimate aim is to develop models that in a more realistic way represent retardation in the natural rock matrix at depth.

### A1.1.1    Background

The topic of radionuclide transport and retardation in the geosphere is of high importance for assessing the safety of geological repositories for radioactive waste in fractured crystalline rock. Matrix diffusion of solutes in the microporous system of the rock matrix is perceived to be well understood and has been discussed for over 60 years. For the past 35 years, matrix diffusion coupled with sorption has been discussed in the context of retardation of radionuclides migrating from a geological repository for nuclear waste.

In recent safety assessments (e.g. SKB 2011, Posiva 2012), the importance of solute exchange between flowing fracture water and stagnant pore water has been stressed in regard to the waste containers' capability of isolating spent nuclear fuel over long time periods. This has, for example, been done in the context of copper corrosion due to intruding oxygenated water and due to sulphide. It is noted that matrix diffusion is one of the processes influencing both the oxygen and sulphide concentrations at depth. In addition, the performance of buffer materials such as bentonite has been shown to depend on concentrations of the groundwater's main constituents, which in turn are affected by matrix diffusion and groundwater interactions with rock minerals. Finally, the groundwater flow rate at depth depends on the water density, which in turn is affected by solute exchange between the flowing water and stagnant water. This has expanded the field of solute transport and retardation to include not just consideration of radionuclides, which has been the traditional focus, but also the performance of the engineered barriers, hydrogeochemistry, and hydrogeology.

The extended scope of solute transport and retardation makes it more difficult to establish what input data values are conservative for safety assessment modelling. As the relationship between radiological risk and these transport and retardation parameters is not necessarily simple and/or monotonic, this evokes the need for improving the realism in the modelling.

Even though the subject of matrix diffusion coupled with sorption has been studied for decades, the modelling approaches used for explaining tracer test results in natural rock have not developed at a significant rate lately[6]. Such development is needed to explain discrepancies between experimental observations and results obtained from inverse modelling of the same experiments. In general, at least within the field of radionuclide transport, inverse modelling of tracer tests is based on Fickian diffusion in homogenous media coupled with equilibrium sorption. In doing this, in-diffusion cases are typically modelled where a water phase tracer cocktail is surrounded by the rock matrix (for example in a drillhole in situ) or where the tracer cocktail surrounds a sample of rock (typically in

---

[6] In this statement the advances in reactive transport modelling is disregarded, as it will take substantial time until such approaches can be applied to natural systems.

the laboratory). Alternatively, the tracer diffuses out of the rock matrix or through the rock matrix, although such experiments are less common in situ.

In in-diffusion experiments, commonly the decline in tracer concentrations in the water phase is measured and modelled, as well as the tracer penetration profiles in the rock matrix. When predicting the tracer penetration profiles, generally Fickian diffusion coupled with equilibrium sorption is assumed. In many cases the rock matrix is assumed to be homogenous. With these modelling prerequisites, the predicted shapes of the penetration profiles will always follow the same pattern. However, such predicted shapes were not observed in the in-situ experiment LTDE-SD, as shown in Figure A1-4.

### A1.1.2  Summary of the Long Term Sorption Diffusion Experiment, LTDE-SD

One of few recent in-situ studies focusing on tracer transport in the stagnant pore water of the rock matrix has been conducted in Sweden at the Äspö Hard Rock Laboratory, within the LTDE-SD campaign (Long Term Sorption Diffusion Experiment). Here the LTDE-SD in-situ experiment is summarised in a generalised way, omitting details that are needed at a later stage in Task 9. For a full description of LTDE-SD, Nilsson et al. (2010) and Widestrand et al. (2010a, b) are recommended. More details, such as dimensions and resulting data, will also be given in task descriptions of subtasks concerning LTDE-SD (e.g. Task 9B).

In the in situ experiment, a cocktail of both sorbing and non-sorbing tracers was allowed to contact a natural fracture surface, as well as the unaltered rock matrix, for a time period of 200 days. The experiment was carried out at a depth of about 410 m below sea level. The illustration in the lower right of Figure A1-1 shows the location of LTDE-SD in the Äspö HRL tunnel system. In the centre of the figure, the local tunnel section is shown together with the different boreholes drilled from the site. These boreholes include the LTDE-SD borehole and the closely located pilot borehole. These two boreholes intersect a water-conducting natural fracture at a distance of about 11 m from the tunnel wall, which is the experiment's target fracture. The LTDE-SD borehole was drilled with different diameters, roughly described as follows. Up to the fracture plane the borehole has a large diameter and beyond the fracture plane a small diameter was used. This is simplistically illustrated in the lower left of Figure A1-1. The borehole is indicated by the solid black line and the intersected fracture is indicated by the curved blue line. Orange areas indicate packed-off volumes, whereas light blue areas indicate volumes of the tracer cocktail. The red arrows symbolise in-diffusion of tracers from the large-diameter borehole through the fracture surface and into the underlying altered rock matrix. They also symbolise diffusion into the unaltered rock matrix from the small-diameter borehole. The dashed black line indicates the rock volume that was overcored at the end of the tracer test.

The tracers injected were Na-22, S-35, Cl-36, Co-57, Ni-63, Se-75, Sr-85, Nb-95, Zr-95, Tc-99, Pd-102, Cd 109, Ag-110, Sn-113, Ba-133, Cs-137, Gd-153, Hf-175, Ra-226, Pa-233, U-236, and Np-237. Speciation calculations were made using PHREEQC. PEEK tubing connected the tracer cocktail volumes with experimental equipment in the tunnel. Hence, the decreasing tracer concentrations, as well as environmental parameters, could be monitored during the 200 days the tracer test progressed. After that the surrounding rock volume was overcored, and from the overcored volume a number of smaller drill cores were excavated, as illustrated in Figure A1-2. Here the natural fracture surface is located on the right-hand side of the overcored rock volume.

A large number of the drill core samples of Figure A1-2, but not all, were cut into subsamples as illustrated in Figure A1-3, enabling the subsequent evaluation of tracer penetration profiles.
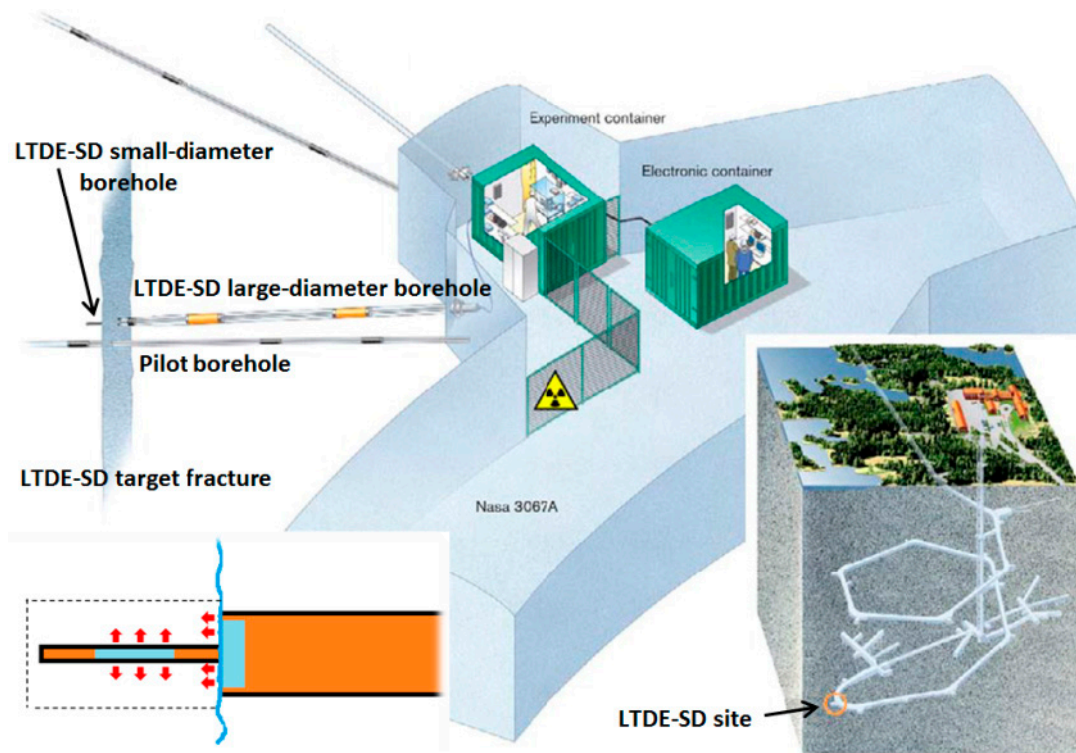
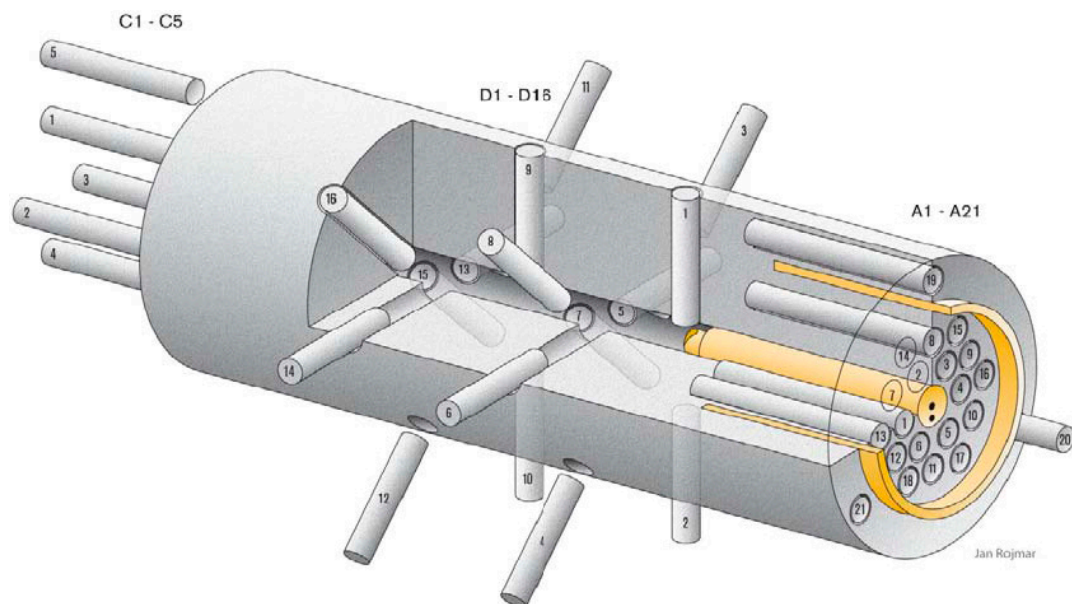***Figure A1-1.*** *Illustrations of the LTDE-SD experimental setup.*



***Figure A1-2.*** *Illustration of drill cores drilled from the overcored rock volume.*
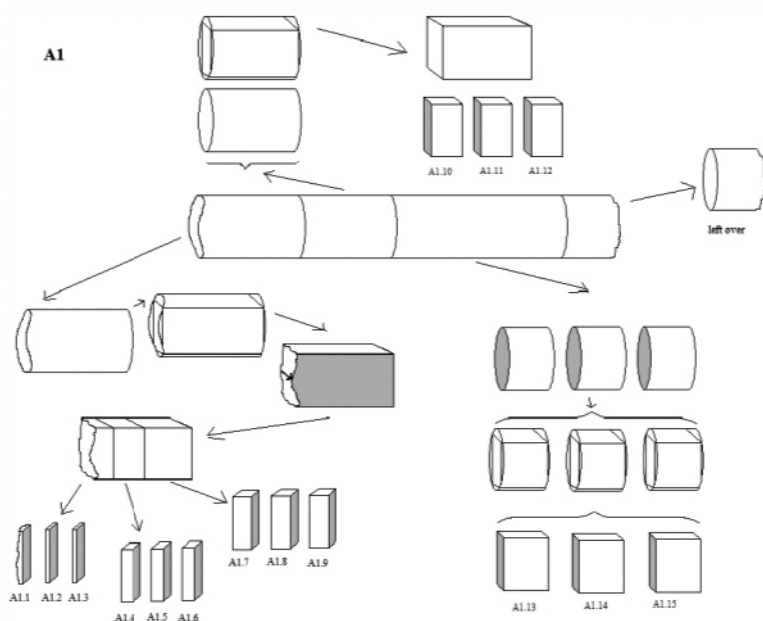
***Figure A1-3.*** *Illustration of the sampling of the overcored rock volume in LTDE-SD.*

The first three slices closest to the tracer cocktail/rock interface were cut into a thickness of ~1 mm, with the discrepancy that the very first slice that samples the natural fracture surface may have been slightly larger due to the fracture surface roughness. The next three slices were cut with a thickness of ~3 mm; the following three slices were ~5 mm thick; the following three slices were 10 mm thick; and the last three slices had a thickness of 20 mm.

Tracer concentrations (or activities) in the rock were obtained by a number of analysis methods, including autoradiography on intact samples; direct activity measurements on intact and crush samples; and leaching or dissolution of intact and crush samples, followed by water phase measurements. Although the methodology and results from the experimental campaign have been finally reported (Nilsson et al. 2010, Widestrand et al. 2010a, b), the outcomes have not yet been subjected to the scrutiny of a broader community of researchers and modellers.

Concerning the shape of the penetration profiles, the expected predicted general shape was not observed; neither for the natural fracture surface nor for the unaltered rock matrix. Figure A1-4 shows the experimental concentration shapes of the in-diffusing tracers Na-22 and Cl-36 by diamonds, as well as the modelled profiles by the solid curves. Here the discrepancy of the curve shapes should be highlighted, whereas the discrepancy in relative curve positions is of lesser importance.

The heterogeneous nature of the rock matrix, in terms of both the microporous network and mineral surfaces available for sorption, has been qualitatively offered as an explanation for the discrepancy (Nilsson et al. 2010). However, other features, events, and processes that are traditionally not included in such modelling may add to the observed discrepancy. It may also be that using the fundamental prerequisites of the modelling, that is the Fickian diffusion equations and the equilibrium sorption approach, may add to the discrepancy.

Increasing the realism when modelling experimental results from LTDE-SD is intended to be an important part of Task 9, without imposing restrictions on the modelling groups in terms of how they should increase this realism. LTDE-SD also featured an extensive laboratory programme on site specific rock samples providing sorption, diffusion, and porosity data, as well as mineralogical characterizations. Hence, a large body of supporting data is available for the modelling groups, if requested.
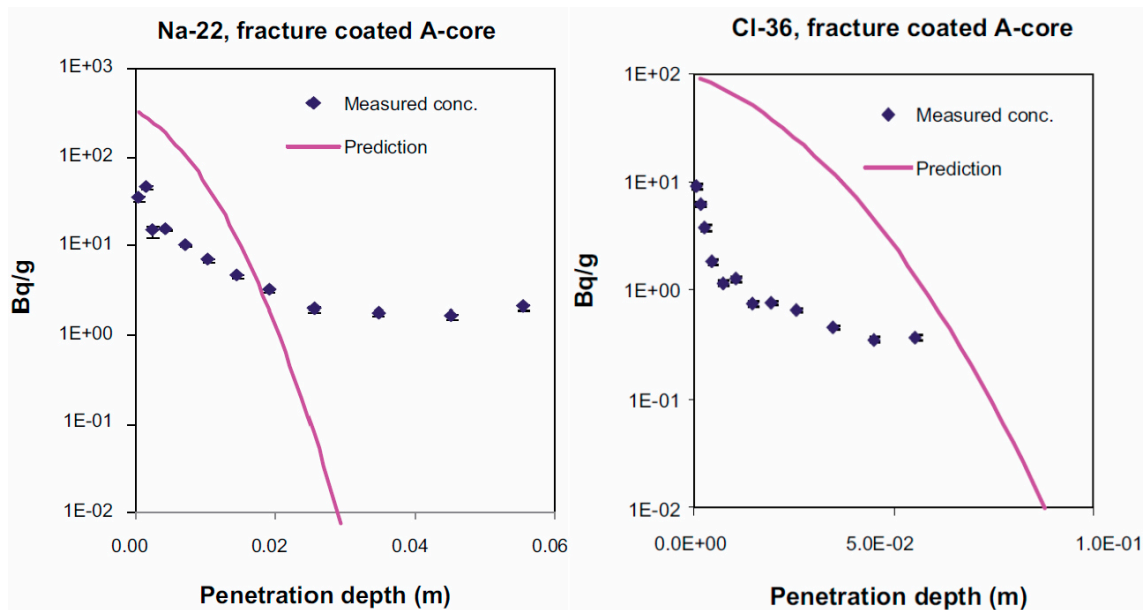
***Figure A1-4.*** *Results from the in-situ in-diffusion experiment LTDE-SD through a natural fracture surface. Modelled Na-22 and Cl-36 penetration profiles (solid curves) in comparison with the measured profiles (diamonds). Na-22 activities in the rock matrix were obtained on intact or crushed rock slices and Cl-36 activities were obtained by leaching of intact or crushed slices. Excerpts from Nilsson et al. (2010, Figures 4-1a and 4-2a).*

### A1.1.3 Summary of REPRO in-situ experiments WPDE-1, WPDE-2 and TDE

The REPRO project is presently carried out by Posiva at the ONKALO underground rock characteri-sation facility in Finland, where REPRO is short for Rock matrix REtention PROperties. This project is in part carried out in situ, and in part as an extensive laboratory programme. Concerning the in situ experiments; two water phase diffusion and sorption campaigns are carried out from the REPRO niche at about 400 m depth, from which a number of drillholes have been drilled (see Figure A1-5). These campaigns are the WPDE (Water Phase Diffusion Experiment) series of experiments and the TDE experiment (Through Diffusion Experiment). As the REPRO project is on-going, it offers the possibility of both inverse and predictive modelling in Task 9. The in-situ part of REPRO aims to tackle the topics of diffusion, sorption; anion exclusion; and rock matrix anisotropy. The laboratory part has, in addition, focused on small scale rock characterisation. This provides a wealth of input data that can be incorporated in the modelling.

**Water Phase Diffusion Experiment**

The WPDE campaign features advection-diffusion-sorption experiments which are carried out in a defined section of drillhole ONK-PP323, about 18 to 20 m away from the niche wall (see Figure A1-5). Here a 1.9 m long section has been packed off, and in this section a dummy that is coaxial with the drillhole has been placed. The dummy diameter is 54 mm whereas the drillhole diameter is 56.5 mm, leaving a 1.25 mm gap between the drillhole wall and the dummy. This gap is regarded as an artificial fracture of relatively well-defined geometry. In this gap a very low steady state water flow has been applied, directed towards the niche. This is achieved by injecting the water at the far end of the packed-off section, as shown to the upper right in Figure A1-5. To date, two experiments have been performed at different flow rates; WPDE-1 (20.1 μL/min) and WPDE-2 (10.0 μL/min). A third flow rate may be utilised in a third experiment, should such an experiment be carried out.
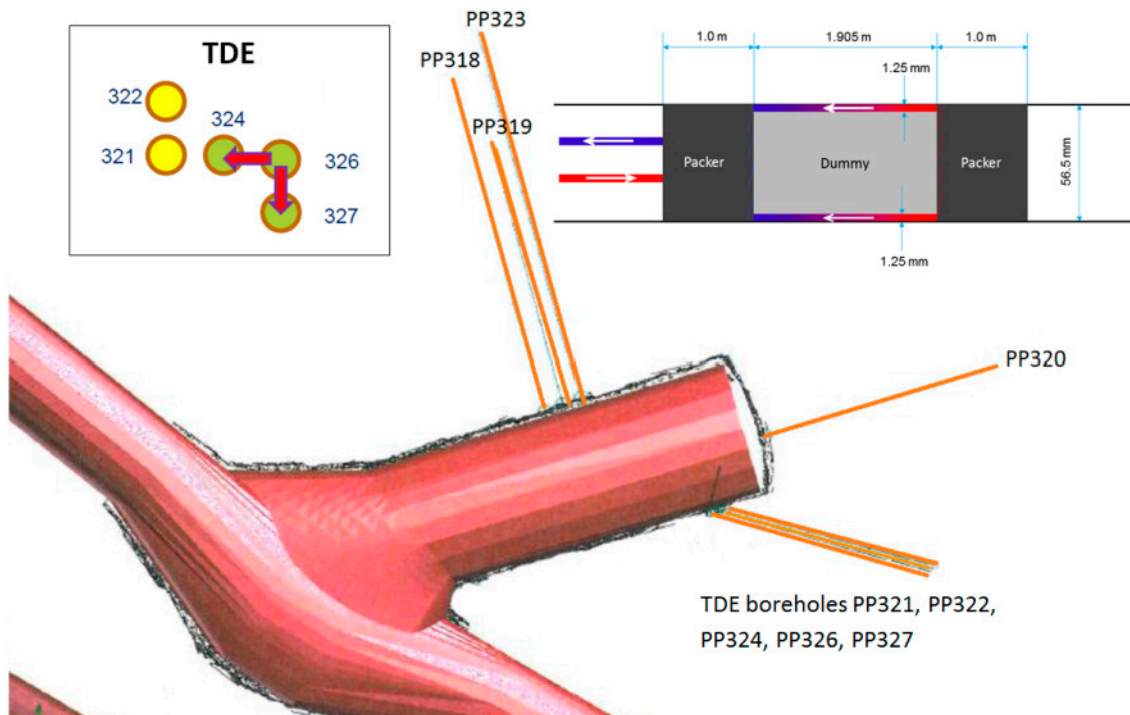
*Figure A1-5. The REPRO niche at the 401 m level at ONKALO, and some of the drillholes drilled from the niche. Drillhole ONK-PP323 is utilized for WPDE 1, WPDE 2, and drillholes ONK-PP324, ONK-PP326, and ONK-PP327 for TDE. The REPRO niche is also labelled Investigation niche 5(ONK-TKU-4219).*

In this water flow the active tracers HTO, Na-22, Cl-36, and I-125 were injected in WPDE-1, and HTO, Na-22, Cl-36, Sr-85 and Ba-133 in WPDE-2. For each experiment, injection was made as a few hours long pulse at the far end of the experimental section. Except for the active tracers, the tracer cocktails contained synthetic groundwater. The idea behind the experimental setup is that as the tracer pulse travels with the water flow; its tracers will diffuse into the rock matrix surrounding the drillhole, where they may also sorb. As the pulse passes, the concentration gradients are reversed and the tracers will diffuse out of the rock matrix and into the flowing water. By detecting their activities in the water phase at the end of the drillhole, breakthrough curves are obtained which can be analysed by modelling.

The tracer concentrations were measured both by online Na(Tl)I-scintillation detection and by analysing water samples in the laboratory. Breakthrough curves have been obtained over half a year and about one and a half a year for WPDE-1 and WPDE-2, respectively. The rock volume surrounding the experimental section, affected by in-diffusion, is not planned to be overcored.

**Through Diffusion Experiment**

The TDE experiment will be carried out between three parallel drillholes arranged as a right-angled triangle. Drillhole ONK-PP326 will be used as the injection hole and drillholes ONK-PP324 and ONK-PP327 as observation holes (see Figure A1-5, upper left corner). The experiment will be carried out in 1 m long packed-off sections, at a distance of about 11 to 12 m from the tunnel wall. The distances between the drillholes are between 10 and 15 cm. Any advective flow between the drillholes is foreseen to be insignificant, as the experiment takes place in a rock volume that lacks water-bearing fractures.

The tracers HTO, Na-22, Cl-36, Ba-133, and probably Cs-134 are planned to be injected. The decreasing tracer concentrations in the injection hole and (foreseen) increasing tracer concentrations in the observations holes will be analysed. This is done on extracted water samples in the laboratory; by liquid scintillation counting and High Resolution GXRS (gamma measurements). Furthermore, online measurements will be performed for the injection hole and observation holes by a High Performance Germanium detector and a Na(Tl)I-scintillation detector, respectively. Tracer concen-

trations in the injection hole will be measured at a higher frequency at the first part of the experiment, while focus will be shifted towards analysing breakthrough concentrations in the observation holes as the experiment progresses. Tracer concentrations will not be measured in adjacent drillholes ONK-PP321 and ONK-PP322 (see Figure A1-5). Breakthroughs of non-sorbing tracers are foreseen within the timeframe of Task 9, although unexpectedly low pore diffusivities may prevent this from happening. For tracers that do not break through within the time frame of Task 9, TDE can be modelled as an in-diffusion experiment similar to that in the small-diameter borehole of LTDE-SD.

The tracers were chosen to make overcoring and analysis of tracer penetration profiles possible, although this option is presently not included in the REPRO planning.

### A1.1.4 Roadmap of Task 9

Figure A1-6 shows the proposed roadmap of Task 9. As can be seen, the task integrates the LTDE-SD and REPRO experiments, utilising both inverse and predictive modelling. For each new step, information from, and knowledge gained in, the previous steps should be incorporated in the modelling. This is intended to lead to an increased realism in process description in the solute transport modelling codes. In Figure A1-6, grey boxes mark activities. When summarising the proposed activities below, the labelling 9A, 9B, 9C, etc. has been used. However, the actual division of Task 9 into different subtasks concerning Task 9C–9F needs to be decided at a later stage. Traditionally, the exact content of each subtask is open for discussion during the lifetime of the task. Task 9 is no exception and the participating organisations are welcome to suggest modifications. As always in the Task Force GWFTS, reporting and publications of papers are encouraged.

**Task 9A:** Task 9 is suggested to start with semi-predictive modelling of WPDE-1 and WPDE-2 of the REPRO project. Traditional solute transport data, that are site specific for ONKALO, are used as input in what the modellers perceive as traditional solute transport codes. Preliminary results from WPDE-1 and WPDE-2 have been shown in PowerPoint presentations at a few Task Force meetings and workshops during 2013 and 2014. In addition, the official WPDE-1 report is intended to be published by Posiva in 2015. The modellers will be asked to disregard these presentations and this publication during the subtask. Even so, the modelling cannot properly qualify as being fully predictive. With this in mind, the subtask is labelled semi-predictive in the roadmap and can also be seen as a "warm-up" case for Task 9. Assuming that the modellers will honour the request to disregard presentations and publications providing the experimental water phase results; an evaluation step consisting of comparison of model and experimental results can be performed.

**Task 9B:** The following modelling subtask is suggested to use results from LTDE-SD; specifically results on tracer concentrations in the water phase and in the rock matrix will be used. In this subtask, the modellers may request data originating from the extensive rock matrix characterisation at the Äspö HRL, as well as geochemical characterisation data. This means that modellers will have a wealth of supporting data in setting up refined models for solute transport in heterogeneous media, for incorporating non-traditional processes, or for incorporating other aspects at the modellers' choosing. This subtask is intended to lead to an increased complexity in the modelling setup, with the ultimate aim to better reflect the reality and the experimental results.

**Task 9C/D:** In this subtask, the penetration profile of Cl-36, Cs-137 and Ni-63 into the LTDE-SD rock matrix will be modelled in a predictive fashion using the models developed in Task 9B. There are drill cores from LTDE-SD that have not yet been analysed in respect to tracer concentrations. Thus, the tracer activities of Cl-36 and/or Cs-137, and/or Ni-63 can still be measured at a reasonable effort, and this can be done on more than one drill core. The resulting profiles can be used for evaluation of the predictive modelling.

**Task 9C/D:** By using the increased realism in the modelling setup from previous subtasks, together with detailed rock and geochemical characterisation data from the REPRO laboratory program, the results from WPDE-1 and WPDE-2 are revisited and new and, hopefully, more complex and realistic inverse modelling is achieved, enabling a better understanding of the experimental data.

**Task 9E:** By using information from all of the above subtasks, predictive and inverse modelling is suggested to be performed for TDE in REPRO. It is uncertain whether or not breakthrough curves will be obtained from this experiment during the Task 9 lifespan. However, during the first few

years, before breakthrough occurs, TDE can be viewed as an in-diffusion experiment. Measurements of the declining tracer activities in the injection hole are planned, with the intention of achieving sufficient resolution for, at least, the sorbing tracers. Based on the progress of the experiment, the evaluation needs to be decided at a later stage.

**Optional Task 9F:** As an optional last subtask, the increased realism in the solute transport codes may be put in the perspective of safety assessment time scales. This is to highlight if different aspects of matrix diffusion and sorption, utilising codes with increased complexity and realism, may have any consequence for long-term retardation. Different safety assessments use different time scales and conditions. Accordingly, the specifics of this exercise need to be decided at a later stage. Some waste management organisations may want to perform such a consequence study within their own programme, and not within Task 9.

For all subtasks, special focus will be put on carefully describing the conceptual models that the computational codes aim to describe. Importantly, known simplifications in describing the natural system should be highlighted. This enables comparisons of the used conceptualisations between subtasks, and between modelling groups.

### A1.1.5 Time frame and organisation

Task 9 is suggested to be carried out during 2015 to 2018. The task was officially launched at the TF GWFTS workshop in Helsinki, Finland between the 22nd and 23rd of April 2015. At this workshop, Task 9A was initiated. The following meeting was held in Kalmar, Sweden, between the 20th and 22nd of October 2015 at the Task Force meeting #33. At this meeting the first results from Task 9A were presented and in addition, Task 9B-1 was initiated. The next meeting, i.e. Task Force meeting #34, will be held in spring 2016, tentatively in May in Prague, Czech Republic. At this meeting, the final results of Task 9A will be presented and shortly thereafter the modellers should submit their complete reports on Task 9A (see Section 2.5.5). At the spring meeting the modellers will also present their first results on Task 9B-1. Moreover, Task 9B-2 will be initiated. Task 9B (i.e. 9B-1 and 9B-2) is intended to be modelled throughout 2016.

Beyond Task 9B the time schedule has not yet been fully defined. Task 9C will tentatively concern predictive modelling of the TDE experiment at the REPRO site and is scheduled to be initiated during the autumn of 2016. Later subtasks are hopefully performed during 2017 and 2018. The roadmap of Task 9 was further discussed at the Helsinki workshop and Kalmar meeting and will be further discussed as Task 9 progresses. As one of the bases for such a discussion, a list of scientific challenges relevant to TASK 9 is appended in Appendix A.

The members of the TF GWFTS Task 9 technical committee are:

- Jan-Olof Selroos, Ph.D., Manager Groundwater flow modelling at SKB, and SKB Task Force Delegate.
- Björn Gylling, Ph.D., Manager Solute transport modelling at SKB, and SKB Task Force GWFTS Secretary.
- Lasse Koskinen, Ph.Lic., Head of the long-term safety team at Posiva, and Posiva Task Force Delegate.
- Martin Löfgren, Ph.D., Niressa AB. TF GWFTS Task 9 Principal Investigator.
- Kersti Nilsson, Ph.D., Geosigma AB. TF GWFTS Task 9 Data coordinator and Principal Investigator.
- Antti Poteri, D.Sc. (Tech), VTT Technical Research Centre of Finland.

The Scientific Chairman of Task Force GWFTS is:

- Bill Lanyon, MA., Fracture Systems Ltd.

The evaluator of Task 9 is:

- Josep Maria Soler Matamala, PhD., Institute of Environmental Assessment and Water Research (IDAEA-CSIC).
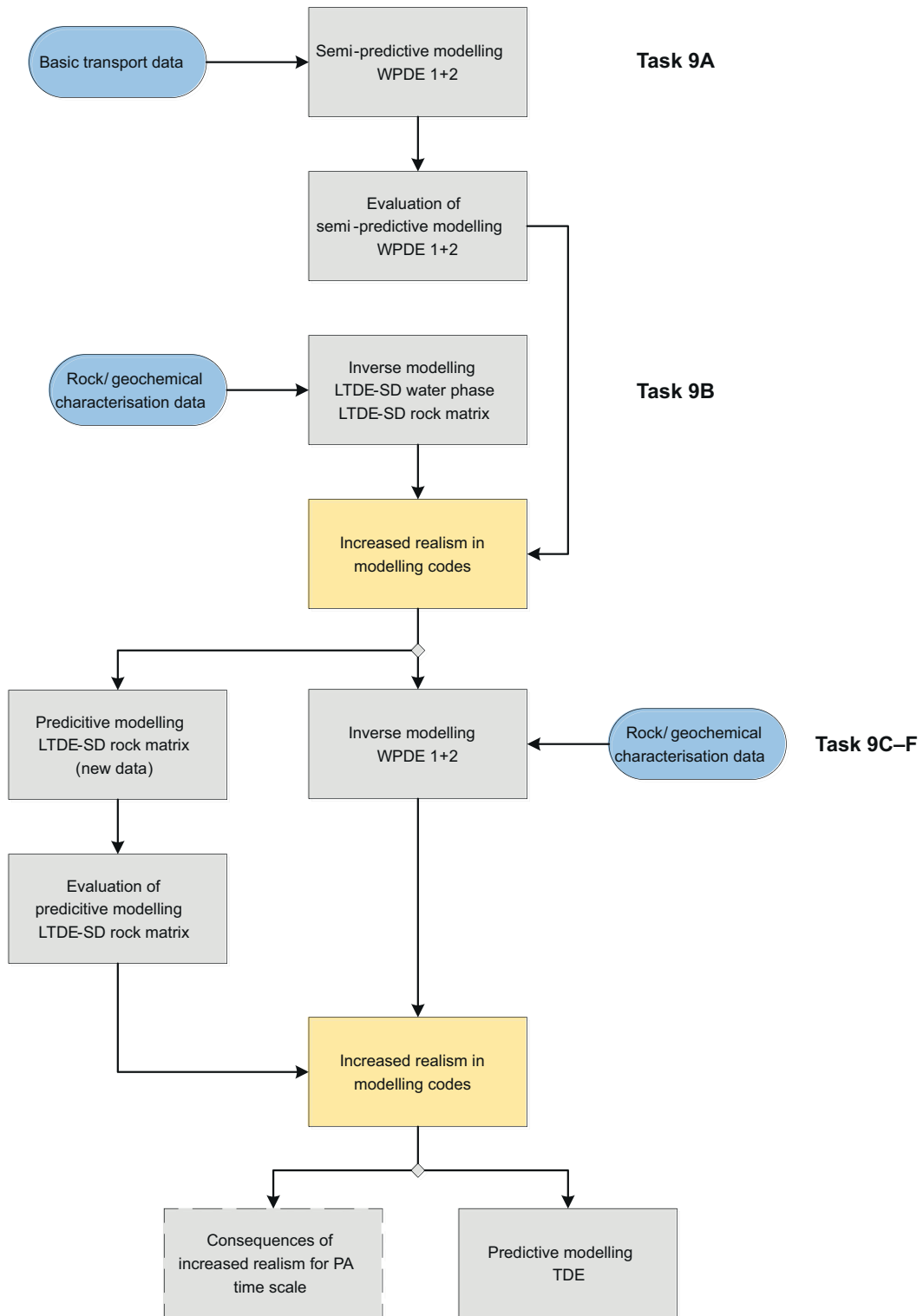
***Figure A1-6.*** *Suggested roadmap of Task 9. Grey boxes mark activities.*

# List of scientific challenges

## A2.1 Background

Task 9 focuses on the realistic modelling of coupled matrix diffusion and sorption in the hetero-geneous crystalline rock matrix at depth. Within this scope there are a great number of scientific challenges that may need further examination; either with the aim at better understanding field-scale tracer tests or at better estimating the long-term radionuclide transport within safety assessment. For Task 9, a flowchart1 has been presented that illustrates the proposed subtasks, and how they link to the different field-scale tracer test within REPRO and LTDE-SD. However, there is still much room for setting the direction of the different subtasks; allowing for the participating organisations to focus on issues of extra concern for their particular research and development programs.

Discussions on the general direction of Task 9, and its constituting subtasks, are planned to be held at the Task 9 workshop in Helsinki, on the 22nd to 23rd of April 2015. These discussions are envisaged to primarily set the direction of Task 9B and subsequent subtasks, while the start-up of Task 9A is scheduled at the Helsinki workshop. The task description of Task 9A is presently being prepared but is not planned to be sent out to workshop participants until the 1st of April. This gives the organisa-tion delegates some time to also give comments and suggestions on the direction of Task 9A, compared to what is outlined in the General Task 9 Task Description (Appendix 11). This may be done in the light of the provided list of scientific challenges.

## A2.2 List of scientific challenges

As an input to the discussions at the Helsinki workshop this document provides a list of scientific challenges associated with better understanding of coupled matrix diffusion and sorption in heterogeneous crystalline rock. The preparation of such a list was requested on the TF#32 meeting at Berkeley. It seems unlikely that all the listed topics can be a focus of attention in Task 9, and hence the list is intended as input when choosing topics that deserve special attention. Of course, the list is not complete and other topics may need highlighting. For some topics it may be that modelling results cannot be verified against experimental results. This is partly due to limitations in the experimental resolution. However, the experiments may also have been carefully designed to avoid some of the processes and features that may be of interest. An example is the general avoidance of sharp concentration differences for non-tracer solutes between the tracer cocktail and natural groundwater. This should not hinder the modelling of the particular process or feature, and comparing the results with those of other models that handle the process or feature differently. This gives Task 9 the opportunity to go beyond the scope otherwise limited by the experimental design; if preferring such an approach.

### A2.2.1 Do laboratory data represent in situ conditions?

In situ tracer tests are rare and expensive and cannot be performed to characterise the entire rock volume hosting a geological repository. Hence, bringing rock samples to the laboratory and perform-ing sorption and diffusion characterisations is a vital strategy in site investigations. In this respect, in situ tracer tests have their greatest value in giving us something to compare our laboratory data with. The main question is if the data we obtain, and the processes we observe, in the laboratory represent in situ conditions.

Concerning sorption data:

- Are laboratory derived sorption data, obtained at laboratory conditions and on crushed rock of different size fractions or on small intact rock samples, relevant for the in-situ rock?

- Are the laboratory data relevant for the different layers of fracture adjacent rock, i.e. the fracture coating; alteration rim; and undisturbed rock matrix? If not, do we need to adjust our laboratory strategy for measuring flow path adjacent rock properties?

- Does the laboratory aqueous chemistry well enough represent the in situ geochemical conditions?

Concerning diffusion data:

- Are laboratory derived diffusivity data, obtained at laboratory scale and conditions, relevant for the in-situ rock?
  - Do we see significant disturbances in the laboratory that originate in stress release and excavation induced damage?
  - Does the laboratory scale, where often short drill core samples are used, induce artefacts?

- Are the laboratory data relevant for the different layers of fracture adjacent rock, i.e. the fracture coating; alteration rim; and undisturbed rock matrix? If not, do we need to adjust our laboratory strategy for measuring this?

- Do we see differences in anion exclusion in the laboratory compared to in situ, as the anion exclusion factor may depend on the rock stress situation? Furthermore, is the magnitude seen in the laboratory dependent on the sample size?

In addressing the above questions one must not forget that some artefacts, especially those originating in rock disturbances, may be similar for laboratory and in situ experiments.

### A2.2.2  Heterogeneous sorption and diffusion

It is well known that radionuclides sorb more or less strongly to different mineral surfaces and that diffusion occurs at different rates in different micropores. Still, sorption and diffusion are often modelled to occur in a homogenous rock matrix where all sorption sites, and all micropores, are equal. Alternatively, the fracture adjacent rock may be described as a few layers of homogenous rock. Depending on the penetration depth, and the studied time frame, these simplifications are more or less valid.

Concerning heterogeneous sorption and diffusion:

- Is it sufficient to model the rock mass as a homogenous medium or as having homogenous layers, or do we see experimental evidence of unaccounted heterogeneous sorption and/or diffusion?

- In REPRO and LTDE-SD, much effort has been made to improve the microstructural model of the rock matrix. Can such improvements lead to an increased and sufficient understanding of sorption and diffusion?

- Is heterogeneous sorption and diffusion sufficiently well described by considering differences, from location to location, in:
  - Layers normal to the fracture surface (i.e. the fracture coating; alteration rim; and undisturbed rock)?
  - Thicknesses and coverages of different fracture minerals?
  - The rock type?
  - The mineralogical composition and lithology within a rock type (i.e. on the scale of the laboratory sample)?
  - Sorption affinity to different mineral grains (e.g. quartz, feldspar, biotite, and clay minerals)?
  - Diffusion rates in different micropore classes defined in the microstructural model (i.e. micro fractures, grain boundary pores, sheet-silica pores, and other pores)?
  - Pore water composition, where there is a gradient from the fracture surface/experimental surface into the rock matrix?

- Do we see evidence of limited in situ pore connectivity in part of, or in all of, the rock volume?

- Do we see evidence of an in situ porous system at the percolation threshold, giving rise to non-Fickian diffusion?

- Is it sufficient to use a constant anion exclusion factor, or do we need to assign different factors for different layers normal to the fracture surface, or other volumes describing the rock heterogeneity?

### A2.2.3 Sorption mechanisms and modelling

In safety assessment (SA) calculations, the $K_d$-concept is often utilised. Frequently, variation in groundwater composition is neglected, or treated in a much simplified manner. Presently attempts are made to use a more realistic sorption concept in SA calculations, called the smart-$K_d$ concept, taking local variability in groundwater composition into account. However, as the smart-$K_d$ concept is fairly new there is room for improvement. Furthermore, simplifications that are appropriate for SA calculations may not be sufficient for understanding tracer tests. For studying sorption in detail, more fundamental understanding may be required. Examples of models that more realistically try to represent the natural system are surface complexation and reactive transport models.

Concerning sorption mechanisms:

- Can the laboratory and in situ data be explained by the traditional $K_d$-concept?

- Do we need to consider non-linear sorption, precipitation, co-precipitation, recrystallisation, or other immobilisation mechanisms to explain the experimental data?

- In general, can the smart $K_d$-concept, only accounting the variation in the groundwater/pore water chemistry, better reproduce experimental results?

- Is it sufficient to discriminate between different water compositions when assigning smart $K_d$-values, or do we also need to account for changes in mineralogy, lithology, or other micro-structural features? Such features may vary normal to, or parallel with, the fracture surface.

- Can observations of solute transport in the rock matrix be better explained if using more funda-mentally based models, taking for example reactive transport, surface complexation, and electric charge conditions at the mineral surfaces into account?

As mentioned earlier the experimental design of REPRO and LTDE-SD aims at avoiding differences in tracer cocktail and groundwater main compositions. Hence, the spatial and temporal variation in the water composition around the injection hole is likely small. Hence, it is likely difficult to use experimental data for the evaluation of different modelling approaches of the smart $K_d$-concept.

### A2.2.4 Diffusion mechanisms and modelling

In safety assessment modelling, and for understanding tracer tests, Fickian diffusion is generally assumed. This is even though Fick's law was not derived for ionic transport in a charged porous media. This discrepancy is, for example, demonstrated by the need to assign different effective diffusivities for anions and cations/neutral species; by introducing the anion exclusion factor. Moreover, diffusion in a homogenous medium is generally assumed, where no account is taken for the fact that different pore types, or porous systems, have different diffusion rates and degrees of anion exclusion and surface enhanced diffusion (if such exist).

Concerning diffusion mechanisms:

- Is it sufficient to use the Fickian diffusion theory?
    - Is it sufficient to only consider diffusion in the bulk pore water of the micropores?
    - Do we need to consider the charge situation of the pore walls and electric double layer to understand surface enhanced diffusion and anion exclusion?
    - Do we need to consider multicomponent transport of ionic solutes, accounting for electro-neutrality in transport calculations (as better described by, for example, the Maxwell-Stefan diffusion model)?

- Do we see experimental evidence for anion exclusion and/or surface enhanced diffusion, for example from interpretations of the penetration profiles?

- Do we see experimental evidence of multicomponent transport effects that influences the penetration profiles? Would multicomponent transport modelling foresee such an influence?

### A2.2.5 Speciation calculations

In both REPRO and LTDE-SD, aqueous cocktails of tracers are affected by in situ geochemical conditions. To have a detailed description of the source term, aqueous speciation calculations have been, or can be, performed by using computational codes such as PHREEQC.

Concerning speciation calculations:

- Is there evidence of unforeseen reactions in the aqueous tracer cocktail, changing the chemical speciation of the tracers and hence the source term?

- Could the speciation change with depth into the rock matrix, and if so, could this be accounted for? Would it be possible to couple transport calculations in the rock matrix with speciation calculations in the pore water. Furthermore, is it sufficient to consider the composition of the bulk pore water, or does one also need to consider the altered composition in the electric double layer?

- Would the above suggestion make the smart $K_d$-approach even smarter?

### A.2.2.6 Other transport mechanisms

In addition to gradients in tracer concentrations or chemical potentials, giving rise to diffusion, there may be other gradients over the rock/fracture interface that affect solute transport. Obvious gradients are the hydraulic gradient that is likely enhanced by the presence of the tunnel system and experimental boreholes; and the electric potential gradient that will affect the migration rate and direction of ionic solutes. Both test sites are located nearby nuclear power plants where the grounding of power transmissions is expected to give rise to greatly enhanced Earth currents, and electrical potential gradients, as compared to the natural situation.

Concerning other transport mechanisms:

- Do we see evidence of an advective flow through the rock matrix, affecting the penetration profiles?
  - If so, is it sufficient for groundwater flow and solute transport modelling to use the simple division between flowing fractures and the rock matrix, or is there a need to refine the hydraulic description of the rock matrix. The latter would benefit from the wealth of micro-structural information available from the two sites.

- Do we see evidence of an electromigratory and/or electroosmotic flow through the rock matrix, affecting the penetration profiles?

- Do we see evidence of other transport mechanisms in the rock matrix?

# Letter to modellers

The following e-mail was composed by Chairman Bill Lanyon and Task evaluator Josep Soler and was sent to the modellers on the 20th of November, 2015.

**Dear Task 9A Modellers,**

After looking at the results presented at the Kalmar meeting, it was obvious that the results for conservative tracers (HTO, $^{36}$Cl) showed two different groups of results. One (KTH, CFE) gave very sharp arrivals and narrow tracer peaks, while the other group showed much wider and shorter peaks, with very early first arrival times.

In Figure A3-1, Pep Soler has used the analytical solution to the 1D Adv-Disp equation, without any matrix diffusion, for an instantaneous tracer release at x=0. Initial mass in the calculation is 1 mol, spread over a cross section area of 1 m$^2$ (so disregard the absolute magnitudes of the concentrations). The teams using classical dispersivity in the slot in their calculations seemed to use a value of dispersivity about 0.2 m. KTH, for instance, used something like $2 \times 10^{-9}$ m$^2$/s for the dispersion coefficient (similar for instance to only diffusion). Pep has calculated the breakthrough curves for these cases. As you can see, the large dispersivity (0.2 m) causes the flat curves and very early arrivals.
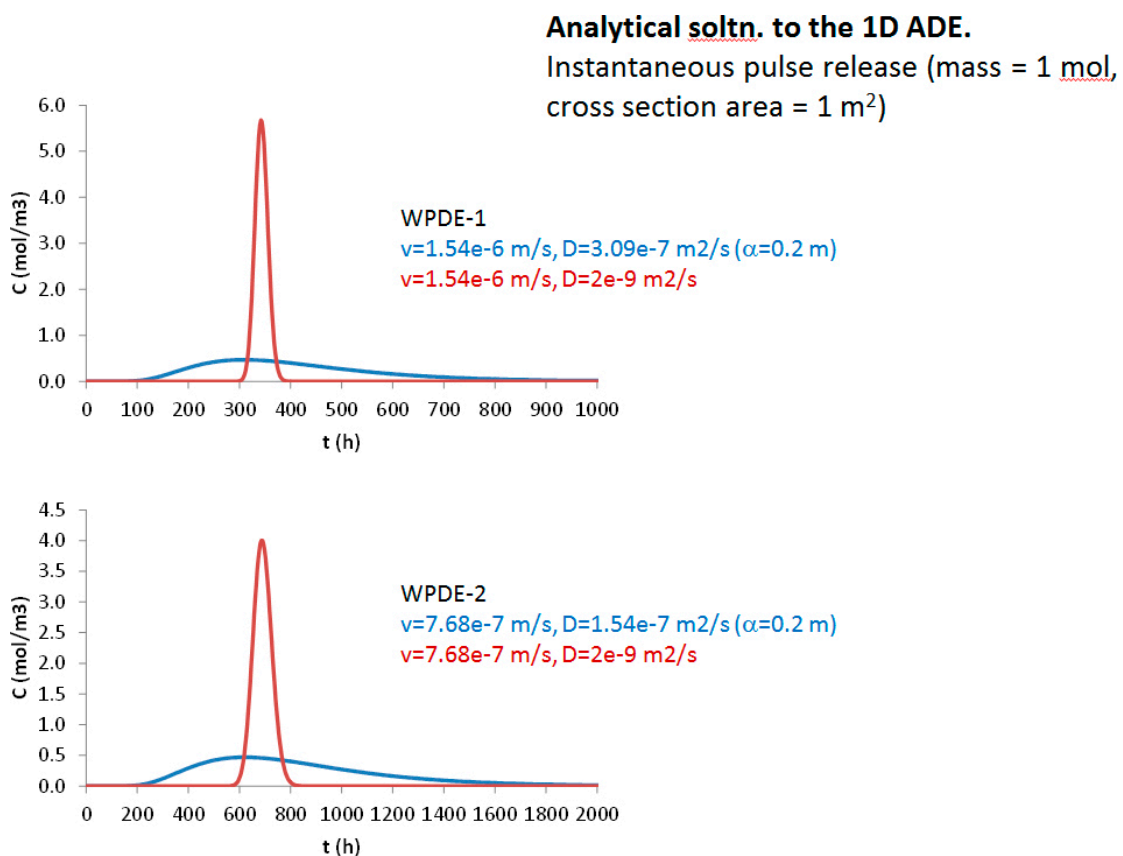


**Figure A3-1.** *Analytical solution to the 1D advection dispersion equation, with matrix diffusion neglected.*

Additionally, Antti Poteri and Kersti Nilsson have mentioned these points as potential causes for large dispersivities:

- Possibility for uneven distribution of the tracers into different injection points.

- The spatial scale of the roughness of the drillhole wall.

- Possible variations in the shape of the drill hole cross-section.

- Accuracy in centering of the drill hole dummy into the drill hole.

Some of these system properties cannot currently be evaluated but are expected to lead to dispersivities in excess of that from Taylor-dispersion and diffusion. These points will be considered further in the planned detailed modelling of the WPDE experiments later in the task.

For the current work most groups have used a dispersivity of about 10 % of the artificial fracture length. In order to facilitate comparison of the tailing within the models, we'd like to ask whether the groups who have used a significantly smaller dispersion can provide a simulation with a comparable dispersivity (suggested value 0.19 m), in addition to your original simulation. In addition, this could serve as an illustration of the sensitivity of the results to dispersion.

It is intended to amend the Task 9A description to include this discussion at a future date but has been sent out now because you may be working on your revised models.

Best wishes

Bill Lanyon

## Data for Task Description 9A

In this appendix, data from the Excel-file constituting data delivery #2 are tabulated. The Excel-file is comprised of 11 spreadsheets where the first one gives the content of the following ten. Data that are tabulated in Chapter 2 are not duplicated. In some cases, the spreadsheets contain too many rows to reproduce.

### A4.1 Experimental setup and geometries

The data of this spreadsheet relate to Section 2.3.1 of the task description. For numerical data on the caliper measurements, data delivery 2 is referred to.

**Table A4-1. Data relating to Section 2.3.1.**

| Description | Data | Unit |
| --- | --- | --- |
| Length of drillhole ONK-PP323 | 21.65 | m |
| Dip of drillhole ONK-PP323 | −10 | ° |
| Length of experimental section | Cf. Table 2-1 | m |
| From borehole length | 17.945 | m |
| To borehole length | 19.850 | m |
| Dummy diameter | Cf. Table 2-1 | m |
| Drillhole diameter* | 0.0565 | m |
| Aperture of annular slot | Cf. Table 2-1 | m |
| Inner diameter of PEEK tubing | Cf. Table 2-1 | m |
| Length of inlet PEEK tube | Cf. Table 2-1 | m |
| Length of outlet PEEK tube to online detector | Cf. Table 2-1 | m |
| Length of outlet PEEK tube to sampling valve | Cf. Table 2-1 | m |

\* This value is somewhat contradicted by caliper data (see below). Choice is up to modeller.
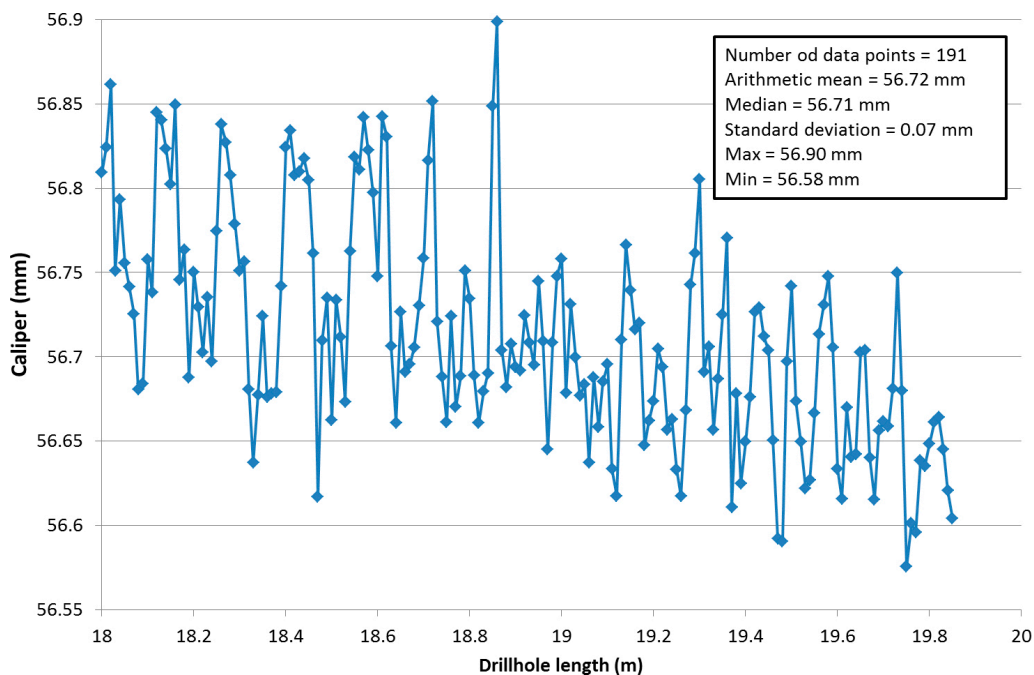


*Figure A4-1.* Caliper data from in-borehole diameter measurements in the WPDE borehole ONK-PP323. Unpublished data obtained by POSIVA. Data is saved to Posiva's research database POTTI.

## A4.2 Flows, experimental pressures and temperature

The data of this spreadsheet relate to Section 2.3.2 of the task description. For numerical data on flow rates and ambient pressures, data delivery 2 is referred to.

**Table A4-2. Data relating to Section 2.3.2.**

| Description | Data | Unit |
|---|---|---|
| Daily averaged flow rates WPDE-1 | Plotted in Figure 2-4 | |
| Daily averaged flow rates WPDE-2 | Plotted in Figure 2-4 | |
| Length of packed-off guard section | 1 | m |
| From borehole length | 6.09 | m |
| To borehole length | 7.09 | m |
| Location of flowing fracture in guard section | 7.64 | m |
| Ambient pressure in experimental section WPDE-1 | Plotted in Figure 2-4 | |
| Ambient pressure in guard section WPDE-1 | Plotted in Figure 2-4 | |
| Ambient pressure in experimental section WPDE-2 | Plotted in Figure 2-4 | |
| Ambient pressure in guard section WPDE-2 | Plotted in Figure 2-4 | |
| Assumed experimental temperature | 11 | °C |
| Upper temperature in container | 17 | °C |
| Lower temperature in container | 14 | °C |

## A4.3 The tracer injection solution and injection data

The data of this spreadsheet relate to Section 2.3.3 of the task description.

**Table A4-3. Data relating to Section 2.3.3.**

| Description | Data | Unit |
|---|---|---|
| Length of injection loop WPDE-1 | 1.24 | m |
| Weight of injected solution in WPDE-1 | 0.999 | g |
| Rate of flushing flow WPDE-1 | 2.0E-05 | L/m |
| Period of flushing WPDE-1 | 3 | h |
| Time of injection WPDE-1 | 2012-03-08 14:12 | yy-mm-dd hh:mm |
| Injected HTO activity WPDE-1 | Cf. Table 2-2 | |
| Injected Na-22 activity WPDE-1 | Cf. Table 2-2 | |
| Injected Cl-36 activity WPDE-1 | Cf. Table 2-2 | |
| Length of injection loop WPDE-2 | 3.70 | m |
| Weight of injected solution in WPDE-2 | 2.963 | g |
| Rate of flushing flow WPDE-2 | 1.0E-05 | L/m |
| Period of flushing WPDE-2 | 25 | h |
| Time of injection WPDE-2 | 2013-01-23 14:27 | yy-mm-dd hh:mm |
| Injected HTO activity WPDE-2 | Cf. Table 2-2 | |
| Injected Na-22 activity WPDE-2 | Cf. Table 2-2 | |
| Injected Cl-36 activity WPDE-2 | Cf. Table 2-2 | |
| Injected Sr-85 activity WPDE-2 | Cf. Table 2-2 | |
| Injected Ba-133 activity WPDE-2 | Cf. Table 2-2 | |
| Half-lives of tracers HTO | Cf. Table 2-2 | |
| Half-life Na-22 | Cf. Table 2-2 | |
| Half-life Cl-36 | Cf. Table 2-2 | |
| Half-life Sr-85 | Cf. Table 2-2 | |
| Half-life Ba-133 | Cf. Table 2-2 | |

## A4.4 Water chemistry

This spreadsheet contains no data, but only the following instruction/statement:

- In Task 9A the synthetic groundwater of the tracer cocktail should be assumed to represent the matrix pore water and geochemical conditions should be assumed to be constant in space and time. Hence there is no straightforward way to incorporate the groundwater chemistry data given in Section 2.3.4 in the modelling. Therefore the data are not reproduced here.

## A4.5 Detection of tracers

The data of this spreadsheet relate to Section 2.3.5 of the task description.

**Table A4-4. Data relating to Section 2.3.5.**

| Description | Data | Unit |
|---|---|---|
| Start of online detection WPDE-1 | 2012-03-08 | yy-mm-dd |
| End of online detection WPDE-1 | 2012-08-16 | yy-mm-dd |
| Start of water sampling WPDE-1 | 2012-03-08 | yy-mm-dd |
| End of water sampling WPDE-1 | 2012-08-21 | yy-mm-dd |
| Start of online detection WPDE-2 | 2013-01-23 | yy-mm-dd |
| End of online detection WPDE-2 | 2014-08-13 | yy-mm-dd |
| Start of water sampling WPDE-2 | 2013-01-21 | yy-mm-dd |
| End of water sampling WPDE-2 | 2014-07-07 | yy-mm-dd |

## A4.6 Rock type, lithology, and mineralogy

These data of this spreadsheet relate to Section 2.4.1 of the task description.

**Table A4-5. Data relating to Section 2.4.1.**

| Description | Data | Unit |
|---|---|---|
| Assumed fraction of VGN surrounding the WPDE section | 90 | % |
| Assumed fraction of PGR surrounding the WPDE section | 10 | % |
| Assumed maximum foliation angle relative to drillhole axis, upper value | 90 | ° |
| Assumed maximum foliation angle relative to drillhole axis, lower value | 60 | ° |

Moreover, the following instruction/statement is given:

- Data in Section 2.4.1 should be used as background information when setting up a representation of the rock volume surrounding the experimental section. How this is done is decided by each modelling group and a range of different approaches could be used. Hence, the data from Section 2.4.1 on rock type, lithology and mineralogy are generally not reproduced, with exception for the assumed foliation and rock type distribution.

## A4.7 Rock samples of the REPRO laboratory campaign

This spreadsheet contains no data, but only the following instruction/statement:

- Data in Section 2.4.2 only concern the partitioning of drill cores into rock samples. Measurement data on these rock samples are provided in subsequent sections. Hence, no data from Section 2.4.2 are reproduced.

## A4.8 Porosity

The data of this spreadsheet relate to Section 2.4.3 of the task description and are found in Table 2-8.

Rock matrix effective diffusivity and permeability

The data of this spreadsheet relate to Section 2.4.4 of the task description and are found in Table 2-9 and Table 2-10. Moreover, it is suggested that the ratio between diffusivity in gas phase and liquid phase is 11 600.

## A4.9 Sorption partitioning coefficients

The data of this spreadsheet relate to Section 2.4.5 of the task description and are found in Table 2-11.

## Description of the tracer inlet for Task 9A

This appendix reproduces data delivery 3, titled "Description of the tracer inlet for Task 9A: flow path of the water and tracer at the inlet and outlet of the experiment section".

**May 2015**
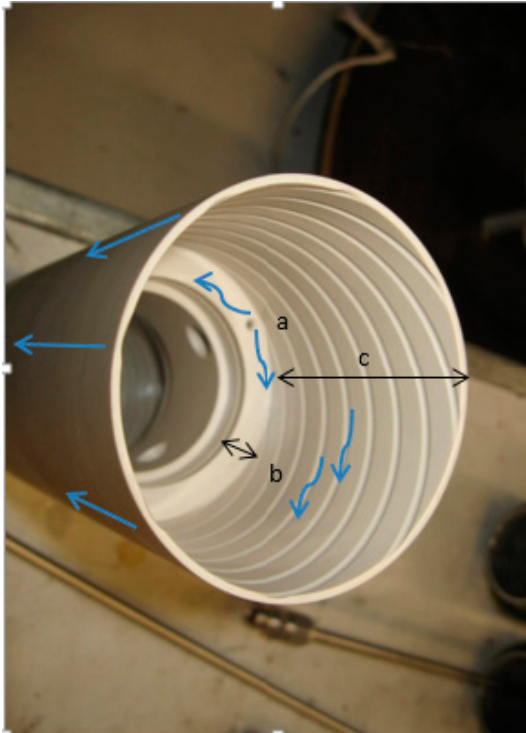


***Figure A5-1.*** *Photo of the inside of the socket for water/tracer inlet/outlet. Blue arrows indicate water/tracer flow. The large hole in the middle of the socket is sealed with a rod, delimiting the inner part of the slit (b) at the bottom. The labels and dimensions a) to d) are identical for Figures A5-1 and A5-2 and Table A5-1.*
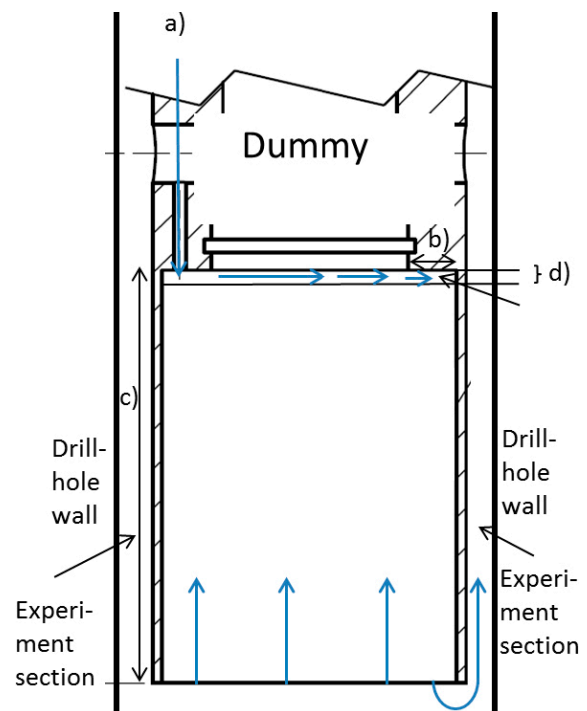


***Figure A5-2.*** *Details of the water/tracer inlet (view from the outside; a) Inlet, b) socket "shelf"/slit at the bottom, c) length of the socket and d) height of the slit between the socket bottom and the packer sleeve. Blue arrows indicate water/tracer flow. The inlet is at the far side of the drillhole, relative to the tunnel. (see Figure 3) Accordingly the flow in the PEEK tubing and the grooves is directed towards the end of the drillhole while the flow in the annular slot is directed towards the tunnel. This explains the curved blue arrow in the lower right of the figure.*

1. Water and the tracer pulse are pumped through the PEEK tubing and then through the inlet hole (a) (See Figure 1 and 2). The design of the water/tracer outlet is identical. The dimensions of the socket are given in Table 1 below.

2. The large hole in the middle of the socket (Figure 1) is sealed with a rod, delimiting the inner part of the slit (b) at the bottom.

3. From the inlet (a), the water/tracer reach the slit (b).

4. From the slit (b), the water/tracer flow arrives first to the closest groove, which is spiralled through the socket with a gradient of 50 mm length per 360° turn. The individual 8 grooves are each sealed-off by a teflonized packer sleeve (green in Figure 4 below), which fills the whole socket except for the slit in the bottom.

5. The water/tracer will then flow successively in the slit (b) to the following grooves and is led through these grooves to the end of the socket, where a packer ("golden", in Figure 4) forces the water to "turn back" and flow outside the socket/PEEK dummy, between the dummy and the drillhole wall.

**Table A5-1. Dimensions of the in- and outlet to/from the experiment section of WPDE-1 and WPDE-2.**

| Parameter | Value (mm) |
|---|---|
| a) Diameter of the inlet hole | 2.0 |
| b) Width of the slit at the socket bottom | 5.9 |
| c) Length of the socket | 71.0 |
| d) Slit between socket and packer | 1.0 |
| Diameter of the grooves | 1.5 |
| Length of the grooves | 237 |
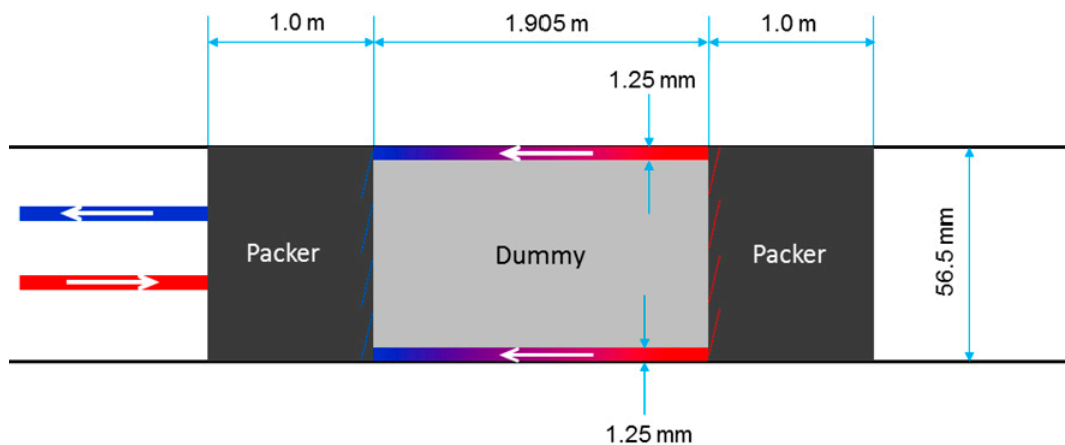


**Figure A5-3.** *Side view of the experimental section.*
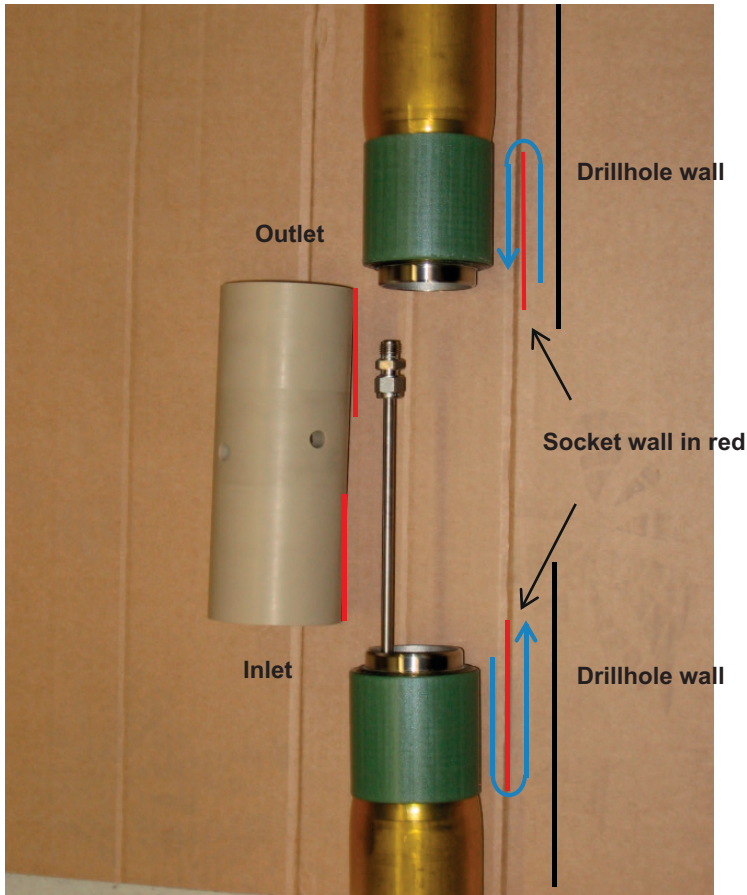
*Figure A5-4.* *A photo showing the packer sleeve (green) covering the grooves. (The equipment in the photo belongs to another experiment with a shorter PEEK dummy.) The water flow (blue arrows) in and out of the section is also displayed.*

## WPDE Photographs with higher resolution

This appendix reproduces the high resolution photos of data delivery 3. The last two figures of the data delivery are already shown in large size in Figure 2-9 and Figure 2-10.



***Figure A6-1.*** *Larger reproduction of Figure 2-2.*
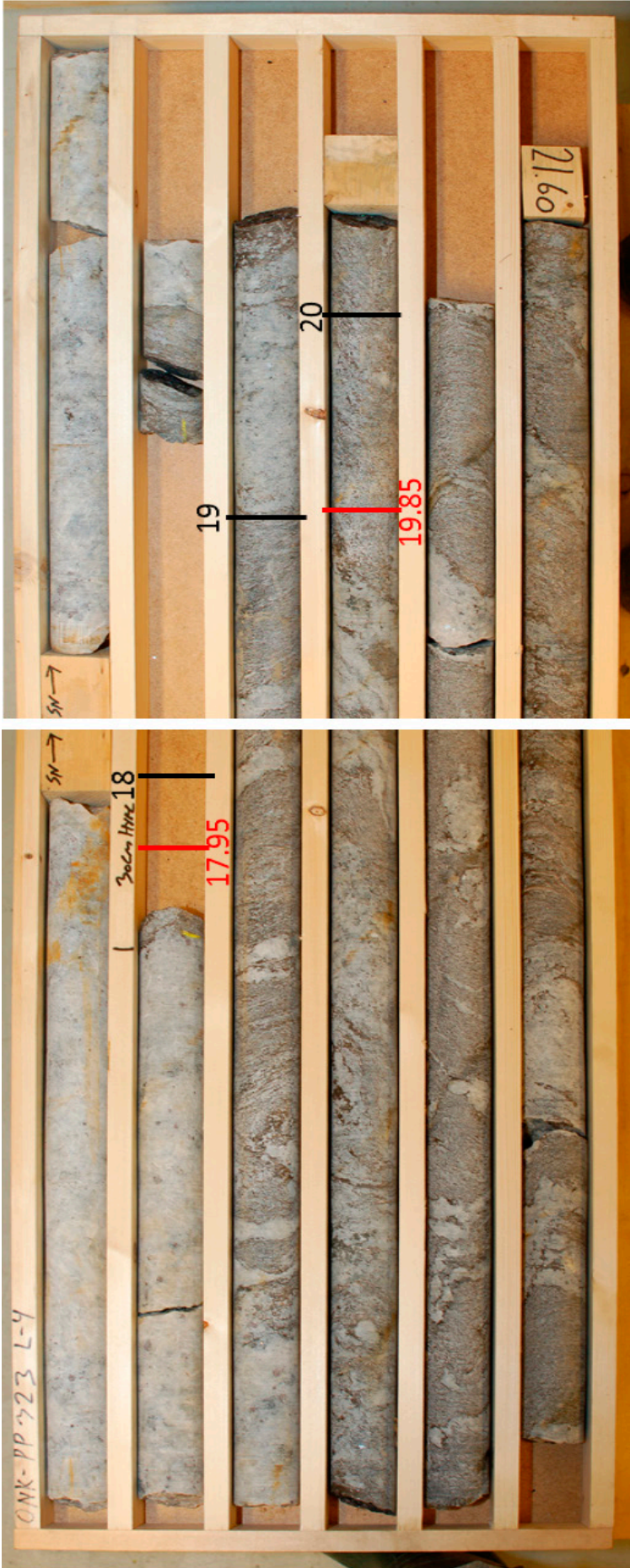
*Figure A6-2. Larger reproduction of Figure 2-8.*

***Figure A6-3.*** *Larger reproduction of Figure 2-8.*

# REPRO WPDE-1 and WPDE-2 (Task 9A) update 2 concerning tracer cocktail densities

*Kersti Nilsson and Johan Byegård, 2017-08-28*

## A7.1    Introduction

In an early draft version of the Posiva Working Report concerning 9A (WPDE-1; Poteri et al. a), two different values for the total chloride concentration in the tracer injection solution of $^{36}$Cl were reported. The presented lower chloride concentration initiated the thoughts of a possible buoyancy driven transport of the tracer cocktail volume in the WPDE experiment section due to the assumed density differences. This theory was presented by Neretnieks et al. in a memo shown in Appendix 8, and at the SKB Task Force GWFTS Workshop in Helsinki in October 2016. Personnel at Helsinki University (HYRL) who prepared the injected tracer cocktails have checked the two presented values, and in this update the correct value of the chloride concentration in WPDE-1 (WPDE-1; Poteri et al. a) is reported together with the correct value for WPDE-2 (WPDE-2; Poteri et al., b). HYRL has also performed density measurements of produced replicates of the two tracer cocktails as well as the REPRO Synthetic groundwater. The effect of temperature differences on densities has been evaluated.

Since Task 9A was set up to be a predictive "warm-up" case, this PM is not considered to be a part of the 9A Task Description, but consists of complementary information.

---

**Clarification or comment**

Poteri et al. a, b should be Poteri et al. 2018 a, b.

---

## A7.2    Updated REPRO WPDE-1 and WPDE-2 tracer cocktail densities

### A7.2.1    Chemical composition

The tracer cocktails in WPDE-1 and WPDE-2 consisted only of the tracer stock solutions and no added salts (WPDE-1; Poteri et al. a; WPDE-2; Poteri et al. b). Of the stock solutions, only the $^{36}$Cl solution is reported to contain significant amount of carrier (6.5 and 16 mg/mL Cl in the NaCl form, in WPDE-1 and WPDE-2, respectively). Thus, $Na^+$ and $Cl^-$ are the dominating species adding density to the solution and the contribution of other ions can be considered negligible ($[H^+]$ is included in WPDE-2). Results from density calculations using PHREEQC (Parkhurst and Appelo 1999) at 9 °C (see Section A7.4 to A7.10) together with the measured density are shown in Table A7-1. The compositions of the solutions as well as the measured density values are presented in Section A7.7 to A7-10.

The experimentally determined density results at 20–22 °C performed by HYRL in April 2017 are included in the given uncertainties. I.e. the combined uncertainty given in Table A7-1 is the sum of a) the difference between the calculated value at 9 °C and the measured value at 20–22 °C and b) the measurement uncertainty at 20–22 °C.

### A7.2.2    Temperature effects

Also temperature differences have been discussed as a cause of density differences. At the time for injection, the measured temperature in the experiment container was 14.7 °C, while the estimated temperature in the experiment section was 10.7±0.2 °C. The estimation of temperature was based on measured temperatures in six different drillholes at elevations down to −850 m. An estimation of the density difference between the two temperatures in water with salinity corresponding to the tracer cocktail is 0.6 kg/m³. This density difference is not likely to cause a significant buoyancy effect.

**Table A7-1. Results from PHREEQC calculations (9 °C) and experimental determination of densities (20–22 °C) included in the uncertainties.**

| Solution | Density (g/cm³) | Uncertainty | Source |
|---|---|---|---|
| REPRO Synthetic Groundwater | 1.0081 | | Section A7.4 PhreeqC calculation at 9 °C |
| WPDE-1 Tracer Cocktail | 1.0019 | | Section A7.5 PhreeqC calculation at 9 °C |
| WPDE-2 Tracer Cocktail | 1.0095 | | Section A7.6 PhreeqC calculation at 9 °C |
| REPRO Synthetic Groundwater | 1.0156 | 0.0003 | Section A7.10 HYRL uncalibrated at 20–22 °C |
| WPDE-1 Tracer Cocktail | 1.0089 | 0.0002 | Section A7.10 HYRL uncalibrated at 20–22 °C |
| WPDE-2 Tracer Cocktail | 1.0161 | 0.0002 | Section A7.10 HYRL uncalibrated at 20–22 °C |
| REPRO Synthetic Groundwater | 1.0088 | | Section A7.10 HYRL calibrated pipette volume |
| WPDE-1 Tracer Cocktail | 1.0022 | | Section A7.10 HYRL calibrated pipette volume |
| WPDE-2 Tracer Cocktail | 1.0093 | | Section A7.10 HYRL calibrated pipette volume |
| REPRO Synthetic Groundwater | 1.0081 | 0.0008 | Best estimate & uncertainty |
| WPDE-1 Tracer Cocktail | 1.0019 | 0.0004 | Best estimate & uncertainty |
| WPDE-2 Tracer Cocktail | 1.0095 | 0.0003 | Best estimate & uncertainty |
| Potential magnitude of temperature effect | ~0.0006 | | |

## A7.3 Conclusion

The best estimate densities and uncertainties in Table A7-1 suggest that buoyancy effects, as described by Neretnieks et al. in Appendix 8, may be significant in WPDE-1 but not in WPDE-2.

## A7.4 PHREEQC calculations for REPRO Synthetic Groundwater at 9 °C

```
                              REPRO_9.docx
   Input file: K:\60_Externt\6044xx\604413_SKB_Task 9 GWFTS, Task 9B, 9C\Task
9B-3\density\phreeqe calc\After HYRL 20170607\REPRO_9.pqi
   Output file: K:\60_Externt\6044xx\604413_SKB_Task 9 GWFTS, Task 9B, 9C\Task
9B-3\density\phreeqe calc\After HYRL 20170607\REPRO_9.pqo
Database file: C:\Program Files (x86)\USGS\Phreeqc Interactive
2.18.5570\database\phreeqc.dat

------------------
Reading data base.
------------------

        SOLUTION_MASTER_SPECIES
        SOLUTION_SPECIES
        PHASES
        EXCHANGE_MASTER_SPECIES
        EXCHANGE_SPECIES
        SURFACE_MASTER_SPECIES
        SURFACE_SPECIES
        RATES
        END
------------------------------------
Reading input data for simulation 1.
------------------------------------

        DATABASE C:\Program Files (x86)\USGS\Phreeqc Interactive
2.18.5570\database\phreeqc.dat
        SOLUTION_SPREAD
          temp     9
           Br     C(4)    Ca      K      Mg         Na          Si      Sr
     Cl
          0.62   0.1599  31.12   0.24   1.41    121.4656       0.101   0.126
186.152
------------------------------------------------
Beginning of initial solution calculations.
------------------------------------------------

Initial solution 1.

--------------------------Solution composition----------------------------

        Elements          Molality        Moles

        Br                6.200e-004      6.200e-004
        C(4)              1.599e-004      1.599e-004
        Ca                3.112e-002      3.112e-002
        Cl                1.862e-001      1.862e-001
        K                 2.400e-004      2.400e-004
        Mg                1.410e-003      1.410e-003
        Na                1.215e-001      1.215e-001
        Si                1.010e-004      1.010e-004
        Sr                1.260e-004      1.260e-004

--------------------------Description of solution--------------------------

                                    pH  =    7.000
                                    pe  =    4.000
                 Specific Conductance (uS/cm, 9 oC) = 12671
                          Density (g/cm3)  =    1.00807
                          Activity of water  =    0.994
                             Ionic strength  =    2.196e-001
                        Mass of water (kg)  =    1.000e+000
                    Total alkalinity (eq/kg)  =    1.353e-004
                        Total CO2 (mol/kg)  =    1.599e-004
                        Temperature (deg C)  =    9.000
                     Electrical balance (eq)  =    1.103e-004
    Percent error, 100*(Cat-|An|)/(Cat+|An|)  =    0.03
                              Iterations  =    6
                                 Total H  = 1.110130e+002
                                 Total O  = 5.550708e+001
                                   Sida 1
```

```
-------------------------Distribution of species-------------------------

                                                  Log        Log        Log
          Species            Molality    Activity  Molality   Activity   Gamma

          H+                 1.253e-007  1.000e-007  -6.902    -7.000    -0.098
          OH-                3.772e-008  2.660e-008  -7.423    -7.575    -0.152
          H2O                5.551e+001  9.942e-001   1.744    -0.003     0.000
Br             6.200e-004
          Br-                6.200e-004  4.293e-004  -3.208    -3.367    -0.160
C(4)           1.599e-004
          HCO3-              1.186e-004  8.840e-005  -3.926    -4.054    -0.128
          CO2                2.513e-005  2.644e-005  -4.600    -4.578     0.022
          CaHCO3+            1.073e-005  8.000e-006  -4.969    -5.097    -0.128
          NaHCO3             4.274e-006  4.496e-006  -5.369    -5.347     0.022
          MgHCO3+            6.437e-007  4.818e-007  -6.191    -6.317    -0.126
          CaCO3              3.614e-007  3.802e-007  -6.442    -6.420     0.022
          CO3-2              9.041e-008  2.791e-008  -7.044    -7.554    -0.510
          SrHCO3+            4.277e-008  3.188e-008  -7.369    -7.496    -0.128
          NaCO3-             2.677e-008  2.004e-008  -7.572    -7.698    -0.126
          MgCO3              9.629e-009  1.013e-008  -8.016    -7.994     0.022
          SrCO3              4.306e-010  4.529e-010  -9.366    -9.344     0.022
Ca             3.112e-002
          Ca+2               3.111e-002  1.002e-002  -1.507    -1.999    -0.492
          CaHCO3+            1.073e-005  8.000e-006  -4.969    -5.097    -0.128
          CaCO3              3.614e-007  3.802e-007  -6.442    -6.420     0.022
          CaOH+              2.210e-008  1.654e-008  -7.656    -7.781    -0.126
Cl             1.862e-001
          Cl-                1.862e-001  1.323e-001  -0.730    -0.879    -0.148
H(0)           1.593e-025
          H2                 7.964e-026  8.377e-026 -25.099   -25.077     0.022
K              2.400e-004
          K+                 2.400e-004  1.705e-004  -3.620    -3.768    -0.148
          KOH                5.588e-012  5.878e-012 -11.253   -11.231     0.022
Mg             1.410e-003
          Mg+2               1.409e-003  4.862e-004  -2.851    -3.313    -0.462
          MgHCO3+            6.437e-007  4.818e-007  -6.191    -6.317    -0.126
          MgCO3              9.629e-009  1.013e-008  -8.016    -7.994     0.022
          MgOH+              5.093e-009  3.812e-009  -8.293    -8.419    -0.126
Na             1.215e-001
          Na+                1.215e-001  9.044e-002  -0.916    -1.044    -0.128
          NaHCO3             4.274e-006  4.496e-006  -5.369    -5.347     0.022
          NaCO3-             2.677e-008  2.004e-008  -7.572    -7.698    -0.126
          NaOH               5.648e-009  5.941e-009  -8.248    -8.226     0.022
O(0)           0.000e+000
          O2                 0.000e+000  0.000e+000 -47.710   -47.688     0.022
Si             1.010e-004
          H4SiO4             1.009e-004  1.061e-004  -3.996    -3.974     0.022
          H3SiO4-            1.125e-007  8.421e-008  -6.949    -7.075    -0.126
          H2SiO4-2           5.797e-014  1.820e-014 -13.237   -13.740    -0.503
Sr             1.260e-004
          Sr+2               1.260e-004  4.077e-005  -3.900    -4.390    -0.490
          SrHCO3+            4.277e-008  3.188e-008  -7.369    -7.496    -0.128
          SrCO3              4.306e-010  4.529e-010  -9.366    -9.344     0.022
          SrOH+              2.817e-011  2.079e-011 -10.550   -10.682    -0.132

---------------------------Saturation indices---------------------------

          Phase          SI  log IAP   log KT

          Aragonite     -1.30    -9.55    -8.25  CaCO3
          Calcite       -1.15    -9.55    -8.41  CaCO3
          Chalcedony    -0.22    -3.97    -3.75  SiO2
          Chrysotile   -10.18    24.11    34.29  Mg3Si2O5(OH)4
          CO2(g)        -3.32    -4.58    -1.25  CO2
          Dolomite      -3.72   -20.42   -16.70  CaMg(CO3)2
          H2(g)        -22.00   -25.08    -3.08  H2
          H2O(g)        -1.95    -0.00     1.95  H2O
                              Sida 2
```

```
          Halite          -3.47    -1.92    1.54   NaCl
          O2(g)          -44.93   -47.69   -2.76   O2
          Quartz           0.26    -3.97   -4.23   SiO2
          Sepiolite       -6.75     9.45   16.20   Mg2Si3O7.5OH:3H2O
          Sepiolite(d)    -9.21     9.45   18.66   Mg2Si3O7.5OH:3H2O
          SiO2(a)         -1.12    -3.97   -2.85   SiO2
          Strontianite    -2.65   -11.94   -9.29   SrCO3
          Talc            -7.15    16.17   23.33   Mg3Si4O10(OH)2
```

```
------------------
End of simulation.
------------------


-----------------------------------
Reading input data for simulation 2.
-----------------------------------


-----------
End of run.
-----------
```

## A7.5 PHREEQC calculations for WPDE-1 Tracer Cocktail at 9 °C

```
                           WPDE1_9_degree.pqo
   Input file: K:\60_Externt\6044xx\604413_SKB_Task 9 GWFTS, Task 9B, 9C\Task
9B-3\density\phreeqe calc\After HYRL 20170607\WPDE1_9_degree.pqi
   Output file: K:\60_Externt\6044xx\604413_SKB_Task 9 GWFTS, Task 9B, 9C\Task
9B-3\density\phreeqe calc\After HYRL 20170607\WPDE1_9_degree.pqo
Database file: C:\Program Files (x86)\USGS\Phreeqc Interactive
2.18.5570\database\phreeqc.dat

------------------
Reading data base.
------------------

        SOLUTION_MASTER_SPECIES
        SOLUTION_SPECIES
        PHASES
        EXCHANGE_MASTER_SPECIES
        EXCHANGE_SPECIES
        SURFACE_MASTER_SPECIES
        SURFACE_SPECIES
        RATES
        END
----------------------------------
Reading input data for simulation 1.
----------------------------------

        DATABASE C:\Program Files (x86)\USGS\Phreeqc Interactive
2.18.5570\database\phreeqc.dat
        SOLUTION_SPREAD
        temp      9
          Na      Cl
        48.97   48.97
-----------------------------------------
Beginning of initial solution calculations.
-----------------------------------------

Initial solution 1.

-------------------------Solution composition------------------------------

        Elements          Molality        Moles

        Cl                4.897e-002   4.897e-002
        Na                4.897e-002   4.897e-002

-------------------------Description of solution----------------------------

                              pH  =    7.000
                              pe  =    4.000
        Specific Conductance (uS/cm, 9 oC) = 3646
                      Density (g/cm3)  =    1.00191
                     Activity of water =    0.998
                       Ionic strength  =    4.897e-002
                    Mass of water (kg) =    1.000e+000
                  Total alkalinity (eq/kg) = -8.126e-008
                   Total carbon (mol/kg) =    0.000e+000
                     Total CO2 (mol/kg) =    0.000e+000
                   Temperature (deg C)  =    9.000
                  Electrical balance (eq) =    8.126e-008
 Percent error, 100*(Cat-|An|)/(Cat+|An|) =    0.00
                          Iterations  =    4
                             Total H  = 1.110124e+002
                             Total O  = 5.550622e+001

-------------------------Distribution of species---------------------------

                                             Log      Log       Log
        Species          Molality  Activity  Molality Activity  Gamma

        H+               1.166e-007 1.000e-007  -6.933   -7.000   -0.067
        OH-              3.269e-008 2.671e-008  -7.486   -7.573   -0.088
                                  Sida 1
```

```
     H2O                     5.551e+001  9.983e-001     1.744    -0.001    0.000
Cl                4.897e-002
     Cl-                     4.897e-002  4.008e-002    -1.310    -1.397   -0.087
H(0)              1.657e-025
     H2                      8.284e-026  8.377e-026   -25.082   -25.077    0.005
Na                4.897e-002
     Na+                     4.897e-002  4.058e-002    -1.310    -1.392   -0.082
     NaOH                    2.646e-009  2.676e-009    -8.577    -8.572    0.005
O(0)              0.000e+000
     O2                      0.000e+000  0.000e+000   -47.689   -47.684    0.005

----------------------------Saturation indices----------------------------

          Phase               SI  log IAP   log KT

          H2(g)            -22.00   -25.08    -3.08  H2
          H2O(g)            -1.95    -0.00     1.95  H2O
          Halite            -4.33    -2.79     1.54  NaCl
          O2(g)            -44.93   -47.68    -2.76  O2

------------------
End of simulation.
------------------


-----------------------------------
Reading input data for simulation 2.
-----------------------------------


-----------
End of run.
-----------
```

## A7.6 PHREEQC calculations for WPDE-2 Tracer Cocktail at 9 °C [a)]

```
                           WPDE2_9_degree.pqo
    Input file: K:\60_Externt\6044xx\604413_SKB_Task 9 GWFTS, Task 9B, 9C\Task
9B-3\density\phreeqe calc\After HYRL 20170607\WPDE2_9_degree.pqi
   Output file: K:\60_Externt\6044xx\604413_SKB_Task 9 GWFTS, Task 9B, 9C\Task
9B-3\density\phreeqe calc\After HYRL 20170607\WPDE2_9_degree.pqo
Database file: C:\Program Files (x86)\USGS\Phreeqc Interactive
2.18.5570\database\phreeqc.dat

------------------
Reading data base.
------------------

        SOLUTION_MASTER_SPECIES
        SOLUTION_SPECIES
        PHASES
        EXCHANGE_MASTER_SPECIES
        EXCHANGE_SPECIES
        SURFACE_MASTER_SPECIES
        SURFACE_SPECIES
        RATES
        END
-----------------------------------
Reading input data for simulation 1.
-----------------------------------

        DATABASE C:\Program Files (x86)\USGS\Phreeqc Interactive
2.18.5570\database\phreeqc.dat
        SOLUTION_SPREAD
            temp      9
            ph        2
             Cl    Na
        252.01  206.3
-------------------------------------------
Beginning of initial solution calculations.
-------------------------------------------

Initial solution 1.

-------------------------Solution composition------------------------------

        Elements         Molality        Moles

        Cl              2.520e-001  2.520e-001
        Na              2.063e-001  2.063e-001

-------------------------Description of solution--------------------------
                                   pH  =    2.000
                                   pe  =    4.000
        Specific Conductance (uS/cm, 9 oC) = 18594
                           Density (g/cm3)  =    1.00945
                          Activity of water =    0.992
                             Ionic strength =    2.354e-001
                          Mass of water (kg) =   1.000e+000
                      Total alkalinity (eq/kg) = -1.257e-002
                        Total carbon (mol/kg) =   0.000e+000
                          Total CO2 (mol/kg) =   0.000e+000
                        Temperature (deg C)  =    9.000
                      Electrical balance (eq)  = -3.314e-002
  Percent error, 100*(Cat-|An|)/(Cat+|An|)  =   -7.04
                               Iterations  =    4
                            Total H  = 1.110250e+002
                            Total O  = 5.550622e+001

-------------------------Distribution of species--------------------------

                                                 Log      Log       Log
        Species         Molality  Activity  Molality Activity   Gamma

        H+              1.257e-002  1.000e-002   -1.901   -2.000   -0.099
                                    Sida 1
```

a)

```
                              WPDE2_9_degree.pqo
     OH-                3.794e-013  2.654e-013   -12.421    -12.576    -0.155
     H2O                5.551e+001  9.920e-001     1.744     -0.003     0.000
Cl              2.520e-001
     Cl-                2.520e-001  1.777e-001    -0.599     -0.750    -0.152
H(0)            1.587e-015
     H2                 7.935e-016  8.377e-016   -15.100    -15.077     0.024
Na              2.063e-001
     Na+                2.063e-001  1.529e-001    -0.686     -0.816    -0.130
     NaOH               9.494e-014  1.002e-013   -13.023    -12.999     0.024
O(0)            0.000e+000
     O2                 0.000e+000  0.000e+000   -67.713    -67.690     0.024

---------------------------Saturation indices-----------------------------

        Phase              SI log IAP  log KT

        H2(g)            -12.00  -15.08   -3.08  H2
        H2O(g)            -1.95   -0.00    1.95  H2O
        Halite            -3.11   -1.57    1.54  NaCl
        O2(g)            -64.93  -67.69   -2.76  O2

------------------
End of simulation.
------------------


----------------------------------
Reading input data for simulation 2.
----------------------------------


-----------
End of run.
-----------
```

## A7.7 Composition of REPRO Synthetic Groundwater

**Repro water (WPDE-1 and WPDE-2).**

|         | **M**     |
|---------|-----------|
| SrCl$_2$  | 0.000126  |
| KCl     | 0.000240  |
| MgCl$_2$  | 0.00141   |
| CaCl$_2$  | 0.03112   |
| NaCl    | 0.1206    |
| NaF     | 0.0000857 |
| NaBr    | 0.00062   |
| NaHCO$_3$ | 0.000599  |
| SiO$_2$   | 0.000101  |

| **Substance** | **C (mmol/kg)** |
|---------------|-----------------|
| Sr            | 0.126           |
| K             | 0.24            |
| Mg            | 1.41            |
| Ca            | 31.12           |
| F             | 0.0857          |
| Br            | 0.62            |
| HCO$_3$         | 0.1599          |
| Na            | 121.4656        |
| Cl            | 186.152         |
| Si            | 0.101           |

## A7.8 Composition of WPDE-1 Tracer Cocktail

−1.5 mL of tracer containing Na-22 about 1.5 MBq, HTO about 15 MBq, Cl-36 about 1.5 MBq and I-125 about 4.5 MBq.

HTO + $H_2O$
Na-22 (NaCl 0.0000004 M)
Cl-36 (NaCl 0.04897 M; carrier concentration 6.5 g/L)
I-125 (NaOH 0.0001 M, $Na_2SO_3$ 0.000006 M)
KI 0.000000024 M

| | |
|---|---|
| Na | 48.97 mmol/kg |
| Cl | 48.97 mmol/kg |

(All other additions are considered as negligible.)

## A7.9 Composition of WPDE-2 Tracer Cocktail

−1.5 mL of tracer containing HTO 26 MBq, Na-22 1.5 MBq, Cl-36 6.1 MBq, Sr-85 7.4 MBq and Ba-133 2.4 MBq.

HTO ($H_2O$)
Na-22 (NaCl 0.0000023 M)
Cl-36 (NaCl 0.2063 M; carrier concentration 16 g/L)
Sr-85 (HCl 0.02857 M, $SrCl_2$ 0.0000009 M)
Ba-133 (HCl 0.01714 M, $BaCl_2$ 0.000082 M)

| | |
|---|---|
| Na | 206.3 mmol/kg |
| Cl | 252.01 mmol/kg |
| $H^+$ | 45.71 mmol/kg |

(All other additions are considered as negligible.)

## A7.10 Measured density values obtained from HYRL

| Waters | Density (g/ml) |
|---|---|
| MilliQ water | 1.0047 ± 0.0002 |
| Repro water (WPDE1 and WPDE2) | 1.0156 ± 0.0003 |
| Simulated tracer WPDE1 | 1.0089 ± 0.0002 |
| Simulated tracer WPDE2 | 1.0161 ± 0.0002 |

The density for the MilliQ water is not what should be expected from literature value. An average of the literature values in the 20–22 °C gives a value of 0.9980 g/ml and using this as a calibration yields that the 5 ml pipette used by HYRL in their determination actually had a volume of 5.034 ml.

Using the operation above as a calibration will result in the following densities:

| | Before calibration | After calibration |
|---|---|---|
| MilliQ water | 1.0047 | (0.9980) |
| Repro water | 1.0156 | 1.0088 |
| WPDE1 | 1.0089 | 1.0022 |
| WPDE2 | 1.0161 | 1.0093 |

# A note on the breakthrough curves in Repro experiments. Exploration of possible impact of gravity differences between tracer solution and water.

*Ivars Neretnieks, Luis Moreno and Longcheng Liu*
*Department of Chemical Engineering and Technology, Royal Institute of Technology, KTH,*
*Stockholm, Sweden*
*September 27, 2016*

## Abstract

It is assumed that the readers of this note are familiar with the REPRO experiments and the Task 9 description of them.

The interpretation of tracer experiments in the REPRO project is revisited. The observed very early arrival of tracers is not readily understood by *known* flowrate anomalies in the equipment. We seek other reasons that can be supported by the known design, physics and chemistry of the system. It is found that the less dense tracer solution slug can migrate rapidly, along the inclined, 10 degrees, experimental slot to the outlet end, driven by density differences causing buoyancy effects. The outlet end lies higher than the inlet. This is also supported by a scoping experiment presented in Section A8.7 in this Note. Two consequences of this are explored.

One is that the less dense tracer collects at the top of the slot from which it cannot flow downward and out through the uppermost groove, due to the buoyancy difference.

Eventually, by molecular diffusion, the tracer diffuses downward to the level of a lower groove entrance. It also becomes denser by taking up salt from the denser GW, decreasing the buoyancy. Then the liquid can be carried away out through the exit hole. This explains that the tracer could start to arrive at less than a third of the mean GW residence time. It also explains the subsequent long "even" concentration plateau. Mathematical modelling supports this, which gives a reasonably good prediction of the tracer breakthrough curves based on only the geometry and the physical and chemical properties of the system.

The system is very sensitive to the density differences. Should the tracer solution be denser than the GW the opposite effect would occur, namely that the tracers collect at the bottom near the entry to the slot. Then the first arrival would be expected to be at the mean GW residence time PLUS that predicted for the less dense tracer solution case. That is $353 + \sim 50 = \sim 400$ hours. The tracer solution and the GW must have a very small density difference, probably considerably less than 1 kg/m$^3$ for either very early or delayed arrival NOT to occur.

Another consequence of the slug migration is that due to its small volume it may not move as a rigid slug but exchange solutes by molecular diffusion with the water it moves in and decrease the density difference to the water in different parts of the slug. This will generate an internal "circulation" in the slug driven by a combination of diffusion in the direction perpendicular to the buoyancy driven flow and the differences in the velocities in different location in the slug. These effects are explored by a simple model presented in Section A8.8. It is found that for the expected concentration differences between tracer slug and water the dilution of the slug underway is moderate and that the slug could start to arrive at the effluent in hours, which is considerably shorter than the flowing water residence time.

There are several uncertainties in the underlying data and in the presented modelling. It is found that both the trapping of the slug as well as the dilution by slug circulation may lead to a surprisingly early arrival of the tracers. The phenomena could be further studied by some simple experiments as well as by more detailed modelling.

## A8.1 Background

In the analysis of the breakthrough curves in REPRO experiments WPDE-1 and WPDE-2, as defined in the Task 9A description, it was suggested that the traced water flows in a concentric slot between a borehole wall and a cylindrical dummy. From the information in the task description the residence time of the water in the slot for WPDE-1 was 343 hours (14.3 days) and the delay time of the water in the tubing 32.5 hours (1.35 days). Surprisingly, the first tracer arrival was at about 100 hours (4 days) and the breakthrough was very sharp, reaching maximum concentration after about 5 days for all three tracers.

Figure A8-1 shows the breakthrough curves, BTC's, for the three tracers. The vertical dashed line shows the mean water residence time.

Predictions of the BTC using advection-dispersion models with Fickian dispersion caused by Taylor dispersion and Multi-channel model with Taylor dispersion as well as dispersion based on reasonable variations in slot apertures predicted very sharp rise of the concentration at around the mean water residence time, a quite sharp peak around the same time but a tailing similar to that in Appendix A in Soler et al. 2019.

The sharp early rise at a time about one third of the mean residence time, RT, could not be obtained by the models without considerably tweaking several parameters and using unsupported assumptions. Simulations were made to explore if a misalignment between borehole and dummy centres causing variations in water velocity in different locations around the slot showed that this could not give so large difference between peak arrival time and mean water velocity. Other reasons that might have caused the unexpected BTC's were explored e.g. clogging of inlet and outlet grooves around the dummy could be discarded by modelling because water velocity between adjacent inlet points (grooves) rapidly evens out downstream. See Section A8.9. Other ideas including the presence of stagnant water zones were tested. It was found to be possible to generate combinations of flowrate distributions and stagnant water zones that gave good fits to the experimental results. However, as it was not possible to find physical reasons to support such assumptions, this was not further pursued.
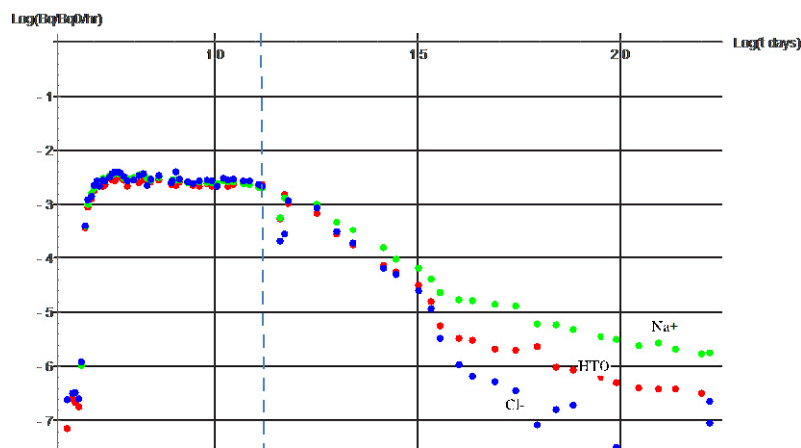


***Figure A8-1.*** *BTC's for Cl⁻, HTO, and Na⁺ for WPDE-1 experiment.*[7]

---

[7] Voutilainen, M., A. Poteri, K. Helariutta, M. Siitari-Kauppi, P. Andersson, J. Byegård, K. Nilsson, M. Skålberg, P. Kekäläinen, J. Timonen, P. Pitkänen, K. Kemppainen, J. Liimatainen, and L. Koskinen, In-situ experiments to investigate rock matrix retention properties in ONKALO, Olkiluoto, Finland, Key Topics in Deep Geological Disposal, Cologne, Germany, 25-26 September, 2014.

## A8.2　An alternative interpretation of the physical situation

**Migration of tracer along slot to the outlet driven by buoyancy**

First we consider the migration of a less dense tracer slug injected at the lower end of the experimental slot around the dummy in the ten degrees downward sloping borehole.

The time for the traced water to flow, driven by buoyancy, along the slot is estimated as follows. The transmissivity $T$ of a slot for laminar flow according to the "cubic law" is,

$$T = b^3 \frac{\rho_w g}{12 \mu_w} \tag{A8-1}$$

$b$ is the slot aperture, $\rho_w$ and $\mu_w$ the water density and viscosity respectively and $g$ the gravitational constant. The impact of the small differences in $\rho_w$ and $\mu_w$ between traced water and GW is negligible for determining $T$.

For a hydraulic gradient $grad$ caused by gravity difference in the 10 degree sloping slot.

$$grad = \frac{\Delta \rho}{\rho_w} \sin\left(\frac{\pi}{18}\right) \tag{A8-2}$$

The velocity of traced water for a density difference of 1 kg/m$^3$ and viscosity of $1.3 \times 10^{-3}$ Pa·s (at 10–11 °C) for $b = 1.25 \times 10^{-3}$ m superimposed on the velocity driven by pumping is:

$$u = \frac{T}{b} \, grad = 1.7 \times 10^{-4} \, m/s \tag{A8-3}$$

This is much larger than the mean velocity of the pumped water, $1.5 \times 10^{-6}$ m/s.

For a slot length of 1.905 m the time to tracer flow along the slot is 3.1 hours if the slug were not diluted by diffusion underway. Accounting for the gradual decrease in density difference cause by diffusional exchange between a rigid slug and GW during the slug migration the time increases to around 5.0 hours. This also was found to the case for a non-rigid slug with internal circulation. See Section A8.8. Obviously a small density difference suffices to let the traced solution to rapidly flow to the upper end of the slot. The traced water would thus move toward the outlet in a much shorter time than the mean water residences time in the slot, 343 hours, and give rise to a much shorter early arrival. However, in the equipment used, the slug is "trapped" near the outlet as explained in a later section. It will eventually escape aided by molecular diffusion, as will be described below. Section A8.5 presents data on the outlet section with the grooves and shows the importance of the pressure drop in them. Section A8.6 presents and discusses density data. Section A8.7 presents the results of very simple experiment that shows that a tracer slug rapidly can migrate driven by the buoyancy caused by a small density difference. In Section A8.8 it is also explored how the velocity of the slug and the arrival time is influenced by diffusion internally and between the slug and the surrounding water.

## A8.3　Subsequent fate of the tracer

**Details of the in and outlet sections**

For the subsequent modelling and discussion we need to be familiar with the rather complicated in- and outlet sections because especially the outlet section plays a central role in the modelling.

We consider the case when the injected traced water has a small density difference $\Delta \rho$ compared to the synthetic groundwater, GW, pumped through the slot. The borehole dips downward with angle of 10 degrees. The injected GW passes through a hole inside the dummy and is released into the borehole between the dummy and the packer at the bottom of the dummy, i.e. near the bottom of the borehole. The water is distributed inside of the hollow dummy and the packer through 8 spiral grooves. These circle the packer by one full turn. The small traced water volume, 1 ml, is less dense than the GW. It will "rapidly" flow up to the top of the slot driven by the density difference. It collects at the top ceiling of the slot at the exit end. At the upper end of the slot the water turns around the hollow dummy end into 8 grooves inside the dummy. The grooves circle the packer. See Figures A8-2 and A8-3. In the groove with the uppermost inlet where the less dense traced water has collected, the water has to be forced downward as the groove circles the packer. This is against the buoyancy force of the denser water in the groove. The tracer slug is about 4 cm wide at the outlet end, see Figure A8-3, at the widest location and probably only contacts the uppermost grove. In the

other grooves the water at their inlets has no or small density difference and can freely flow. The pressure drop in these grooves determines what buoyancy difference the less dense traced water must overcome to begin to flow. The needed density difference to hinder flow is 1.7 kg/m$^3$. The density difference is estimated to be between 1.3 and 2.9 kg/m$^3$, see Section A8.6. If it were not sufficiently large, the tracer slug would flow away from the top of the slot in less than a few hours and exit as a very narrow pulse with no additional delay. That is not what is observed.

Figure A8-2 illustrates how the traced water collects at the top of the circular slot. In the figure and for the subsequent modelling the circular slot is "unfolded" and straightened. The triangular region with the tracer is 2$b$ thick as both sides were folded together. The triangle symbolises the semi-triangular slug, which is 4.5 cm long and 3.9 cm wide in the slot if seen from above. Its volume is 0.999 cm$^3$. This is illustrated in Figure A8-2, which shows a cross section view of the dummy outlet end where the straight line shows the lowest elevation of the tracer slug at the end of the dummy. The slug extends only 4.5 cm along the slot because it slopes downward. In the mathematical model a rectangular slug with the same volume is used, shown by the dash-dot rectangle.

The borehole has 56.5 mm diameter and the dummy outer diameter is 54 mm. Because of the gravity difference the flowing water cannot force the low-density water down the groove toward the exit hole. See Figure A8-3. Thus the synthetic GW will not contain any tracer at early times although the tracer already has arrived at the exit end of the dummy.

Figure A8-3 combines the view of the outside of the dummy where the slot is located with the interior of the dummy where the spiral grooves lead the water back into the inside of the dummy to an outlet as if they were outside the dummy. This picture tries to illustrate that buoyancy of the traced water can hinder it to flow down the groove. The traced water is pushed a distance downward, indicated red in the figure, down the groove but cannot move further. The arrangement and flowpaths are described in more detail in Figures A8-3 and A8-4.

Figure A8-4 shows the arrangement at the end of the hollow dummy with the slot outside the dummy and the grooves inside the dummy. In the upper picture the water in the slot flows to the right, turns 180 degree at the end of the dummy and flows into the grooves inside the dummy and then to the left circling the packer in the grooves inside the dummy. After leaving the grooves the water will find its way to the exit hole shown in Figure A8-3 but not in Figure A8-4.
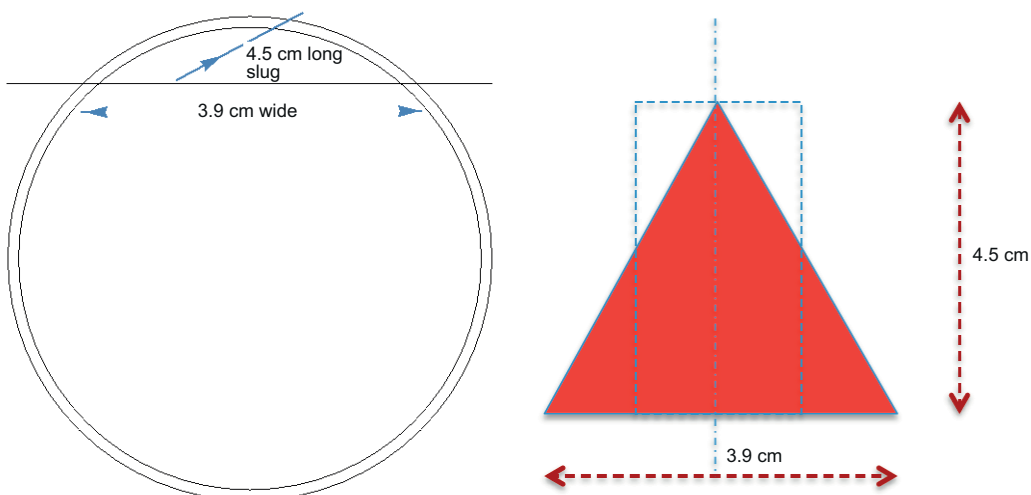


*Figure A8-2.* Cross section view of the dummy end. In the left figure the straight line shows the lowest elevation of the tracer slug at the end of the dummy. The right figure shows the tracer slug seen from above.
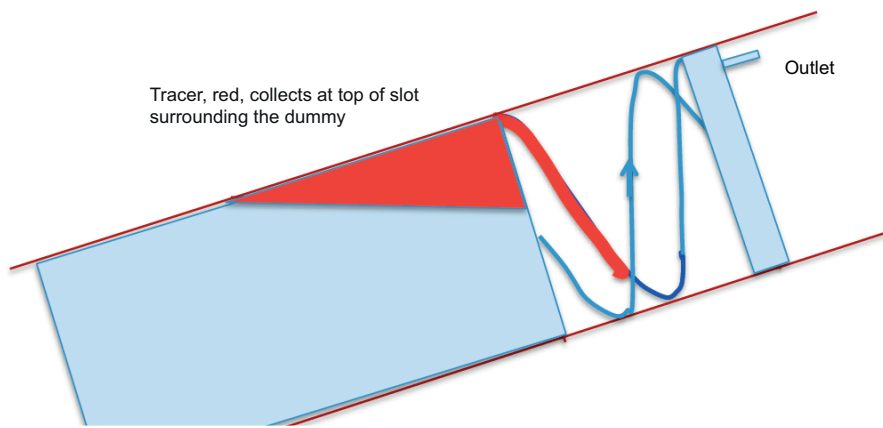
**Figure A8-3.** *Projection of slot around the dummy near the outlet end seen from the side, not to scale. Triangle illustrates where the traced water has collected in the slot surrounding the dummy. Two grooves surrounding the packer are shown as if they were outside the dummy although they actually are located inside the dummy and reversed to the left and downward in the figure. One with GW, blue, one with light traced water, red, that due to buoyancy cannot reach the lower portion of the groove.*
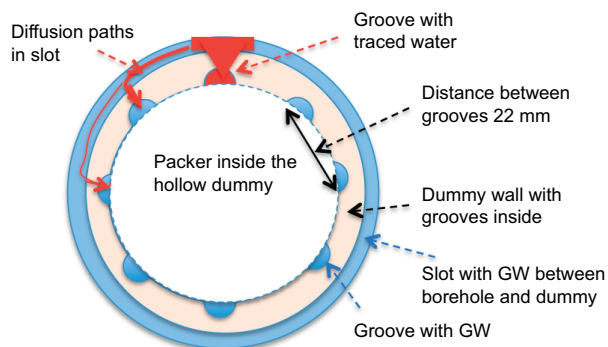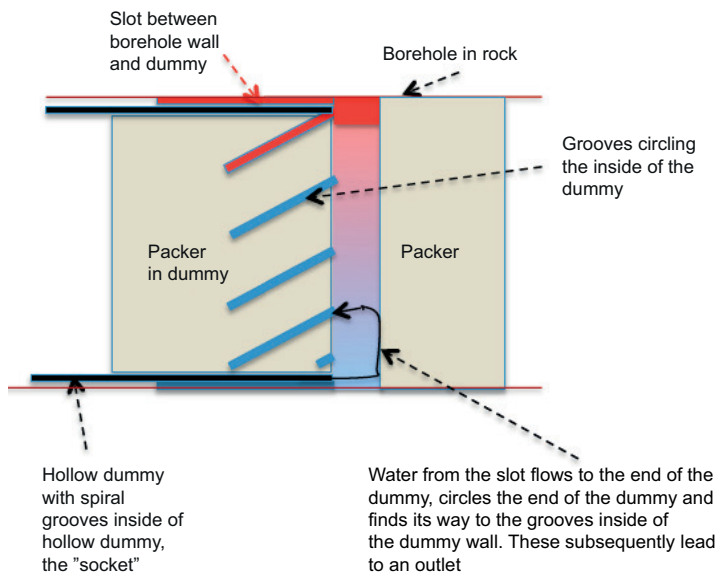




**Figure A8-4.** *Arrangement of slot connecting slot and grooves at the end of the dummy at the outlet section. Not to scale.*

The tracers from the slug trapped at the top of the dummy diffuse downward in the water in the slot to where the flowing water brings it into a slot. This is indicated in the upper picture.

The lower picture of Figure A8-4 shows how the grooves are arranged inside the dummy. The tracer, flowing from left to right then collects at the "ceiling" of the slot. It is in contact with the uppermost groove at the right end of the dummy (upper figure). The "red" water cannot flow as explained above. However, the tracers can migrate by molecular diffusion downward around the slot and be carried into the next or next-next groove by the water that is denser and can flow down the groove without encountering the buoyancy barrier. The tracers from the slug trapped at the top of the dummy diffuse downward in the water in the slot to where the flowing water brings it into a slot. This is indicated in the upper left part of the upper picture.

The diffusional exchange between slug and GW is directed both to and from the slug. The lower density of the slug will take up salt from the synthetic GW and the density difference will decrease. This is a rather rapid process for the *slug*. Its density would start to approach that of the more abundant GW in hours[8]. Then the slug would gradually loose it buoyancy and flow through the uppermost groove, were it not that that groove has become filled with the slug water with its original low density. This water acts as a stagnant plug hindering flow through the uppermost groove. Eventually the stagnant water plug in the groove also will be diluted by diffusion of salt form both ends of the "plug" in the groove. The length of the plug is on the order of 120 mm, if filled from the top to its lowest point. This is about 100 times as long as the height of the slug residing at the top of the slot. The time to considerably decrease its density by diffusion is proportional to the height squared of the slug as well as the plug. The latter is about 100 times larger so it would take on the order of many of thousands of hours for the plug to start to flow. When it does the remaining water of the slug will rapidly (less than a few hours) flow away. However, when the slug suddenly flows away after thousands of hours the flowing water will be supplied with tracers that re-emerge by diffusion from the rock matrix given rise to the long tail observed.

The mode and distance for the tracer to migrate by molecular diffusion from its location in the slot to the grooves where water can flow is crucial for the model. The diffusion paths are complex and we use $x_o$ as some unspecified mean distance. It is *the adjustable parameter in the model*. We have taken $x_o$ to be 5 cm in the simulations and will revisit

We are very conscious of the uncertainties involved in the above description but will nonetheless try to model and simulate the consequences of the above scenario.

**Mathematical modelling**

After the tracer slug has arrived at end of the slot it takes some time for the first traces of it to reach a groove with flowing water. This time is denoted by $t_D$. It can be estimated by diffusion modelling. The flowing water can carry it out to the exit region (blue) in Figure A8-3. Solute from above will continuously diffuse downward and be carried away by the GW and will deplete the slug. Gradually more and more solute will be carried away. However, the solute will also diffuse into the pores of the rock matrix around the slot in the *r*- direction (perpendicular to the picture in Figure A8-2). There it will temporarily accumulate. When the solute concentration in the water in the slot has been depleted to low values, the back-diffusion from the matrix will replenish the water.

The time $t_{D,0.01}$ for diffusion in the slot water to reach a concentration $0.01\ C_o$, where $C_o$ is the initial concentration in the traced water and $D_w$ is the diffusion coefficient ($2 \times 10^{-9}$ m²/s) is estimated. To exemplify we choose the arc length in the slot to the exit location to be $x_0 = 0.05$ m. This is about the distance to the second groove the solute must diffuse to exit.

$$t_{D,0.01} = \frac{1}{16}\frac{x_o^2}{D_w} = 21.7\ hrs \qquad\qquad (A8-4)$$

Before this time very little tracer will be carried out by the GW. For times longer than $t_{D,0.01}$ the situation can be conceived as being at pseudo steady state during which, neglecting the even slower matrix diffusion effect, the source is slowly depleted by diffusion into the flowing GW that carries

---

[8] The density difference between slug an GW will also change during the migration of the slug from the inlet end the outlet end where it is trapped. This is modelled and discussed in Section A8.8.

it out through the exit groove. To further simplify the model, the tracer solution is assumed to be rectangular instead of triangular and diffusion *along* the slot is neglected. This leaves only two dimensions, x for diffusion vertically and *r* for the radial diffusion in the matrix. Details of the model and computations can be found in the Mathematica® Notebook:*" Gravity impact radial diffusion.nb"*

The diffusion equation accounting for both the slot water and matrix becomes

$$\frac{\partial c}{\partial t}(\varepsilon(r) + K(r)) = D_e(r)\frac{\partial^2 c}{\partial x^2} + \frac{1}{r}\frac{\partial}{\partial r}\left(D_e(r)r\frac{\partial c}{\partial r}\right) \qquad (A8\text{-}5)$$

Note that this formulation does not specifically separate the water in the slot from that in the pores of the matrix. This is handled by using parameters that are functions of location.

The porosity $\varepsilon(r)$, volumetric sorption coefficient $K(r)$ and effective diffusivity $D_e(r)$ are function of $r$, i.e. the distance from the dummy into the rock matrix. $r_h$ is the radius of the borehole.

$$\varepsilon(r) = (1 - H(r - r_h)) \times 1 + H(r - r_h)\varepsilon_o \qquad (A8\text{-}6)$$

$H$ is the Heaviside function (If arg <0 in $H$(arg), $H$=0 else $H$=1)

$\varepsilon_0$ is the porosity of the rock matrix

$$K(r) = (1 - H(r - r_h)) \times 0 + H(r - r_h)K_o \qquad (A8\text{-}7)$$

$K_0$ is the solute dependent volumetric sorption coefficient of the rock matrix. For the water in the slot $K_0 = 0$.

$$D_e(r) = (1 - H(r - r_h)) \times D_w + H(r - r_h) D_p \varepsilon_o \qquad (A8\text{-}8)$$

$D_p$ is the pore diffusion coefficient of the rock matrix.

The initial condition is that $c$=1 in the region where the solute collected. The boundary conditions are that no solute passes $x$=0 and $r<r_D$, the radius of the dummy. The key boundary condition is that at $x \geq x_0$ the concentration is zero for all $r$. Note that in this way the model (5) does not invoke any specifics of the flowrate of water provided it is sufficiently large to maintain a low concentration while passing the slug. It just means that the flowing water so rapidly can carry away the tracer that concentration build up is negligible.

Figure A8-5 illustrates an example of the initial condition and the region modelled.

The extent of the matrix $r_0$ is chosen such that at the end of the experimental time the tip of solute concentration could barely reach $r_0$. $r_0$ is nuclide dependent.

Equation (A8-8) with the initial and boundary conditions and data in Table A8-1 is solved by the finite element method as implemented in Mathematica®.
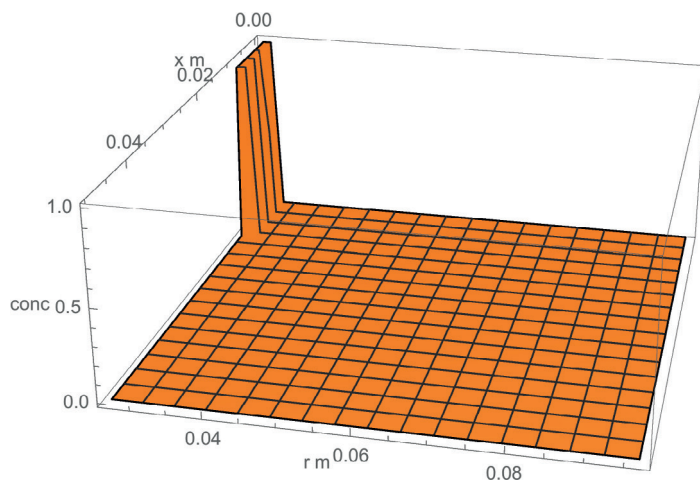


*Figure A8-5. Example of model region and initial condition. Initially the width of the slug is taken to be 1 cm on this side of the symmetric region.*

## A8.4 Results

**Table A8-1. Data table**

| Parameter | Value | Unit | Comment |
|---|---|---|---|
| $D_p$ | $2 \times 10^{-11}$ | $m^2/s$ | Pore diffusion coefficient |
| $D_w$ | $2 \times 10^{-9}$ | $m^2/s$ | Diffusion coefficient in unconfined water |
| $K_0$ | 0 | – | Volumetric sorption coefficient $K_d\rho_s$ HTO and $Cl^-$ |
| $K_0$ | 2.7 | – | Volumetric sorption coefficient $K_d\rho_s$ $Na^+$ |
| $u_0$ | $1.5 \times 10^{-6}$ | m/s | Mean water velocity by pumping |
| $x_0$ | 0.05 | m | Weighted distance for diffusion to the flowing grooves |
| $x_s$ | 0.01 | m | Width of solute region, |
| $\varepsilon_0$ | 0.01 | | Matrix porosity HTO and $Na^+$ |
| $\varepsilon_0$ | 0.0005 | | Matrix porosity $Cl^-$ |

Figure A8-6 shows the predicted effluent concentration of HTO for the data in Table A8-1.

The fist arrival was predicted to be at around 50 hours (2 days) compared to about 100 hours (4 days) found in the experiment. The plateau and tailing are reasonably well predicted.

Figure A8-7 left and right show the results for $Na^+$ and $Cl^-$ respectively. The fluctuation at late times is caused by a numeric artefact for the very low matrix capacity.

The early arrival of all three traces is in error by about 50 hours to early. The difference is much less than earlier predictions based on the advection dispersion plus matrix diffusion mechanisms. These predict an early arrival of 300 hours when Taylor dispersion is assumed to be the main hydrodynamic dispersion mechanism in the slot (Appendix A in Soler et al. 2019). Also the plateau is now better predicted. The HTO and $Cl^-$ tailings are reasonably well predicted but the late time tailing is not well predicted for $Na^+$. This suggests that the laboratory derived sorption coefficient may be too large.

Figure A8-8 shows the sensitivity to the distance $x_o$.

The diffusion distance $x_o = 5$ cm to the flowing groove used in the central case seems to be a rather reasonable choice and is well within the diffusion distances that could be attained in the equipment.

The evolution of the HTO concentration over time in the x-r region is shown in Figure A8-9.

The accumulation/depletion in the pores of the rock matrix quite is clearly seen.
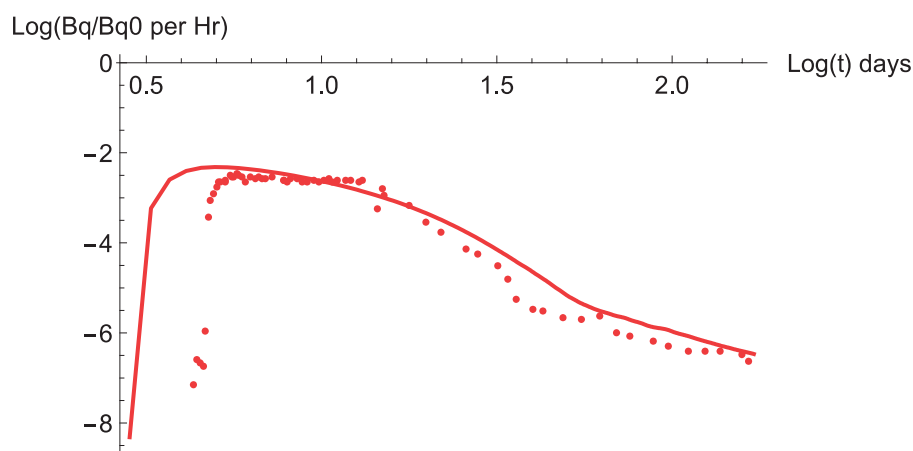


***Figure A8-6.*** *Predicted and experimental BTC for HTO.*
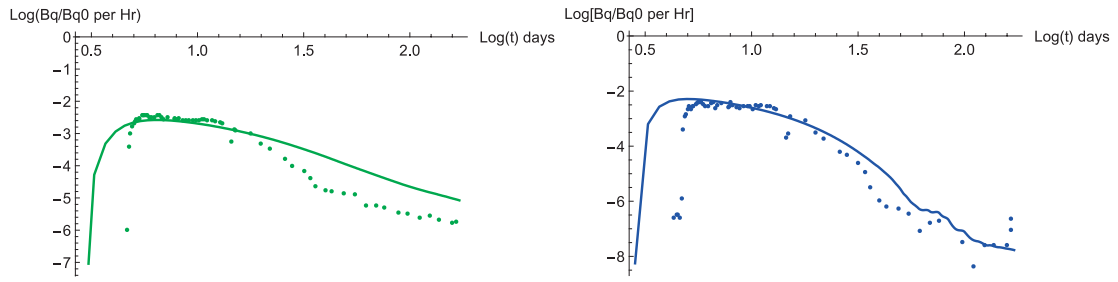
**Figure A8-7.** *Predicted and experimental BTC for Na⁺ left and Cl⁻ right.*
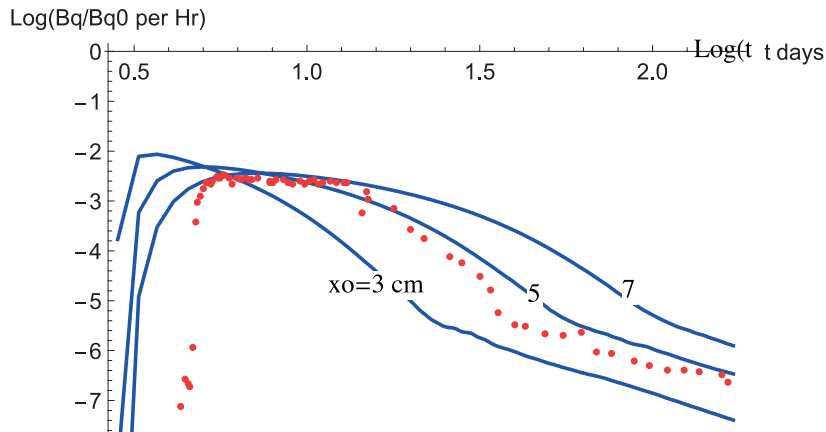


**Figure A8-8.** *Sensitivity to $x_o$ for HTO.*
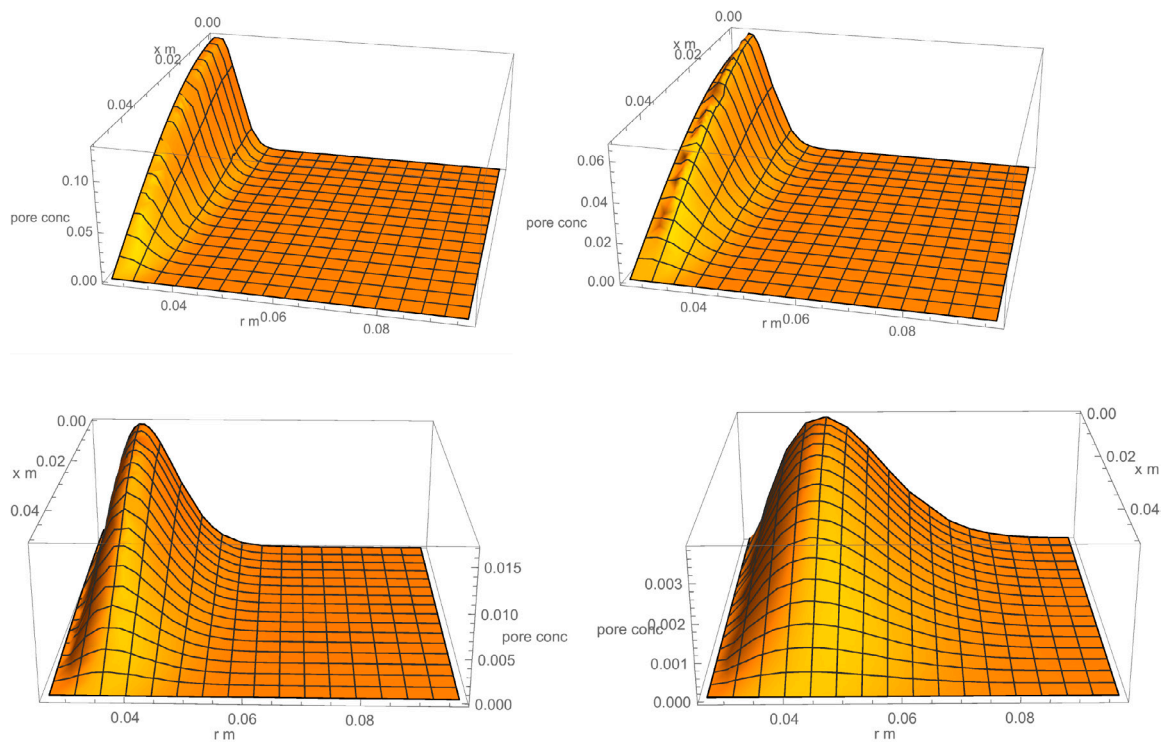


**Figure A8-9.** *HTO concentration 5, 10, 30 and 90 days in the same region as in Figure A8-5, which shows the profile at time zero.*

Figure A8-9 shows the results for HTO for WPDE-2 experiments. In this experiment the injected tracer volume was three times larger than in WPDE-2. This implies that the slug is about 1.7 times longer and wider. The flowrate was half that in the first experiment and the mean water residence time was twice as long.

The diffusion length $x_o$ is longer, which could be caused by the larger slug. Its tip extends to about 7.8 cm from the end of the dummy. In WPDE-1 it was 4.5 cm. See Figure A8-2.

**Discussion and conclusions**

We have presented an alternative interpretation of the Repro experiments. When the borehole slopes downward as in the experiment it is found that as the injected tracer solution has a lower density than the GW, the tracer rapidly flows past the experimental section and collects at the top of the slot. From there it has to diffuse downward before it can leave the system because the buoyancy of the less dense tracer solution hinders downward flow. The simple model describing these phenomena and modelling predictions supports this interpretation but by no means proves that this is the correct interpretation.

There are several uncertainties. One is that the estimated density difference between tracer slug and GW is between 1.3 and 2.9 kg/m³. See Section A8.8. This may or may not be large enough to hinder it to flow away because about 1.7 kg/m³ is needed to counteract the pressure difference between in-and outlet of the grooves. See Section A8.5. The latter is also a quite uncertain figure because already a 10 % underestimation of the groove diameter would lower the need for the density difference to less than 1.2 kg/m³. However, and more important, if flow were to occur of the tracer slug, it would be carried away in less than a few hours to the exit of the equipment. The BTC would be very narrow and there would be no long tailing because the traced water has not been in contact with the rock surface longer than it took for it to reach the end of the slot.

It may at first seem surprising that tailing caused by matrix diffusion is quite similar to what is predicted with the original model in which all GW is assumed to have tracer and this water contacts all the rock surface of the slot. However, this is a consequence of the linear properties of the exchange mechanism between flowing water and rock. The results will be very similar because the water diluted X times, is in contact with X times larger surface. As long as the contact time is the same in both cases the same mass of tracer will enter/leave the matrix. The key entity that determines the residence time of the trapped tracer is $x_o$.
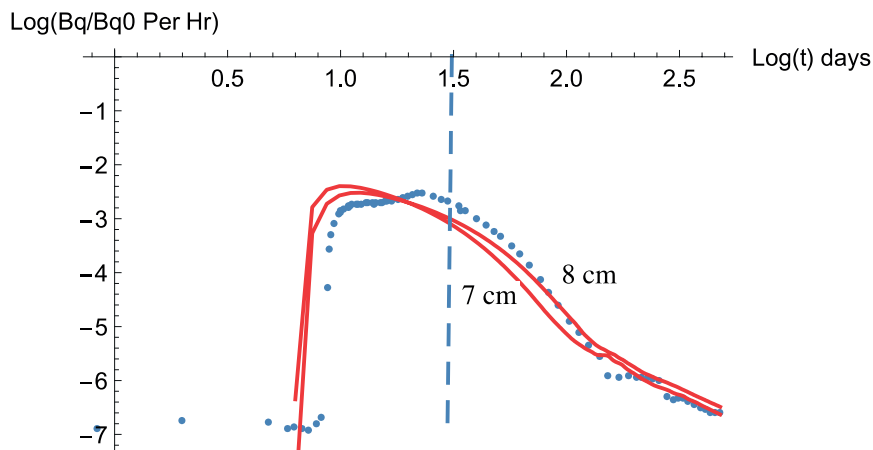


***Figure A8-10.*** *Predicted and experimental BTC for HTO in WPDE-2.' The dashed line indicates the mean flowing water residence time.*

Referring to Figure A8-7 for sodium it is seen that the tailing for this weakly sorbing tracer is poorly predicted. The high tail suggests too high sorption in the model. An attempt was made to see if a better fit could be obtained with a lower sorption coefficient. A better fit can be obtained but the sensitivity to changes in the sorption coefficient is too weak to be able to determine a good value, but at least an order of magnitude lower value would be needed.

The density difference between the tracer slug and the GW are central to the above modelling. A density difference that does not stop flow in the uppermost groove would let the slug flow to the exit in less than a few hours and the BTC would have a very narrow peak. A denser tracer solution than the GW on the other hand would dramatically change the situation, as the tracer solution then would have collected in the bottom of the slot before flowing into and through the slot. It would not have been lifted into the intended flowpath. It would have been delayed and first breakthrough would be considerably after the mean water residence time. This was, however, not observed in the experiments.

There are considerable uncertainties caused by the simplification of the geometry and uncertainties in density data. Nevertheless, this little exercise suggests that density differences could considerably impact the performance and interpretation of tracer experiments. The impact of density driven solute migration seems not to have been considered in most reported laboratory and field experiments.

It is suggested that, if possible, this or similar equipment can be inserted in a transparent tube so that the migration and fate of the tracer slug can actually be observed under well-controlled conditions.

## A8.5    Grooves and pressure drop in Repro experiment.

The eight grooves surrounding the cylindrical packer in inlet and outlet sections are placed symmetrically around the packer. The grooves are 237 mm long. The length of the packer is 71 mm. If we observe the cylinder horizontally with one groove "inlet" on top, this groove circles the packer, first descending until it reaches the bottom of the packer, then rising to the top again. The number of full turns around the cylinder is about one. The groove outlet is therefore at the top of the outlet section near the eccentrically placed outlet hole from the outlet section[9]. In our scenario the light traced liquid accumulates at the top of the slot. It has to flow out through the uppermost groove. The light fluid is first forced downward into the groove that is wound around the packer. To just hinder the light fluid to flow against buoyancy the pressure difference caused by buoyancy of the light liquid must be equal to the pressure difference (drop) between inlet and outlet over the other flowing grooves. The buoyancy pressure caused by the density difference must be similar to the pressure drop $\Delta P_{flow}$ over the flowing grooves. This is given by the following Equation (A8-9). See also Figure A8-11.

$$\Delta P_{flow} = \Delta \rho_w g d_{dummy\ interior} \tag{A8-9}$$

$=\Delta \rho_w$ is the density difference and $d_{dummy\ interior}$ is the vertical height of the light water when this extends to the bottom of the non-flowing groove, h2 in Figure A8-11.

Figure A8-11 shows the rise and fall of the grooves.

$\Delta P_{flow}$ can be assessed by Hagen-Poiseuille equation for laminar flow in a tube.

$$\Delta P_{flow} = \frac{L_{groove} Q\ 8\ \mu_w}{\pi r_{hy}^4} \tag{A8-10}$$

The viscosity of the water at the temperature 10–11 °C of the experiment is $1.3 \times 10^{-3}$ Pa·s, $L_{groove} = 0.237$ m. The flowrate in WPDE-1 in all 8 grooves Q$=20 \times 10^{-9}$ m³/min. $r_{hy}$ is the hydraulic radius of the groove.

$$r_{hy} = \frac{A_{groove}}{P_{groove}} 2 \tag{A8-11}$$

$$A_{groove} = \frac{1}{2} \frac{\pi d_{groove}^2}{4} \tag{A8-12}$$

---

[9]  According to information from the experimentalists it was the aim to have the outlet hole inside the dummy high up but as the equipment still is in place this is not confirmed. Should the outlet hole be much lower the light tracer would again collect at the top of the outlet section and would have to diffuse downward to arrive at the outlet hole. This could generate additional time delay.

$A_{groove}$ is the cross section are of the groove, the half- tube, with diameter 1.5 mm and $P_{groove}$ is the wetted perimeter of the groove.

$$P_{groove} = \frac{\pi d_{groove}}{2} + d_{groove} \qquad (A8\text{-}13)$$

From this $r_{hy}$ = 0.458 mm

and

$\Delta\rho_w = 1.7 \frac{kg}{m^3}$ , See also Figure A8-11 below

This means that the density difference must be larger than $1.7 \frac{kg}{m^3}$ not to let the traced water flow through it. The estimated density difference is between 1.3 and $2.9 \frac{kg}{m^3}$. See Section A8.3. Considering that if flow *were to occur* in the uppermost groove, which is in direct contact with the tracer slug this would be carried away in less than a few hours to the exit of the equipment. The BTC would be a very narrow pulse, less than ten hours and there would be no long tailing because the traced water has not been in contact with the rock surface longer than it took for it to reach and collect at the upper end of the slot. This suggests that the density difference *is large enough* to trap the slug.

## A8.6 Densities of tracer solution and synthetic groundwater

### A8.6.1 Information regarding the tracers in a mail from Martin Löfgren 18 August, 2016. The paragraph below is a direct copy. The yellow highlight is by Ivars and all original references are still there

[3]H and [22]Na were delivered by Perkin&Elmer. Total amount of 37 MBq/ml of ^{3}H and 3.7 MBq of [22]Na were purchased. The producer gives 10 % uncertainty for the products; these are not precision calibrated solutions.[AP2] The activity of [36]Cl solution is 3.81 MBq/ml having carrier chloride concentration of 6.2 mg Cl⁻ in the solution (10 % uncertainty; from Scopus Research). Total amount of 62 MBq of [125]I (Perkin&Elmer) was purchased. Producer gives 15 % uncertainty for the specific activity of the tracer solution. The initial chemical form of [36]Cl and [22]Na was sodium chloride (NaCl) in aqueous solution. The initial chemical form of ^{125}I was sodium iodide (NaI) in phosphate buffer solution. The tracer was bought from MAP Medical Technologies. The pulse was prepared at HYRL on 5th of March 2012. The tracer solution, which was decided to be 1 ml in volume, was placed into a sampling loop after mixing the four radioactive elements in a plastic vial. The loop was transported to ONKALO on the 7th of March in the castle of lead. The loop was kept at ambient pressure closed with 2-way valves during transportation. Table A8-2 lists the amounts of the added stock solutions and their activities. 999 mg of mixed tracer solution was placed into the injection loop, while the rest of the tracer solution, 665 mg, was kept at HYRL, for tracer activity measurements. A few drops of 4M NaOH and 4.693 g of water were added into 347 mg of tracer solution (solution T). Sodiumhydroxide was added to keep iodine in solution. This solution was still diluted to solutions T1 and T2[AP3]. The radioactivities of [22]Na, ^{125}I, [36]Cl and HTO were measured from these diluted T1 and T2 solutions.
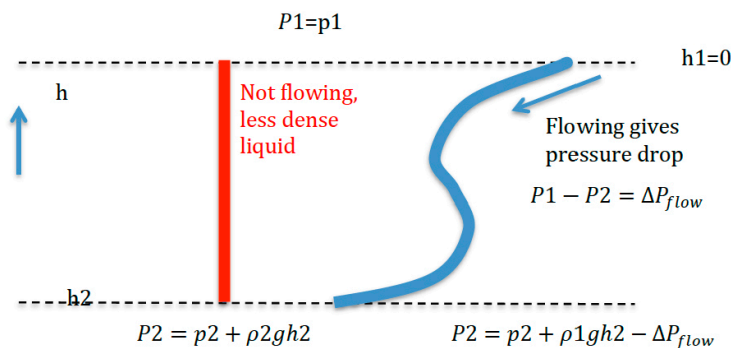


*Figure A8-11.* *Illustration of the density difference needed to just hinder the lighter fluid from flowing. P denotes sum of pressure p and gravitational term ρgh, ρ1 and ρ2. Are the densities of the red and blue liquid respectively?*

**Table A8-2. The amount of radionuclides injected in WPDE1 experiment. Activities and mass of the stock solutions and notes of them are listed. Solutions and measured activities of the injected tracer (mass of 0.999g).**

| Tracer | Activity of stock solution | Mass of stock solution (mg) | Notes | Activity of the tracer (MBq) uncertainties given as 2$\sigma$ |
|---|---|---|---|---|
| HTO | 37 MBq/ml | 791 | | 17.1 ± 0.3 |
| $^{22}$Na | 3.7 MBq/ml | 419 | | 1.38 ± 0.03 |
| $^{36}$Cl | 5.6 MBq/ml | 453 | Carrier concentration 16 mg/ml Cl | 1.25 ± 0.03 |
| $^{125}$I | 2.8 MBq/µl | 2 | Stock solution activity decreased | 1.36 ± 0.04 |

### A8.6.2 Estimation of tracer solution and GW densities based on the above information

The densities of the tracer solution and of the GW are essential to our modeling. As there seem to be uncertainties of a magnitude that can severely affect the interpretation of the results we document our estimated values below. We may have misunderstood the information and present our interpretations so that any errors can be corrected.

1) It is stated that the length of the loop is 124 cm, that the inner diameter is 1 mm (no uncertainty is provided) and that 999 mg of stock solution was used to fill this loop. This gives a density of 1.026 g/ml. However a 1 % error in the *tube diameter* changes this to 1.0056 g/ml. This approach is thus very uncertain.

2) From Table 2-6 the density of the tracer solution is estimated as follows: The carrier concentration of Cl$^-$ in 453 mg of solution is 16 mg/ml. The counterion is Na$^+$, which gives NaCl concentration of 26.4 mg NaCl/ml and a mass of NaCl in the 463 mg (0.453 ml) solution of 12.4 mg NaCl. This solution is mixed with the volumes containing the HTO and the Na$^+$ and I$^-$ radionuclides in pure water (our assumption as nothing else is mentioned). The total mass of solution is 1665 mg (1.665 ml). This gives a NaCl concentration of 7.17 mg/ml. At low concentrations the solution density of NaCl in water acts as if the salt does not change the volume of the water in which it is dissolved so the density of the solution becomes 1.00717 g/ml.

3) In the yellow highlighted text above it is stated that $^{36}$Cl solution contains 6.2 mg Cl$^-$. We interpret this to mean that this is in the 453 mg solution. This gives a NaCl$^-$ concentration of 13.7 ± 1.4 mg/ml. This gives density of the tracer solution 1.00614 g/ml with an uncertainty range 1.00552 to 1.00675 g/ml.

4) The GW density is estimated from the table in the Task description by adding the concentrations of all the ions, of which most is NaCl and approximating the density by assuming that it does not affect the volume in the same way as stated in 2). The density of the GW then is 1.00843 g/ml

The density difference between GW and the tracer solution is then given in the table below.

**Table A8-3. Density differences between traced water and GW estimated from different sources of information.**

| Case # | GW-Tracer kg/m$^3$ | Comment |
|---|---|---|
| 1) 1.00 mm | −1.76 | 1.00 mm tube. Tracer is denser |
| 1) 1.01 mm | 2.8 | 1.01 mm tube. |
| 2) | 1.3 | |
| 3low) | 2.9 | Contradictory data in |
| 3) best estimate | 2.3 | report on carrier concentration, see discussion under 3). |
| 3high) | 1.7 | |
| 4 | 3.91 | PhreeqC[13] |

---

[10] Pesonal communication, Johan Byegård Geosigma. Calcualtions by PhreeqC geochemical code. wwwbrr.cr.usgs.gov/projects/GWC_coupled/phreeqc/

## A8.7 Little experiment showing how a dye slug, driven by gravity, flows in a water filled tube

A simple scoping experiment was made to illustrate how a small fluid slug with a density slightly larger than water (on the order of 4 kg/m³) flows down gradient in a narrow *tube*. A similar experiment will be made in a narrow *slot*. Figure A8-12 shows the progress of the slug. The pictures show the tube from the side.
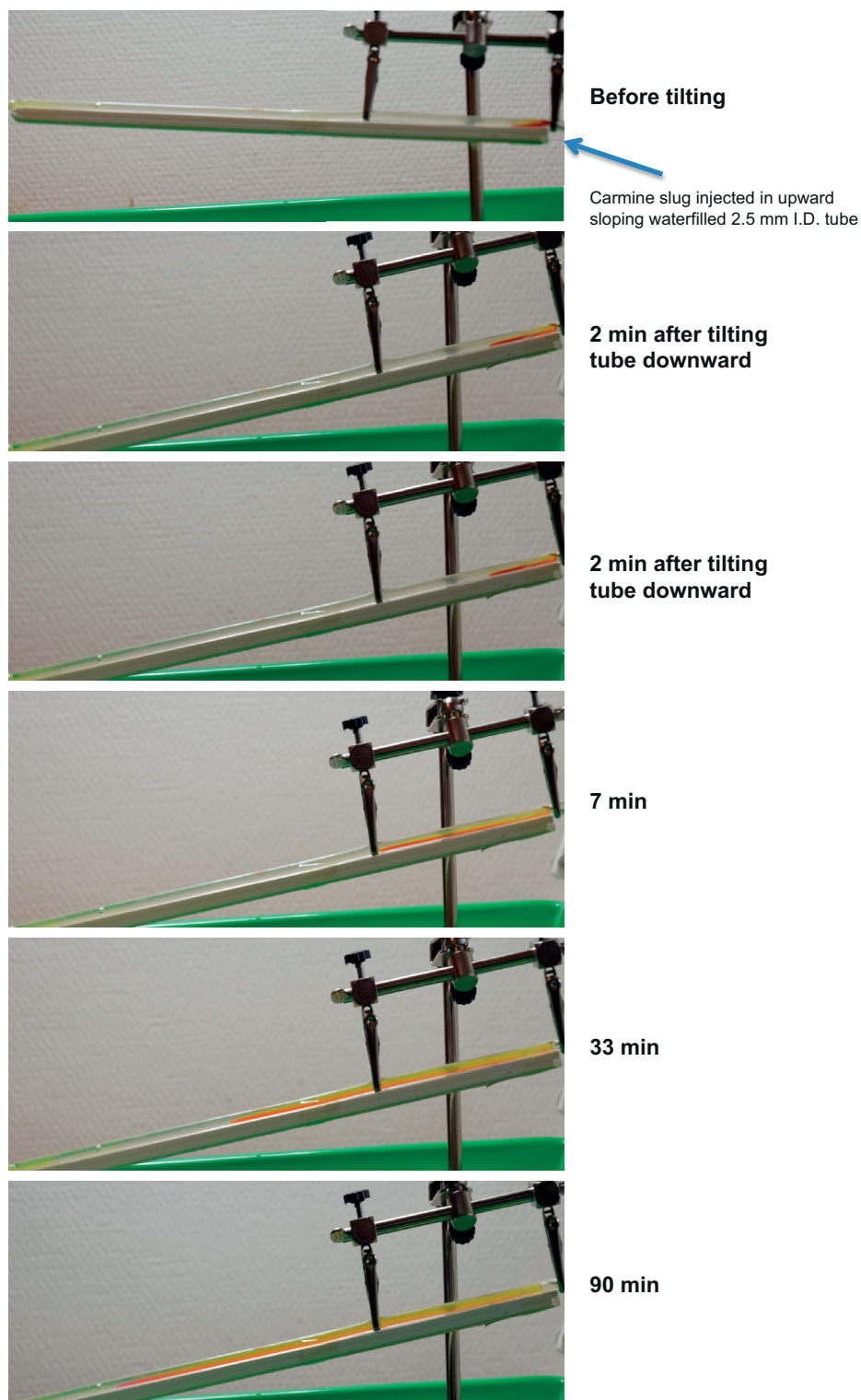


**Before tilting**

Carmine slug injected in upward sloping waterfilled 2.5 mm I.D. tube

**2 min after tilting tube downward**

**2 min after tilting tube downward**

**7 min**

**33 min**

**90 min**

*Figure A8-12.* *Carmine slug sliding down a 2.5 mm I.D. tube filled with water. The tube length seen in picture is 25 cm. The slope is 9.5.*

The tube has an inner diameter of 2.5 mm and is 25 cm long. The approximately 2 cm long slug was injected at the lower end of the tube using a hypodermic needle. After a few minutes, observing that the slug remained in place and did not change shape, the tube was tilted at an angle of 9.5 degrees. A series of pictures followed the slug migration. The migration rate slowed down as the slug moved down gradient and it elongated as it moved leaving a growing tail behind. The tailing is caused by the difference in water velocity between the tube wall and the centre of the tube generated by the mid of the slug moving faster than the portion near the wall. This is not accounted for in the model.

Figures A8-13 and A8-14 show the upper and the lower end to the tube respectively three hours after start of the experiment. These pictures are taken from above.

After three hours the dye has diffused sufficiently to even out the concentration profile across the diameter of the tube but has only marginally affected the concentration profile along the tube.

## A8.8    Impact of dilution by diffusion in slug and between slug and surrounding water

**Migration of rigid but diffusing slug**

In the proposed scenario the tracer slug "rapidly" moves up the inclined slot assuming only a small dilution or mixing with the GW underway. Here we explore this assumption. See: the Mathematica® Notebook *"Flow of blob with increasing density due to diffusion.nb"* for details.

The 0.999 cm$^3$ blob forms a short stubby cylinder when squeezed in the 1.25 mm aperture slot The cylinder area is 8 cm$^3$. Its radius $r_{blob}$=1.6 cm. With time, when the blob is exposed to GW it will exchange solutes with it. The density difference will decrease, decreasing the slug velocity. In a first crude estimate we assume that the entire slug with its increasingly "fuzzy" border moves as a rigid slug. This is explored by solving the instationary diffusion equation, PDE, in radial coordinates, which shows how the density difference changes with time in the slug. Equations (A8-1 to A8-3) are used coupled to the Fickian diffusion equation in radial coordinates. As the velocity of the blob is proportional to the density mean difference we can by integration of the velocity over time determine the time it takes to travel the length of the slot.

Figure A8-15 shows how the local density evolves over time and radius in the blob.

By integration of the entire blob the mean density difference is obtained. Figure A8-13 shows how the mean density difference changes with time.
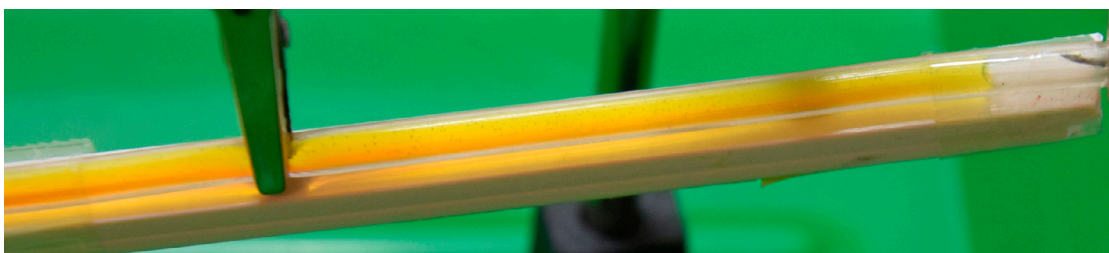


***Figure A8-13.*** *Water with some remaining dye in the upper end of the tube after nearly 3 hours.*
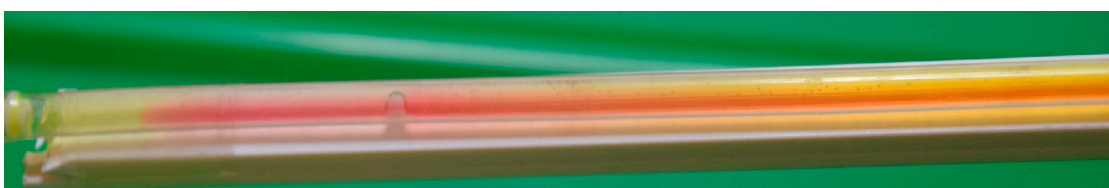


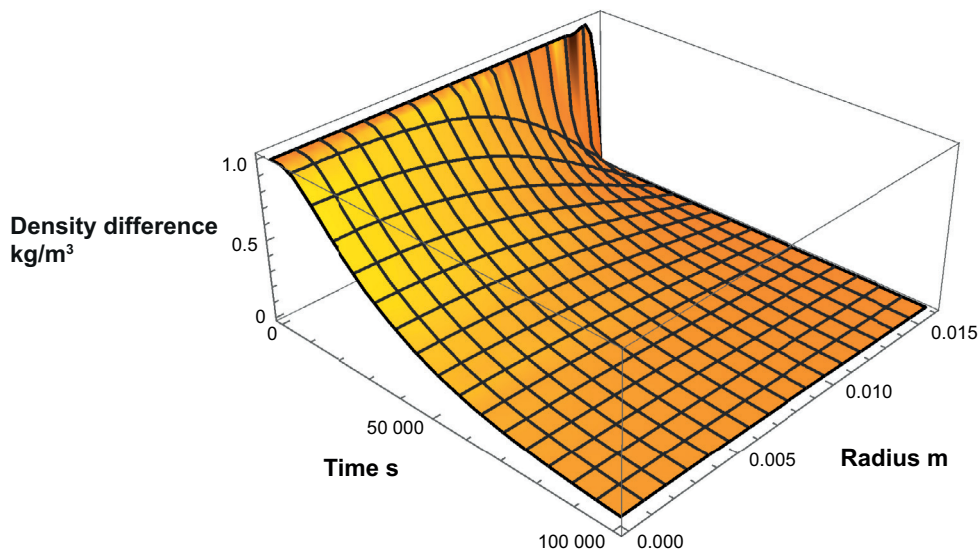***Figure A8-14.*** *Water with dye in the lower end (25 cm) of the tube after nearly 3 hours.*

*Figure A8-15.* *Local density evolution over time and radius in the blob. (Mathematica® Notebook: Flow of slug with increasing density due to diffusion.nb".*
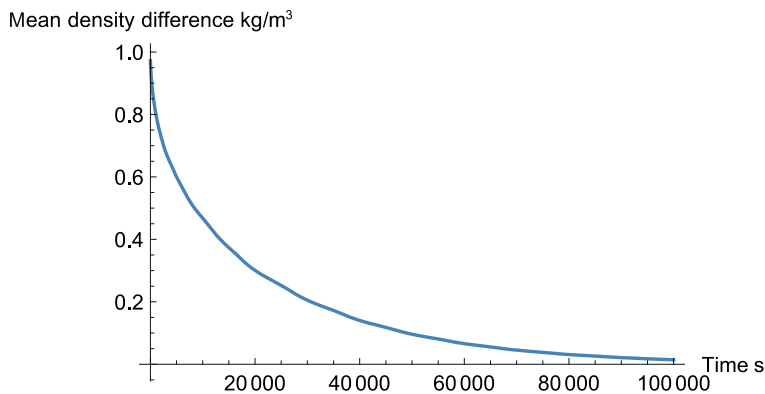


*Figure A8-16.* *Density difference between tracer slug and GW over time.*

The travel distance is obtained by integrating the velocity over time. It takes about 5.5 hours for the tracer slug to travel the length of the inclined slot. This is nearly twice the time it takes for the undiluted blob to migrate the same distance. The original density difference has decreased to one third. This adds further uncertainty to the trapping as the density difference of the slug decreases by 2/3$^{rds}$.

**Modelling a rising non-rigid slug subject to diffusional exchange with the surrounding water**

We use a simple model to explore how dilution by diffusion of the non-rigid slug can influence its delay. The model is very simple and is not expected to give very accurate results. It can, however, indicate if it could be worthwhile to do more exact modelling. This would have to include at least a two-dimensional Navier-Stokes equation and an at least two-dimensional diffusion model coupled via the density of the fluid. The equations will then not have constant coefficients and would demand a capable code and non-trivial effort to verify that the results are correct.

As before, a slug rises in water by buoyancy. The slug is divided into vertical "strips". Diffusion takes place between strips. Each strip flows upward with a velocity that depends on its buoyance in relation to water. It is assumed that the friction between strips can be ignored because the friction against the walls of the narrow slot determines the velocity. The strips exchange solute with neighbouring strips by diffusion. The difference between the mean density of the strip over its height in the slug and the clean water defines the rise velocity of the strip. See Figure A8-17. The figure illustrates the right part of the symmetric slug. The densest strip moves faster because it has the largest density difference. Diffusion carries tracer as shown by arrows.

Circulation pattern of displaced water
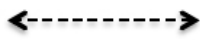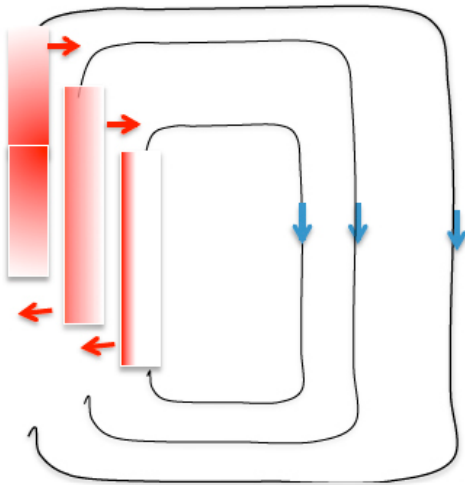
Size of blob grows with $\sqrt{time}$
Due to diffusion

*Figure A8-17. Visualisation of the rising slug. Three strips and the circulation pattern of the displaced water illustrate the idea. Red arrows show direction of diffusion between strips.*

The diffusion between strips changes the density difference and thus the rise velocity of each strip. We model half the slug. A finite difference grid is set up with M cells in x-direction and N cells in y-direction (upward). The slug is located between 1–Mx in x-direction and is one cell thick in the y-direction. The density difference initially is $c[x, y, t] = c_o$ kg/m³. The PDE that describes the migration is

$$\frac{\partial c}{\partial t} = -\frac{\partial c_{mean}}{\partial y}u_y(x) + D_w\frac{\partial^2 c}{\partial x^2} + D_{wT}(u_y(x))\frac{\partial^2 c}{\partial y^2}) \qquad (A8\text{-}14)$$

$D_w$ is the diffusion coefficient in water and $D_{wT}$ is the Fickian dispersion coefficient based on Taylor dispersion in the flow direction. $D_{wT} = D_w\left(1 + \frac{1}{52.5}Pec_w^2\right)$ where $Pec_w = \frac{u_y(x)d_{slot}}{D_w}$. Inspection of the magnitude of the parameters shows that although the Taylor dispersion can be several hundred times $D_w$, the entire term $D_{wT}(u_y(x))\frac{\partial^2 c}{\partial y^2}$ contributes negligibly. The system is strongly dominated by advection in the y-direction except for the very early times when the Taylor dispersion will not have properly developed anyway and cannot be used.[11]

$c_{mean}$ is the mean c in the height of the slug, which grows with $\sqrt{t}$.

It is *assumed* that the height is proportional original width plus how it has grown over time by diffusion in the flow direction. The increase is taken to be the distance $x_{c = 0.01\,c_o}$ to which diffusion has expanded to the concentration where $c = 0.01\ c_o$.

$$x_{c=0.01c_o} = 4\sqrt{D_w t} \qquad (A8\text{-}15)$$

The height of the strips in the slug are taken to be

$$h_{slug} = \Delta y + 2x_{c=0.01c_o} \qquad (A8\text{-}16)$$

where $\Delta y$ is the size of the cell in the y-direction in the discretised grid.

---

[11] Should one wish to set up and solve the problem based on the Navier-Stokes equations the diffusion across the aperture could be included to explore the early time behaviour.

$u_y(x)$ is the velocity in the y direction and is

$$u_o + k_u \times \frac{c_{mean}}{c_o} \qquad\qquad (A8\text{-}17)$$

$u_0$ is the vertical velocity of the flowing water and $k_u \times \frac{c_{mean}}{c_o}$ is the additional velocity of the strip at x with $c_{mean}$ defining the mean buoyance difference of strip x over the height of the strip. The constant $k_u$ accounts for the friction against the walls of the slit for the rising strip. $k_u$ can be interpreted as the velocity a rigid slug with density difference $c_o$ kg/m³ would have in the slot when only friction against the slot walls acts on it.

We repeat Equations (A8-1 to A8-3) from the main part of the note.

$$u = \tfrac{T}{b} \; grad = 1.7\times10^{-4} \; m/s \qquad\qquad (A8\text{-}3)$$

where

$$grad = \tfrac{\Delta\rho}{\rho_w} \sin\left(\tfrac{\pi}{18}\right) \qquad\qquad (A8\text{-}2)$$

$T$ is the transmissivity of the slot and is

$$T = b^3 \tfrac{\rho_w g}{12\,\mu_w} \qquad\qquad (A8\text{-}1)$$

For convenience we use $c_o = \Delta\rho = 1$ kg/m³ in the example calculations. This gives

$$k_u = 1.7\times10^{-4} \; m/s$$

Equation (A8-14) is solved by finite differences with typically 30–90 cells in the x-direction and 15–30 cells in the y-direction. Time steps are set by the stability criterion $dt = Min[(\frac{dx^2}{D_w} + \frac{dy}{u_{y.max}})/2]$. Sometimes dt is decreased further by a factor of 2 or on occasion by 5. To ensure that erratic behaviour is avoided. uy.max = uo+ku. Typical number of time steps ranges from low 100 to several thousand.

**Examples**

Figure A8-18 shows the location and concentration difference of the slug after 3 hours.

The half-width of the slug (x-direction) has expanded from 2 cm to about 3 during this time but extends from 0.7–1.9 m in the flow direction.

Figure A8-19 shows the mean concentration difference across the x-direction as the slug passes the end of the slot at 1.905 m.

A slug width of 1 cm changes the BTC to that shown in Figure A8-20.

A larger concentration difference will increase the migration velocity approximately in proportion to the concentration difference.
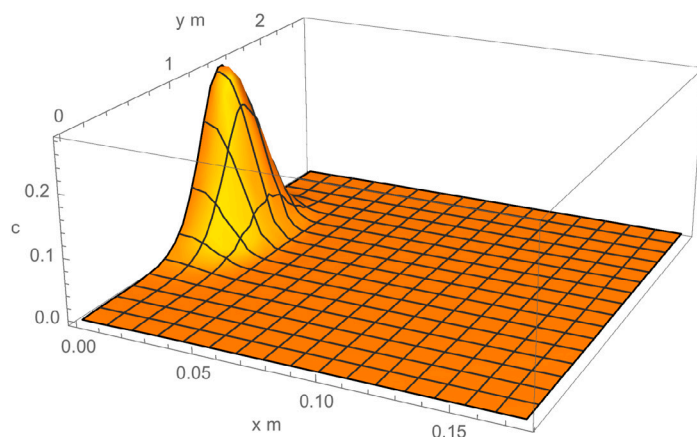


**Figure A8-18.** *Location and concentration of the slug after 3 hours, $c_o$=1 kg/m³ Slug width initially is 2 cm.*
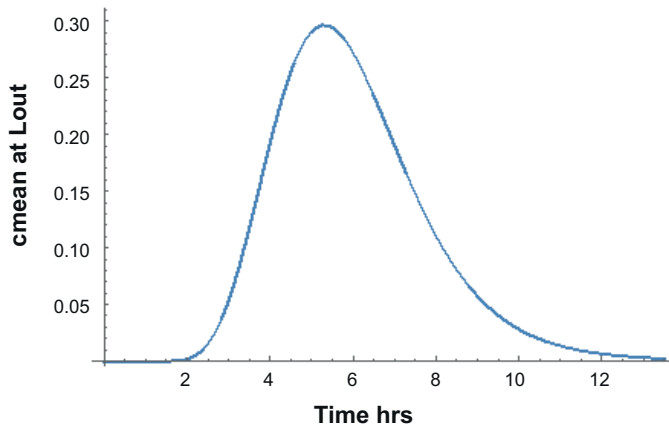
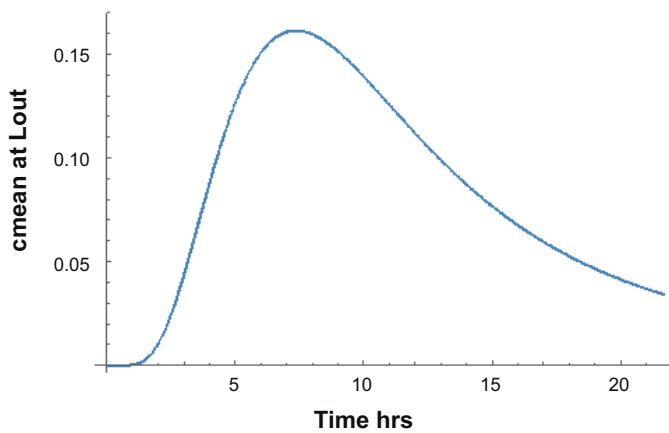***Figure A8-19.*** *Concentration at effluent of the slot. $c_o=1$ kg/m³. Slug width is 2 cm.*



***Figure A8-20.*** *Concentration at effluent of the slot. $c_o=1$ kg/m³. Slug width is 1 cm.*

These simple calculations show that the BTC to the upper end of the slot can be quite sensitive to both initial density difference and to the size of the slug. Nevertheless they support the possibility that the tracer slug rapidly can migrate by buoyancy forces to the end of the slot and that the dilution underway may not be large.

## A8.9 Impact of misalignment of dummy in borehole and impact of clogging of a groove

**Misalignment**

The very early arrival of the first tracer at about 1/3rd of the mean water residence time could be caused by channelling, i.e. part of the circular slot carries most of the water at a higher velocity. The reasons for such behaviour can at present only be speculated on. One such speculation is that the tool (dummy) around which the water flows is not fully centred but is misaligned.

The cylindrical insert tool in the REPRO experiment is slightly smaller than the borehole. If the misalignment of the centres of hole and tool is small, a fraction, $\varepsilon$, of the mean slot aperture, $\delta_m$, the slot aperture will vary, by close approximation, as

$$\delta = \delta m (1 + \varepsilon \sin(\alpha)) \tag{A8-18}$$

around the circumference $2\pi r_m$ of the slot. With a slot length $L$ the volume $V$ of the slot is

$$V = 2\pi r_m L \delta_m \tag{A8-19}$$

The velocity under laminar flow conditions in a planar slot is

$$u = C\delta^2 = C\delta_m^2(1+\varepsilon \sin(\alpha))^2 \qquad (A8\text{-}20)$$

where $C$ is a constant we need not specify. We use this expression also for the circular slot neglecting the impact of curvature. The shear between adjacent streamlines can also be neglected, as the gradient across the narrow aperture of the slot is more than 2 orders of magnitude larger than between adjacent streamlines.

The flowrate $Q_{d\alpha}$ in a small section $r_m d\alpha$ is

$$Q_{d\alpha} = u\,\delta\,r_m d\alpha = C\delta^3\,r_m d\alpha \qquad (A8\text{-}21)$$

The total flowrate in the entire slot is

$$Q_{tot} = \int_0^{2\pi} Q_{d\alpha} = C\pi\,r_m\delta_m^3(2+3\varepsilon^2) \qquad (A8\text{-}22)$$

The mean residence time is

$$t_m = \frac{V}{Q_{tot}} \qquad (A8\text{-}23)$$

The shortest residence time, $t_{min}$, corresponds to the maximum velocity which is found at $\alpha = \pi/2$ where $\delta = \delta_m(1+\varepsilon)$,

$$t_{min} = \frac{L}{u_{max}} = \frac{L}{C(\delta_m(1+\varepsilon))^2} \qquad (A8\text{-}24)$$

Then

$$\frac{t_{min}}{t_m} = \frac{2+3\varepsilon^2}{2(1+\varepsilon)^2} \qquad (A8\text{-}25)$$

This has no real root for $\frac{t_{min}}{t_m} < 3/5$. The shortest early arrival due to misalignment could only reach 3/5 of the mean residence time. Thus the cause for the early arrival cannot be caused by misalignment only.

Figure A8-21 shows how the aperture varies with $\alpha$ for two different values of the misalignment $\varepsilon$.

Figure A8-22 shows how the velocity (normalised) varies with $\alpha$ for two different values of the misalignment $\varepsilon$.

Figure A8-23 shows how $\frac{t_{min}}{t_m}$ varies with $\varepsilon$.

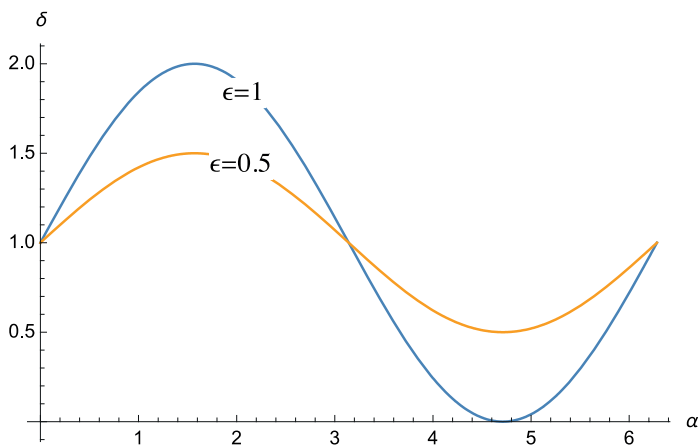The largest decrease of $t_{min} = 3/5\ t_m$ is attained at $\varepsilon = 2/3$.



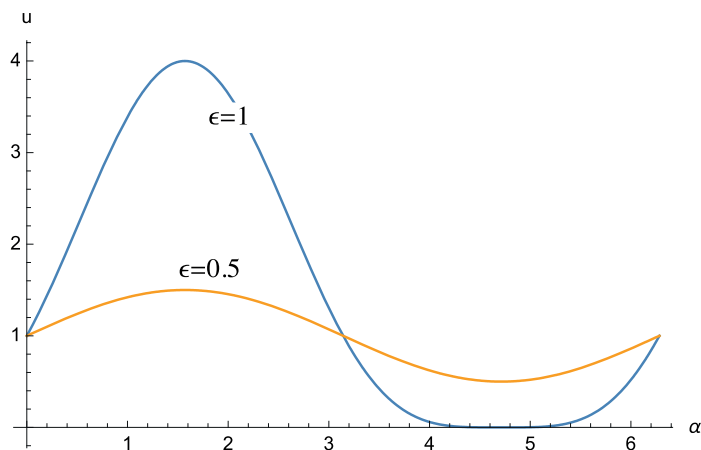**Figure A8-21.** *Aperture variation with α for two different values of the misalignment ε.*

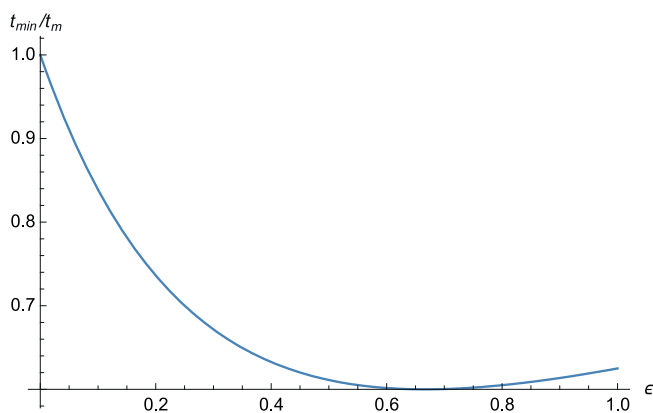**Figure A8-22.** *Normalized velocity variation with α for two different values of the misalignment ε.*



**Figure A8-23.** $\frac{t_{min}}{t_m}$ *variation with ε.*

**Impact of clogging of a groove**

The flowrate in the slot can be modelled as two-dimensional Darcy flow when we neglect the impact of the curvature of the slot. A short section of the slot upstream of two of the eight grooves is modelled. Also two outlet grooves are included in the modelled region. First the pressure distribution in the section with both outlet grooves flowing is modelled. Then one of them is clogged. We want to demonstrate that the impact on the upstream velocity only extends a very short distance compared to the length of the entire slot.

Figure A8-24 shows the pressure driving the flow in the slot along a part of the slot near the exit where 2 grooves collect the water from the slot. The groves are a distance 0.5 in arbitrary units. After a flow distance somewhat smaller than the distance between the grooves the pressure has essentially stabilized at a steady state and the flow is evenly distributed over the entire slot. The pressure difference is also in arbitrary units.

Figure A8-25 shows the velocity in the flow-direction at distances 0.2 (the deepest), 0.4, 0.6 and 0.8 fractions of the distance between grooves. Already at a distance 80 % of that between grooves the velocity is in practice constant over the section.

Figure A8-26 shows a case where the upper groove is clogged. The upstream distance at which the velocity profile is practically even in this case extends to 1.6 times the distance between grooves.
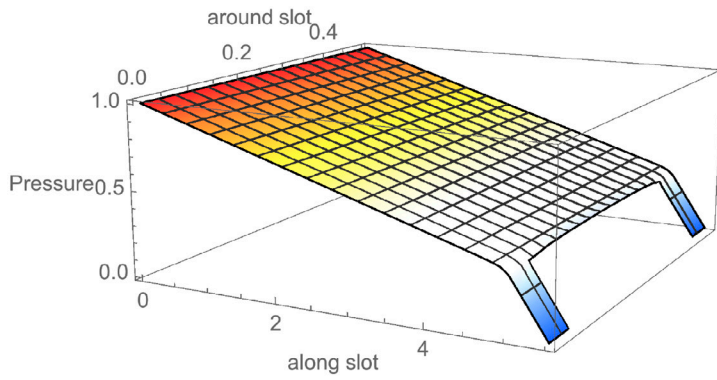
**Figure A8-24.** *Pressure in slots and grooves. Only a small fraction of the length of the slot is shown. Mathematica Notebook: Eccentric insert in Repro experiment.nb*
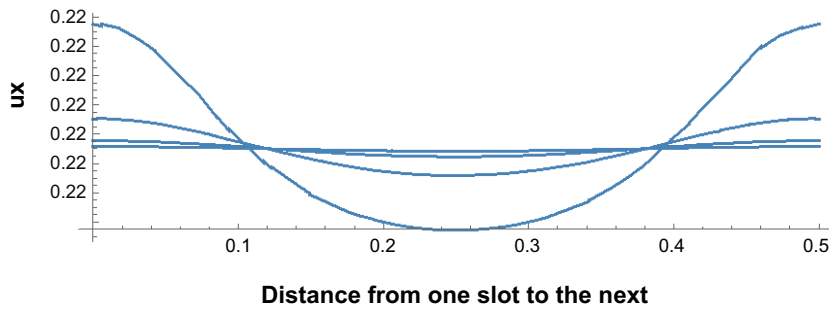


**Figure A8-25.** *Velocity (arbitrary units) in the flow-direction at locations upstream from the grooves at 0.2 (the deepest), 0.4, 0.6 and 0.8 fractions of the distance between grooves.*
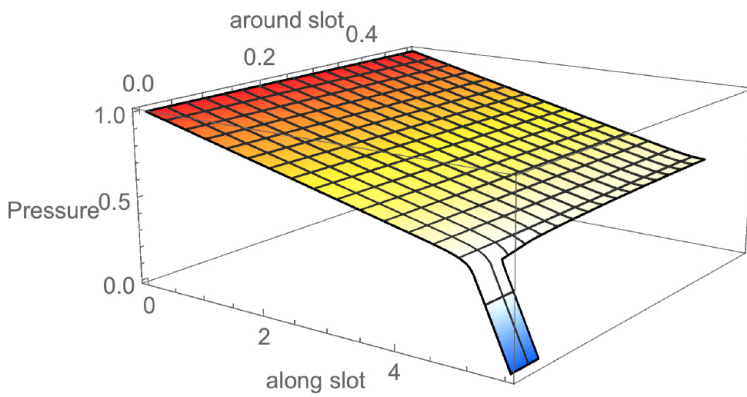


**Figure A8-26.** *Pressure in slot and groove. Upper groove is clogged.*

Considering that the length of the experimental section is 1.9 m and the distance between grooves is 0.022 m, it is concluded that clogging of a few grooves will not have much influence on the water velocity distribution over the slot. Clogging of a few grooves cannot result in a misdistribution of water velocities that lead to the observed early tracer arrival.

# General Task Description Task 9

## SKB Task Force on Modelling of Groundwater Flow and Transport of Solutes Task 9

### Increasing the realism in solute transport modelling – Modelling the field experiments of REPRO and LTDE-SD.

*Author: Martin Löfgren, 2014-11-12*

## A9.1 Summary

Task 9 focuses on the realistic modelling of coupled matrix diffusion and sorption in heterogeneous crystalline rock matrix at depth. This is done in the context of inverse and predictive modelling of tracer concentrations of the in-situ experiments performed within LTDE-SD at the Äspö HRL in Sweden, as well as within the REPRO project at ONKALO in Finland, focusing on sorption and diffusion. The ultimate aim is to develop models that in a more realistic way represent retardation in the natural rock matrix at depth.

## A9.2 Background

The topic of radionuclide retardation in the geosphere is of high importance for assessing the safety of geological repositories for radioactive waste in fractured crystalline rock. Matrix diffusion of solutes in the microporous system of the rock matrix is perceived to be well understood and has been discussed for over 60 years. For the past 35 years, matrix diffusion coupled with sorption has been discussed in the context of retardation of radionuclides leaking from a geological repository for nuclear waste.

In recent safety assessments (e.g. SKB 2011, Posiva 2012), the importance of solute exchange between flowing fracture water and stagnant pore water has been stressed in regard to the waste containers' capability of isolating spent nuclear fuel over long time periods. This has, for example, been done in the context of copper corrosion due to intruding oxygenated water and due to sulphide. It is noted that matrix diffusion is one of the processes influencing both the oxygen and sulphide concentrations at depth. In addition, the performance of buffer materials such as bentonite has been shown to depend on concentrations of the groundwater's main constituents, which in turn are affected by matrix diffusion and groundwater interactions with rock minerals. Finally, the groundwater flow rate at depth depends on the water density, which in turn is affected by solute exchange between the flowing water and stagnant water. This has expanded the field of solute transport and retardation to include not just radionuclides, which has been the traditional focus, but also the performance of the engineered barriers, hydrogeochemisty, and hydrogeology. The extended scope of solute transport and retardation makes it more difficult to establish what input data values are conservative for safety assessment modelling. As the relationship between radiological risk and these transport and retardation parameters is not necessarily simple and/or monotonic, this evokes the need for improving the realism in the modelling.

Even though the subject of matrix diffusion coupled with sorption has been studied for decades, the modelling approaches used for explaining tracer test results in natural rock have not developed at a significant rate lately[12]. Such development is needed to explain discrepancies between experimental observations and results obtained from inverse modelling of the same experiments. In general, at least within the field of radionuclide transport, inverse modelling of tracer tests is based on Fickian diffusion in homogenous media coupled with equilibrium sorption. In doing this, in-diffusion cases are typically modelled where a water phase tracer cocktail is surrounded by the rock matrix (for example in a borehole in situ) or where the tracer cocktail surrounds a sample of rock (typically in the laboratory). Alternatively, the tracer diffuses out of the rock matrix or through the rock matrix, although such experiments are less common in-situ. In in-diffusion experiments, commonly the

---

[12] In this statement the advances in reactive transport modelling is disregarded, as it will take substantial time until such approaches can be applied to natural systems.

decline in tracer concentrations in the water phase is measured and modelled, as well as the tracer penetration profiles in the rock matrix. When predicting the tracer penetration profiles, generally Fickian diffusion coupled with equilibrium sorption is assumed. In many cases the rock matrix is assumed to be homogenous. With these modelling prerequisites, the predicted shapes of the penetration profiles will always follow the same pattern. However, such predicted shapes were not observed in the in-situ experiment LTDE-SD, as is further detailed below.

## A9.3    LTDE-SD

One of few recent in-situ studies focusing on tracer transport in the stagnant pore water of the rock matrix has been conducted in Sweden at the Äspö Hard Rock Laboratory, within the LTDE-SD campaign (Long Term Sorption Diffusion Experiment). In this study, a cocktail of both sorbing and non-sorbing tracers was allowed to contact a natural fracture surface, as well as the unaltered rock matrix, for a time period of 200 days. The decline in tracer concentration in the water phase was monitored. Thereafter the rock was overcored and analysed in regard to tracer concentration profiles in the rock matrix. Numerous core samples from the overcored rock volume were first cut into 1 to 10 mm slices and subjected to autoradiographs. Thereafter, the tracer activities of the slices were obtained by various laboratory methods ultimately allowing for the compilation of tracer penetration profiles. Although the methodology and results from the experimental campaign have been finally reported (Nilsson et al. 2010, Widestrand et al. 2010a, b), the outcomes have not yet been subjected to the scrutiny of a broader community of researchers and modellers. Concerning the shape of the penetration profiles, the predicted general shape discussed in the above paragraph was not observed; neither for the natural fracture surface nor for the unaltered rock matrix. Figure A9-01 shows the experimental shapes of the in-diffusing tracers Na-22 and Cl-36 by diamonds, as well as the modelled profiles by the solid curves. Here the discrepancy of the curve shapes should be highlighted, whereas the discrepancy in relative curve positions is of lesser importance.

The heterogeneous nature of the rock matrix, in terms of both the microporous network and mineral surfaces available for sorption, has been qualitatively offered as an explanation for the discrepancy (Nilsson et al. 2010). However, other features, events, and processes that are traditionally not included in such modelling may add to the observed discrepancy. It may also be that using the fundamental prerequisites of the modelling, that is the Fickian diffusion equations and the equilibrium sorption approach, may add to the discrepancy. Increasing the realism when modelling experimental results from LTDE-SD is intended to be an important part of Task 9, without imposing restriction on the modelling teams in terms of how they should increase this realism.
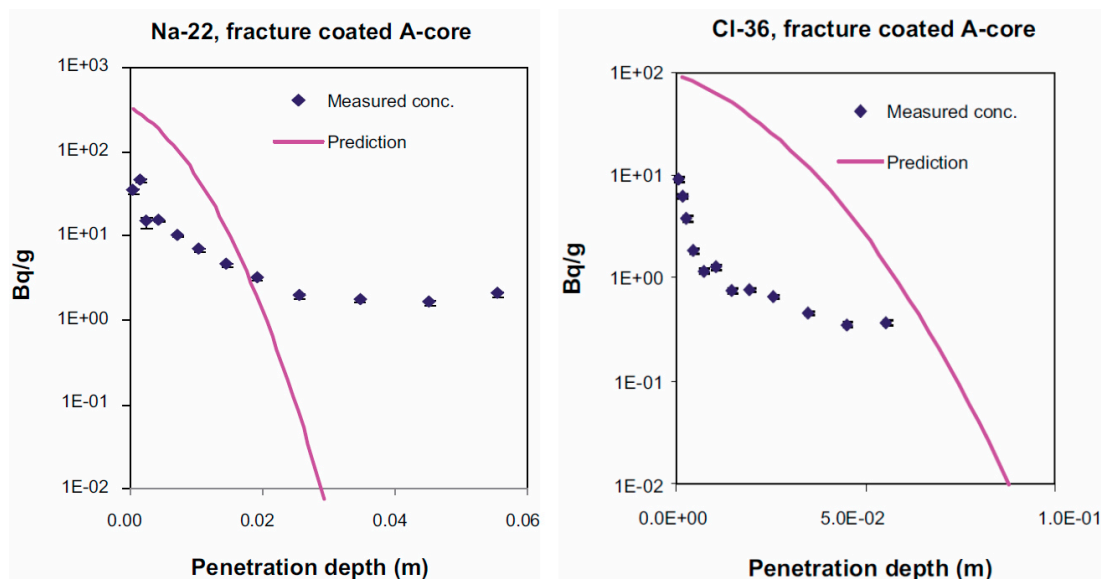


*Figure A9-1.* *Results from the in-situ in-diffusion experiment LTDE-SD through a natural fracture surface. Modelled Na-22 and Cl-36 penetration profiles (solid curves) in comparison with the measured profiles (diamonds). Na-22 activities in the rock matrix were obtained on intact of crushed rock slices and Cl-36 activities were obtained by leaching of intact or crushed slices. Excerpts from Nilsson et al. (2010, Figures 4-1a and 4-2a).*

## A9.4    REPRO

The other important input to Task 9 is the REPRO project which is presently carried out by Posiva at the ONKALO underground rock characterisation facility in Finland. This project is in part carried out in situ, and in part as an extensive laboratory programme. Two water phase diffusion and sorption campaigns are carried out in-situ; WPDE and TDE. The WPDE (Water Phase Diffusion Experiment) series of experiments are advection-diffusion-sorption experiments. A borehole has been drilled into the non-fractured rock matrix, and in this borehole a dummy is inserted creating a 1 mm gap between the borehole wall and the dummy. This gap is regarded as an artificial fracture of relatively well-defined geometry. In this gap a very low steady state water flow has been applied and in this water flow, a tracer cocktail has been injected as a pulse. The active tracers HTO, Na-22, Cl-36, Sr-85, I-125 and Ba-133 have been used. As the pulse travels with the water flow, its tracers will diffuse into the rock matrix. As the pulse passes, the concentration gradients are reversed and the tracers will diffuse out of the rock matrix and into the flowing water. By detecting their concentrations in the water phase at the end of the borehole, breakthrough curves are obtained which can be analysed by modelling. To date, two experiments have been performed at different flow rates; WPDE-1 (20 µL/min) and WPDE-2 (10 µL/min). For these experiments, the breakthrough curves have been obtained over half a year and about one and a half a year, respectively. A third flow rate may be utilised in a third experiment, should such an experiment be carried out.

The TDE experiment (Through Diffusion Experiment) will be carried out between three parallel boreholes situated perpendicular to each other. A tracer cocktail will be injected in one borehole. The solutes are intended to diffuse through about 10-15 cm of intact rock matrix to the other boreholes, where tracer breakthrough curves will be detected in the water phase. This experiment has not yet been initiated, but is assumed to run parallel to Task 9. Currently, a tracer cocktail of HTO, Na-22, Cl-36, Ba-133, and probably Cs-134 is planned to be injected during spring 2015. The tracers were chosen to make overcoring and analysis of tracer penetration profiles possible, although this option is presently not included in the REPRO planning. As the REPRO project is on-going, it offers the possibility of both inverse and predictive modelling. The in-situ part of REPRO aims to tackle the topics of diffusion, sorption, anion exclusion, and rock matrix anisotropy. The laboratory part has, in addition, focused on small scale rock characterisation. This provides a wealth of input data that can be incorporated in the modelling.

## A9.5    Outline of Task 9

Figure A9-2 shows the proposed flow chart of Task 9. As can be seen, the task integrates the LTDE-SD and REPRO experiments, utilising both inverse and predictive modelling. For each new step, information from, and knowledge gained in, the previous steps should be incorporated in the modelling. This is intended to lead to an increased realism in process description in the solute transport modelling codes. In Figure A9-2, grey boxes mark activities. When summarising the proposed activities below, the labelling 9A, 9B, 9C, etc. has been used. However, the actual division of Task 9 into different subtasks concerning Task 9C–9E needs to be decided at a later stage. Traditionally, the exact content of each subtask is open for discussion during the lifetime of the task. Task 9 is no exception and the participating organisations are welcome to suggest modifications. As always in the Task Force GWFTS, reporting and publications of papers are encouraged.

**Task 9A**: Task 9 is suggested to start with semi-predictive modelling of WPDE-1 and WPDE-2 of the REPRO project. Traditional solute transport data, that are site specific for ONKALO, are used as input in what the modellers perceive as traditional solute transport codes. Preliminary results from WPDE-1 and WPDE-2 have been shown in PowerPoint presentations at a few Task Force meetings and workshops during 2013 and 2014. In addition, the official WPDE report is intended to be published by Posiva in 2015. The modellers will be asked to disregard these presentations and this publication during the subtask. Even so, the modelling cannot properly qualify as being fully predictive. With this in mind, the subtask is labelled semi-predictive in the flow chart and can also be seen as a "warm-up" case for Task 9. Assuming that the modellers will honour the request to disregard presentations and publications providing the experimental water phase results; an evaluation step consisting of comparison of model and experimental results can be performed.
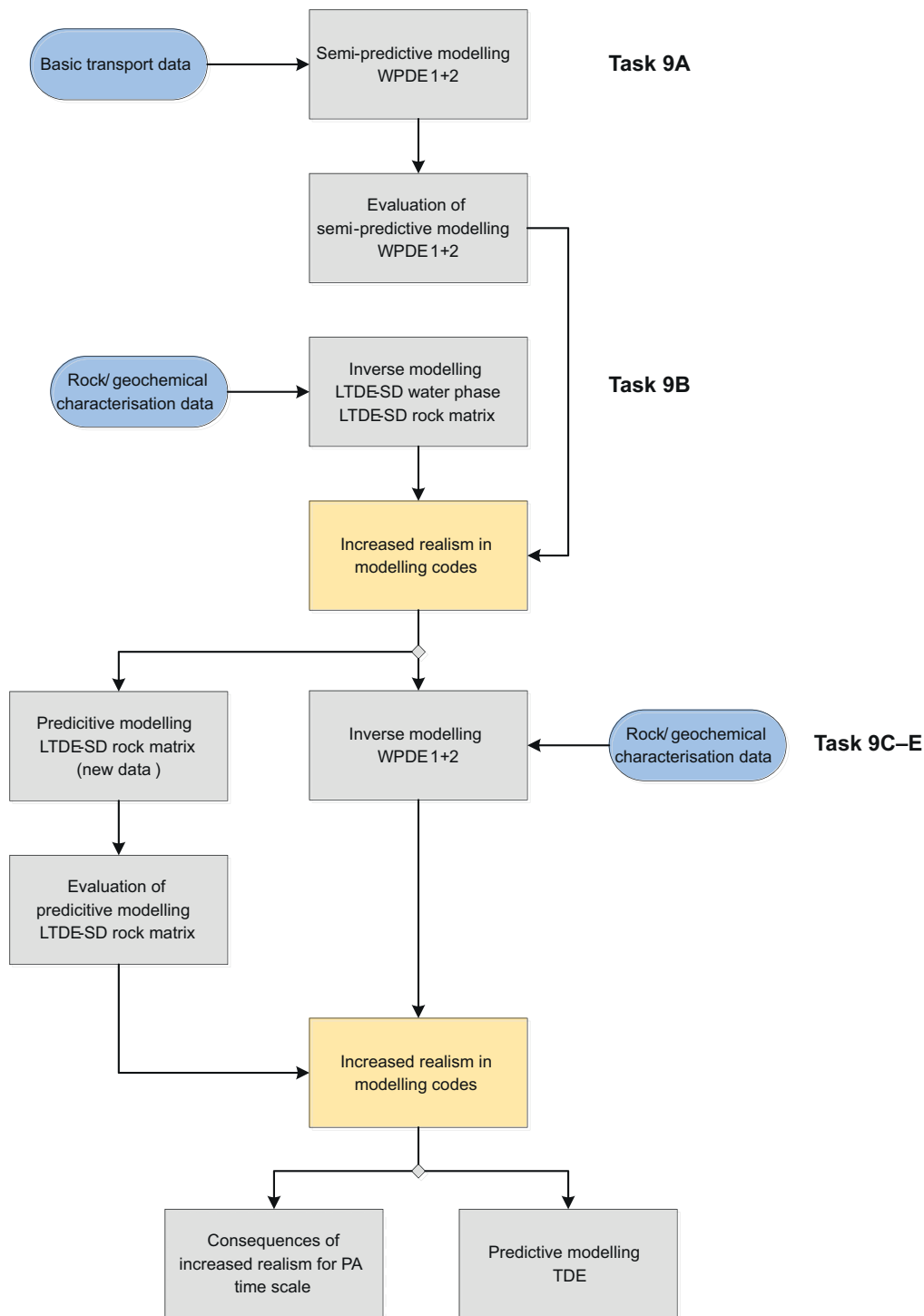
**Figure A9-2.** *Suggested flow chart of Task 9. Grey boxes mark activities.*

**Task 9B**: The following modelling subtask is suggested to use results from LTDE-SD; specifically results on tracer concentrations in the water phase and in the rock matrix will be used. In this subtask, the modellers may request data originating from the extensive rock matrix characterisation at the Äspö HRL, as well as geochemical characterisation data. This means that modellers will have a wealth of supporting data in setting up refined models for solute transport in heterogeneous media, for incorporating non-traditional processes, or for incorporating other aspects at the modellers' choosing. This subtask is intended to lead to an increased complexity in the modelling setup, with the ultimate aim to better reflect the reality and the experimental results.

**Task 9C**: In this subtask, the penetration profile of Cl-36, Cs-137 and Ni-63 into the LTDE-SD rock matrix will be modelled in a predictive fashion using the models developed in Task 9B. There are drill cores from LTDE-SD that have not yet been analysed in respect to tracer concentrations. Thus, the tracer activities of Cl-36 and/or Cs-137, and/or Ni-63 can still be measured at a reasonable effort, and this can be done on more than one drill core. The resulting profiles can be used for evaluation of the predictive modelling.

**Task 9D**: By using the increased realism in the modelling setup from previous subtasks, together with detailed rock and geochemical characterisation data from the REPRO laboratory program, the results from WPDE-1 and WPDE-2 are revisited and new and, hopefully, more complex and realistic inverse modelling is achieved, enabling a better understanding of the experimental data.

**Task 9E**: By using information from all of the above subtasks, predictive modelling is suggested to be performed for TDE in REPRO. It is uncertain whether or not breakthrough curves will be obtained from this experiment during the Task 9 lifespan. However, during the first few years, before breakthrough occurs, TDE can be viewed as an in-diffusion experiment. Measurements of the declining tracer activities in the injection hole are planned, with the intention of achieving sufficient resolution for, at least, the sorbing tracers. Based on the progress of the experiment, the evaluation needs to be decided at a later stage.

**Option:** Optionally at the end of Task 9, the increased realism in the solute transport codes may be put in the perspective of safety assessment time scales. This is to highlight if different aspects of matrix diffusion and sorption, utilising codes with increased complexity and realism, may have any consequence for long-term retardation. Different safety assessments use different time scales and conditions. Accordingly, the specifics of this exercise need to be decided at a later stage. Some waste management organisations may want to perform such a consequence study within their own programme, and not within Task 9.

## A9.6    Time frame and organisation

Task 9 is suggested to be carried out during 2015 to 2018. The task is intended to be officially launched at the TF GWFTS workshop tentatively in April/May 2015. The following meeting, TF#33, is planned to venue in the fall of 2015.

Members of the TF GWFTS Task 9 Technical Committee are:

- Jan-Olof Selroos, Ph.D., Manager Groundwater flow modelling at SKB, and SKB Task Force Delegate.

- Björn Gylling, Ph.D., Manager Solute transport modelling at SKB, and SKB Task Force GWFTS Secretary.

- Lasse Koskinen, Ph.Lic., Head of the long-term safety team at Posiva, and Posiva Task Force Delegate.

- Martin Löfgren, Ph.D., Niressa AB. TF GWFTS Task 9 Principal Investigator.

- Kersti Nilsson, Ph.D., Geosigma AB[13]. TF GWFTS Task 9 Principal Investigator and data coordinator.

- Antti Poteri, D.Sc (Tech), VTT Technical Research Centre of Finland.

- TF GWFTS Task 9 Evaluator: Remains to be appointed; discussions are on-going.

---

[13] Geosigma has been in charge of running the in-situ parts of LTDE-SD and REPRO.

SKB is responsible for managing spent nuclear fuel and radioactive waste produced by the Swedish nuclear power plants such that man and the environment are protected in the near and distant future.

**skb.se**